

**POSSIBLE CLIMATIC CONSEQUENCES OF A MAN-MADE
GLOBAL WARMING**

H. Flohn

RR-80-30
December 1980

*This study was sponsored jointly by the United Nations Environment
Programme and IIASA.*

**INTERNATIONAL INSTITUTE FOR APPLIED SYSTEMS ANALYSIS
Laxenburg, Austria**

Research Reports, which record research conducted at IIASA, are independently reviewed before publication. However, the views and opinions they express are not necessarily those of the Institute or the National Member Organizations that support it.

Copyright © 1980
International Institute for Applied Systems Analysis

All rights reserved. No part of this publication may be reproduced or transmitted in any form or by any means, electronic or mechanical, including photocopy, recording, or any information storage or retrieval system, without permission in writing from the publisher.

FOREWORD

There is increasing concern about man's impact on climate. While studying this problem, one comes to realize that this influence is not so much felt as a variation of the average values of global climate, such as temperature and pressure. Of concern is instead a change in the climatological patterns, with the average values changing very little. This could be a change in rainfall patterns, for example. Among other effects, increasing levels of carbon dioxide could cause a man-made global warming.

While it is impossible to determine such changes in climate patterns given the present state of the art, we consider it perhaps useful to study the changes that occurred in the climate patterns of the past. Today's highly sophisticated knowledge in paleometeorology allows us to undertake such a venture – a research activity that may also be crucial for our understanding of the forthcoming CO₂ problem.

Professor Flohn has studied this question along these lines, making use of information available to him as of March 1980. He wrote this report for the study on "Energy Systems and Climate" [Project Number FP/0700-75-02(717)], sponsored jointly by the United Nations Environment Programme (UNEP) and IIASA.

Wolf Häfele
Leader
Energy Systems Program

SUMMARY

Although climatic changes and modifications are mainly observed in the atmosphere, they in fact occur within the climatic system – the atmosphere, oceans, soil and vegetation, snow and ice – and can affect the multiple interactions between these subsystems. As Figure S1 shows, the time scales relevant to the subsystems can vary between a few days, in the case of the atmosphere, for instance, and up to 10^6 years, in the case of the Antarctic ice dome.

This paper examines both natural processes and man-made effects that may play a role in climate change, to provide the background for the development of a scenario of future climate change. The sensitive internal interactions between the atmosphere and thin drifting sea ice that lead to ice formation and melting are discussed, as well as the interaction between the atmosphere and the oceans in the regions of frequent upwelling along the equator and some coasts. The role of the heavily glaciated Antarctic continent in causing a marked hemispheric asymmetry of both the atmospheric–oceanic circulation and the positions of the large climatic belts is then examined. A possible partial instability of the West Antarctic ice sheet and its role in sea-level changes is also discussed.

The paper turns next to man-made impacts on the climate. Some, such as direct heat output, atmospheric pollution, changes in surface albedo (reflectivity), heat storage, and water budget, are obvious on a local scale. More important, however, are the implications of the increase in carbon dioxide and some atmospheric trace gases. Their long residence time, between 5 and about 50 years, their large-scale turbulent mixing caused by the atmospheric circulation, and, above all, their absorption in the infrared portion of the spectrum produce a combined greenhouse effect, which tends to warm the troposphere and cool the stratosphere.

Attempts to model the relationship between CO_2 concentrations and temperature changes are then reviewed, in order to quantify the greenhouse effect that may be associated with given levels of CO_2 . It is found that the

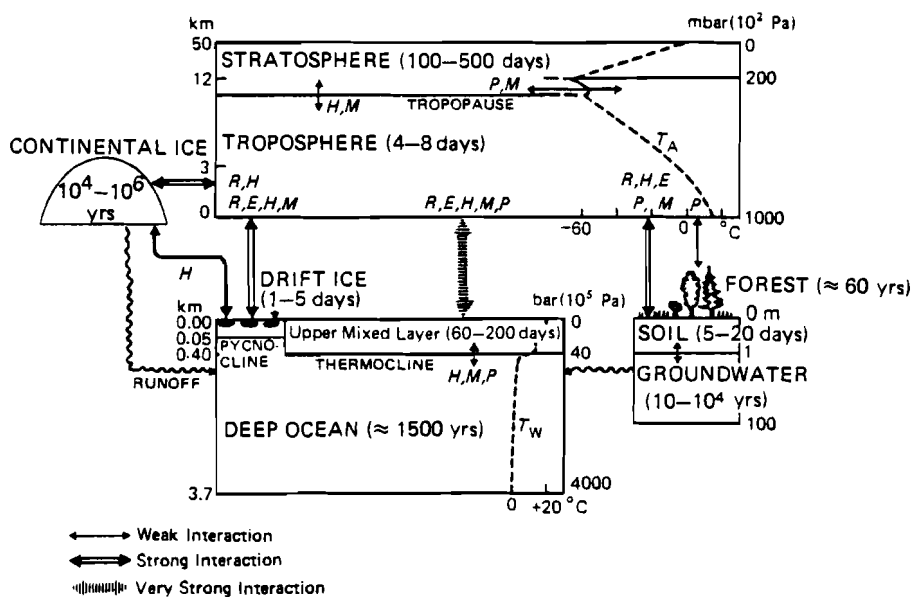


FIGURE S1 The climatic system, showing the time scales characteristic of its subsystems and the interactions between the subsystems. *R* is radiation; *H* is heat; *E* is evaporation; *M* is momentum; *P* is particles or gases; *T_w* is water temperature; and *T_A* is atmospheric temperature.

best models available indicate an average 3 °C warming of the surface layers in low and middle latitudes, with a doubling of the CO₂ concentration. This warming increases to 5–10 °C in polar latitudes, due to the feedback between snow or ice, surface albedo, and temperature. The effect of other trace gases, especially of nitrous oxide, one of the final products of nitrogen fertilizers, adds some 50% or more to the CO₂ effect – accelerating the expected global warming. An estimate of future temperature evolution, dependent on the initial growth rate of CO₂ concentrations, is made, using one of the most reliable radiation models for the relation between CO₂ content and typical temperature change (together with a selection of logistic CO₂ growth functions).

Evidence of temperature fluctuations in recent years is examined next. It is found that a man-made global warming of 0.2 °C, assumed to have occurred over the past 80 years, can be accounted for by natural fluctuations. Evidence shows that an increase of 0.4–0.5 °C is likely to occur between 1990 and 2000.

Paleoclimatic phases characterized by warm temperatures are then identified, to see if current man-made warming and expected future warming has been paralleled by past warm phases during the long historical evolution of the earth's climate, and to study the nature of the climate during the warm phases. Table S1 provides information on selected paleoclimatic warm phases, including estimates of the middle-latitude temperature differences that characterized the phases, and CO₂ levels equivalent to the increased temperatures. The CO₂ levels associated with the estimated temperature differences are based on two extreme versions of the Augustsson–Ramanathan model (1977). “Virtual” CO₂ content refers to a CO₂ level that has been adjusted to reflect the additional greenhouse effect of other trace gases. It is assumed that the increase in other trace gases adds 50% to the greenhouse effect of CO₂ alone (the “real” CO₂ content).

Since really comprehensive models of the climatic system as a whole and its interactions are not yet available and cannot be expected to be forthcoming soon, a scenario based on these warm paleoclimatic phases is discussed in this paper. Such a scenario can be used as a conditional forecast only if the following natural factors remain constant: no change in the solar constant, no major cluster of volcanic eruptions, no disintegration of the West Antarctic ice sheet, and no changes in cloudiness. Furthermore, the changes in the boundary conditions since the occurrence of past warm phases, i.e., changes in vegetation, sea level, and mountain formation, must also be taken into account.

Examination of past climates as a basis for a global warming scenario. Evidence is brought together showing that during the Medieval warm phase (~ 1,000 AD), the sea ice around Greenland retreated, causing more northerly cyclone tracks and frequent dry anticyclonic conditions for Europe. Evidence for the Holocene warm period (~ 6,000 years ago) indicates that it was nearly everywhere more humid than today, especially in the arid belt of the Old World. There the desert was replaced by semiarid grassland densely populated by cattle-raising nomads. The role of natural and man-triggered processes, such as the retreat of the North American ice sheet and the beginning of desertification, during this epoch is also discussed. It is concluded that under present boundary conditions a return to a similar regional climate is unlikely.

During the warmest interglacial period 120,000 years ago, more warming, i.e., +2.0–2.5 °C, occurred, accompanied by marked shifts of vegetation belts and coastal lines due to a sea-level rise of 5–7 m. A partial disintegration of the West Antarctic ice sheet probably played an important role in climatic change during this period. As in the Holocene warm period, the climate was somewhat more moist than today in many areas for which data are available. (Immediately after the Eem sensu stricto phase of this warm interglacial period, an abrupt cooling occurred; such abrupt occurrences of cooling, sometimes of a nearly glacial intensity, have also been observed for other interglacials, lasting for several centuries.)

The real CO₂ level equivalent to a 2.5 °C warming, as occurred during the last interglacial period, can be estimated to be 550 ppm ± 10%, if one assumes

TABLE S1 Atmospheric CO₂ content equivalent to estimated temperature differences (ΔT) during selected paleoclimatic phases.

Paleoclimatic warm phases	$\Delta T(^{\circ}\text{C})^a$	Virtual CO ₂ content ^{b,d} (ppm)	Real CO ₂ content ^{c,d} (ppm)
Medieval warm phase (1,000 yrs ago)	+1.0	420–490	385–430
Holocene warm phase (6,000 yrs ago)	+1.5	475–580	420–490
Eem Interglacial (120,000 yrs ago)	{ +2.0 +2.5	530–670 590–760	460–555 500–610
Ice-free Arctic ocean (12–2.5 × 10 ⁶ yrs ago)	+4.0	780–1150	630–880

^aEstimated temperature increase over the current temperature in low and temperate latitudes.

^bUnit expressing the combined greenhouse effect stemming from real CO₂ and atmospheric trace gases.

^cAssuming a 50% contribution of trace gases to the expected increase in virtual CO₂.

^dThe ranges in virtual and real CO₂ content are based on two extreme versions of the Augustsson–Ramanathan model (1977); the most likely value lies between the extremes.

SOURCE: The data presented in this table are based on results from the Augustsson–Ramanathan model (Augustsson and Ramanathan, 1977).

the contribution of trace gases to the CO₂ greenhouse effect to be 50%. The warming in the Arctic would reach about 6–8 °C, probably reducing the Arctic sea ice to its central core between Siberia and Canada, and causing at the same time a poleward displacement of climatic belts by several hundred kilometers.

If CO₂ concentrations reached 750 ppm ± 16%, an average global warming of 4 °C would occur. *Model studies and paleoclimatic investigations indicate that this value is close to the critical threshold of a complete disappearance of the drifting Arctic sea ice.* The sensitivity of this sea ice (whose average thickness is only 2–3 m) to changes in such climatic factors as length of melting period, heat flow from the ocean, and salinity (due to a possible reduction of freshwater inflow), indicates that such a disappearance would probably take no more than a few decades, or even less. Due to the delay caused by the heat storage capacity of the ocean, the above-mentioned temperature increase of 4 °C may be considered a minimum value.

Paleoclimatic evidence collected by the Deep Sea Drilling Program has revealed that a permanently open Arctic sea existed until 2.5 or 3.0 × 10⁶ years ago. In contrast, the East Antarctic continent has been glaciated for the past 12–14 × 10⁶ years. The evidence shows that for about the last 10 × 10⁶ years before the beginning of the present glacial–interglacial cycle, an Antarctic ice dome of today's height (or higher) coexisted with an open Arctic ocean,

with temperate or boreal forests extending to lat 81–83 °N, interspersed only with some local mountain glaciers; no evidence of tundra or permafrost in the soil has been found.

The implications of a possible coexistence of an ice-free Arctic and a glaciated Antarctic. The evidence from the Deep Sea Drilling Program is quite surprising since such a contrast between a heavily glaciated pole and an ice-free pole must have created a hemispheric asymmetry of the atmospheric–oceanic circulation that was much stronger than the asymmetry existing today. Such an asymmetry of the climate would cause the southern arid areas to expand to the vicinity of the equator, displace the meteorological (and thermal) equator to near lat 10 °N or even more (leaving the equatorial rain belt only in the northern hemisphere), and shift the northern arid belt to lat 35–45 °N, extending it even to the southern part of central Europe. This shift of climatic belts must be seen as a consequence of fundamental circulation theories. With the temperature difference between the equator and the North Pole decreasing, the area of the tropical–subtropical circulation belt increases, while the temperate and subpolar belt of westerlies contracts toward the North Pole. Since no comprehensive climate model of this unexpected pattern has been designed so far, detailed forecasts of regional climates after such an event are not possible. Simple extrapolation of the climate of the late Tertiary ($12\text{--}2.5 \times 10^6$ years ago) is not admissible because of the displacement of continental coasts and the formation and lifting of most of today's mountains at and since that time. Still, the stability of this pattern over a period of as long as ten million years must now be considered a fact. A return to this pattern would most probably lead, after a series of catastrophic weather extremes, to a displacement of the earth's climatic zones by 400–800 km. This would necessarily affect mankind as a whole, beneficially in some areas, but destructively in many others, drastically changing freshwater supply and agricultural productivity.

CONTENTS

1	INTRODUCTION	1
	1.1 Natural Climatogenic Processes	1
	1.2 Man-made Climatogenic Effects	2
	1.3 Methods for Predicting Climatic Change	3
	1.4 Organization of the Report	5
2	NATURAL INTERNAL CLIMATOGENIC PROCESSES	7
	2.1 The Role of Polar Sea Ice	7
	2.2 The Role of the Antarctic Continental Ice Sheet	12
	2.3 The Asymmetry of the Global Atmospheric Circulation	13
	2.4 Equatorial Upwelling, El Niño, and the Hydrologic Balance	15
3	MAN-MADE CLIMATOGENIC PROCESSES: THE “COMBINED GREENHOUSE EFFECT” OF CARBON DIOXIDE AND ATMOSPHERIC TRACE GASES	21
	3.1 Factors Contributing to the Greenhouse Effect	21
	3.2 Estimation of the Future Combined Greenhouse Effect	24
4	RECENT CLIMATIC HISTORY AND THE PERCEPTION OF A GLOBAL WARMING	30
5	EXAMINATION OF PAST CLIMATES AS A BASIS FOR A GLOBAL WARMING SCENARIO	35
	5.1 Medieval Warming	35
	5.2 The Holocene Warm Period and the Humid Sahara	37
	5.3 The Last Interglacial Period (Eem Sensu Stricto)	45

6	IS A COEXISTENCE OF AN ICE-FREE ARCTIC AND A GLACIATED ANTARCTIC POSSIBLE?	48
6.1	Causes and Time Scale of a Possible Opening of the Arctic Ocean	48
6.2	Coexistence of an Open Arctic Ocean and a Glaciated Antarctic during the Late Tertiary	54
6.3	Some Implications of a Unipolar Climatic Asymmetry	61
7	CONCLUSIONS	69
	REFERENCES	73

1 INTRODUCTION

The recent discussion on the physical background of climatic fluctuations aims at one of the basic problems of meteorology and the geophysical sciences as a whole (see GARP 1975). Climatogenesis occurs not only within the atmosphere but within the overall climatic system. As Figure 1 shows, this system consists of several interacting subsystems with quite different time scales (or “memories” in the usual scientific jargon). The climatic history of the past 5,000 years indicates that this system is fairly well balanced, for only secondary climatic fluctuations occurred during this period. But even these seriously disturbed man’s economy and challenged his bare existence in marginal areas of the polar or arid zones.

1.1 NATURAL CLIMATOGENIC PROCESSES

Many climatic changes are caused by natural feedback processes within the climatic system; for example, an expansion of the Arctic sea ice is at the same time both a cause and an effect of climatic fluctuations. Such internal climatogenic processes are discussed in Chapter 2 of this report.

Other natural causes of climatic fluctuations are external and operate with little or no feedback. The examples given most frequently include heavy volcanic eruptions of the explosive (Plinian) type; such eruptions produce large numbers of small particles in the submicron range, which float in the stratosphere (in the Junge layer at about 20–22 km), concentrate in polar regions, and absorb and scatter some components of solar radiation. This leads to worldwide cooling that increases with high-latitude feedback between snow, albedo (reflectivity), and temperature (Mass and Schneider 1977, Oliver 1976, Pollack *et al.* 1976). The frequency with which these eruptions occur varies greatly (Lamb 1970, Kennett 1977a, Kennett and Thunell 1975, 1977b); as in the case of earthquakes, they are apparently triggered by the slow, but discontinuous, motion of the tectonic plates of the earth’s crust.

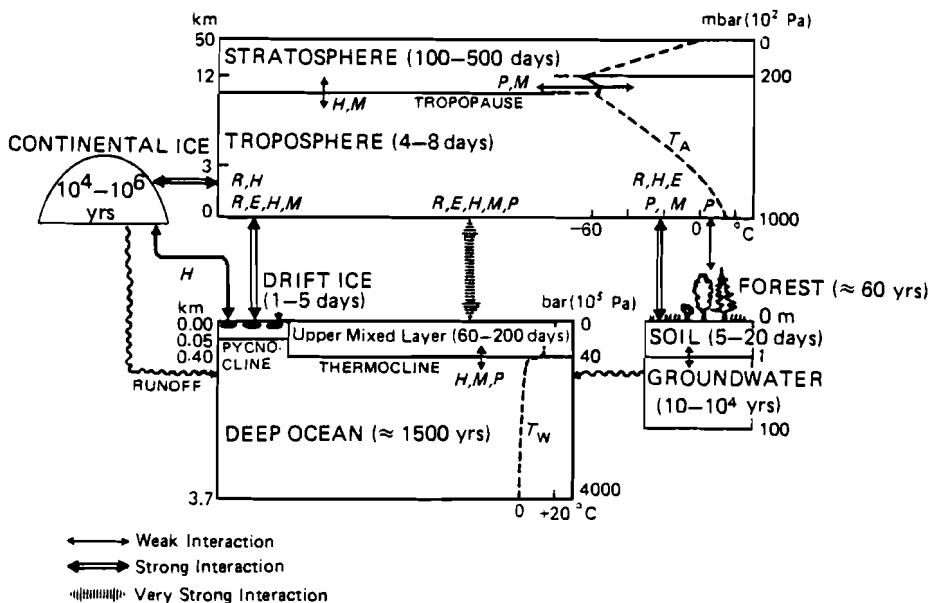


FIGURE 1 The climatic system, showing the time scales characteristic of its subsystems and the interactions between the subsystems. R is radiation; H is heat; E is evaporation; M is momentum; P is particles or gases; T_w is water temperature; and T_A is atmospheric temperature.

The possibility that short-lived fluctuations of solar radiation in the visible and near-infrared part of the spectrum induce climatic change is still controversial among specialists; continuous high-precision measurement above the level of pollutants in the denser layers of the atmosphere is needed, preferably by means of a satellite. There are also strong variations in the particle emission of the sun (protons) and in solar radiation in the far-ultraviolet or roentgen range. The possible role of such variations in the climate- and weather-producing troposphere [below 200 millibars (mbar) or approximately 12 km] is also still controversial and will not be discussed here. Other extraterrestrial factors affecting the climate are negligible.

1.2 MAN-MADE CLIMATOGENIC EFFECTS

It is generally agreed that man-made effects have been perceptible until now only locally or on a microscale, e.g., in cities or industrial centers (see Bach 1976a, 1976b). The role of atmospheric dust (in the 1–10 μm range) has sometimes been overrated, though it may be important in some deserts or semi-

deserts (notably in Central Asia and the Middle East), or in large metropolitan areas. The effect of atmospheric dust depends not only on the size and quality of the particles, but also on the surface albedo; it seems to have a warming effect, at least in continental areas. Waste heat affects the climate only on a local scale; even if it were to increase substantially, the short residence time of enthalpy in the atmosphere – on the order of hours and days – would probably inhibit its impact. In contrast to the rather short residence time of tropospheric particles, which is on the order of days or weeks, the residence time of infrared-absorbing gases, such as CO_2 , is on the order of years and decades. Because of their importance in climatogenic processes, i.e., in creating a “combined greenhouse effect,” a detailed treatment of the role of these pollutants is provided in Chapter 3.

Omitted from this discussion are some slow, but certainly important, man-made changes which affect the climate via the biosphere and the soil. These include destruction of natural vegetation in order to create arable land or pastures (causing soil erosion and desiccation of swamps, lakes, and marshes); large-scale irrigation (now affecting about $2.3 \times 10^6 \text{ km}^2$); building of reservoirs (now covering about $0.5 \times 10^6 \text{ km}^2$, not including the multitude of small tanks and ponds); and sealing of the earth's surface with concrete and other building materials. The climatic effect of these activities occurs through changes in several physical parameters: surface albedo and roughness, soil moisture and evapotranspiration, terrestrial (infrared) radiation, and absorption of radiation by water vapor. All of these processes are first relevant on a local scale; on a global scale they operate quite slowly. Still, continental surfaces have been subject to exponentially increasing changes at least since the Neolithic revolution about 8,000 years ago. Such man-made effects are probably even much older; Paleolithic man already knew how to use fire for hunting (e.g., in Australia).

At least 30% of the continents, some $45 \times 10^6 \text{ km}^2$, are now affected by such activities. According to statistics from the Food and Agriculture Organization (FAO), destruction of natural vegetation has reached an alarming rate (see Polunin 1980). These statistics indicate that the annual rate of destruction of tropical forests (which play a big part in the CO_2 cycle) is $110,000 \text{ km}^2$. These surface changes tend to increase the surface albedo everywhere and are one of the few man-made processes that lead to cooling, at least in cases where the decrease in evapotranspiration does not cause an increase in sensible heating. Recent estimates (i.e., by Sagan *et al.* 1979) indicate that this effect is quite small in the context of the “human time scale” of 50–100 years; however, destruction of vegetation may have contributed to the global cooling since the Neolithic revolution.

1.3 METHODS FOR PREDICTING CLIMATIC CHANGE

Due to the complexity of the climatic system (see Figure 1) and the lack of models suitable for simulating the important interactions between its subsystems,

any attempt to predict climatic changes *in toto* is useless at the present time, at least if the forecast is to cover a period longer than one year. Most sobering in this respect is the fact that external effects on the climatic system are as yet unpredictable and will remain so for some time. Still, there is some hope that *conditional* predictions (also defined rather approximately as “predictions of the second kind”) may be feasible. Such predictions may start with the assumption that external climatogenic effects, and perhaps also some of the internal interactions, do not change. One may then ask the question, What are the climatic consequences of a given man-made process, for instance, an increase in CO₂? If all other factors are held constant, it should be possible, with the help of simplified or more sophisticated models, to outline the possible individual or combined effects of processes produced or triggered off by man. In this way our understanding of climatogenic processes can be systematically improved.

In spite of the remarkable progress we have made in designing physical–mathematical models of atmospheric circulation, no model can yet adequately describe the climatic system as a whole, including the highly effective positive or negative feedback mechanisms within and between its subsystems. Manabe and Holloway (1975) provide a careful and critical evaluation of the existing limitations of surface climate modeling, using Köppen’s classification for comparing model results and reality. No model has yet demonstrated, with sufficient accuracy and horizontal resolution, an ability to simulate the present surface climate with its seasonal variation – one of the most demanding and convincing tests of model capability. A major drawback is the lack of effective parameterization of subgrid-scale processes; another is the limited capability of even the most powerful computers available. Still, these sober statements should not underrate the achievement of enthusiastic model designers. There is little doubt that in the foreseeable future more advanced climate models, probably combining deterministic and stochastic approaches, will be able to present satisfactory solutions, at least for conditional predictions.

In recognition of the present state of modeling, a scenario based on past climate behavior is discussed in this report, and no attempt is made to use comprehensive physical–mathematical models. This scenario is a scientific tool based on historical and geological information. It may be considered essentially (but not exclusively) an empirical approach with specific limitations. Since it is necessary to study climate behavior over many epochs (the Medieval warm period 1,000 years ago, the Holocene warm period 6,000 years ago, the last Interglacial 10⁵ years ago, and earlier epochs reaching back 10⁶–10⁷ years), the boundary conditions of the climatic system vary to such a degree that past experience can only be used as a first guide to what may happen in the foreseeable future – like sensitivity tests for a fairly sophisticated model. Also, in spite of the nearly unimaginable time scale on which the scenario is based, our interest in future climate change has to be restricted to what could be considered man’s time scale, the next 50–100 years.

Because of the unpredictability of and uncertainty about many natural climatogenic processes, a scenario describing the possible future evolution of the climate must assume no major change in solar radiation, no unusual clustering of major volcanic eruptions, and no unusually large advance ("surge") of the Antarctic ice shelves. Because of our present lack of knowledge, it is also necessary to assume no significant variation in average cloudiness, for the interaction between radiation (dependent on wavelength) and clouds (dependent on size distribution of droplets and crystals, on cloud type and altitude, and on pollution particle content) is not well understood. However, many scientists feel that this concern should not be overemphasized (Cess 1976, 1977). One reason is that most clouds are formed or dissolved in ascending or subsiding motion of different scales; due to the law of conservation of mass all vertical motions are well balanced. Only a few percent of low-level stratus and thin cirrus trails can now be manipulated by man. A second reason is that global warming due to infrared absorption (the "greenhouse effect") decreases with height and reverses its sign in the stratosphere. In this case the overall thermal stability of the troposphere will decrease; consequently, the frequency of stratus clouds will also decrease, while vertical mixing will increase. Roads (1978) demonstrated that fractional cloudiness and relative humidity may even decrease with increasing temperature.

Compared with a model, the scenario discussed in this report has one advantage: it describes a situation that has in fact occurred and that may therefore arise again. Learning from history means checking how nature has solved the complete set of equations simultaneously and on-line, in all subsystems and at all scales, with a fully four-dimensional, i.e., time-dependent, approach. Since the boundary conditions are varying slowly, but permanently, climatic history can never repeat itself in all details, but rather only in substance. In this analysis, the main objective of scenarios is to serve as a preliminary guide for impact studies. Since the time scale of the phases of geophysical evolution described in our scenario can vary greatly, the scenario should not be conceived as a necessary sequence or as a substitute for climate prediction.

1.4 ORGANIZATION OF THE REPORT

Natural processes which can play an important role in climate change are presented in Chapter 2 of this report. In section 2.1 the formation and melting of polar sea ice is discussed, with emphasis on factors which may produce changes in the area and thickness of drift ice. Evidence of the recession or advancement of Arctic sea ice in the historical past is also reviewed. Section 2.2 addresses the role of the Antarctic continental ice sheet, focusing on the partial latent instability of the ice, which could possibly lead to catastrophic ice surges or deglaciation of western Antarctica. In section 2.3 the discussion turns to the asymmetry of the global atmospheric circulation at the current time, due to the contrast between the heavily glaciated Antarctic continent and the Arctic,

with its thin cover of drift ice. Finally, in section 2.4 the phenomena of equatorial upwelling of the ocean, El Niño, and the hydrologic balance are discussed, with attention to their significance for ocean water temperatures and evaporation. Changes in the parameters describing these phenomena during selected paleoclimatic phases are reviewed. As a whole Chapter 2 provides the background for the later discussion of a possibly ice-free Arctic and the implications of such a situation for the climate.

Chapter 3 focuses on climatic changes produced or triggered off by man, specifically the “greenhouse effect,” or global warming, caused to a great extent by the release of CO₂ and trace gases into the atmosphere, but also by increases in such factors as the water vapor content of the atmosphere due to human activities, or to equatorial downwelling of the ocean. Attempts to model the relationship between atmospheric concentrations of CO₂ and trace gases, and the magnitude of global warming are then reviewed. Finally, paleoclimatic phases characterized by warm temperatures are identified and associated with levels of CO₂ that could be expected to produce such warming in the future.

In Chapter 4 existing evidence of the most recent temperature fluctuations is examined, taking into account the difficulty of distinguishing natural fluctuations from a real warming trend. The lack of representative data on such parameters as air temperatures, rainfall, and the extension of sea ice at the end of the melting season is discussed.

Chapter 5 focuses on the characteristics of selected warm paleoclimatic phases, i.e., the Medieval warm period, the Holocene warm period, and the last Interglacial period. Underlying this description of climatic history is the question, To what extent could history repeat itself, under varying boundary conditions, if global warming equal to that which obtained in earlier eras is reached in the future? Evidence regarding such factors as the extension of Arctic sea ice, cultivated land areas, tree lines, sea level, air and water temperatures, and rainfall during these eras is presented.

Chapter 6 takes a serious look at one scenario of climate change in the future: the possibility for the coexistence of an ice-free Arctic and a glaciated Antarctic. The discussion begins with a review of factors which could lead to global temperature increases large enough to cause the complete disappearance of Arctic sea ice — temperatures higher than those which obtained during all the warm climatic phases of the past two million years. Particular attention is then paid to the plausibility of the ice-free Arctic—glaciated Antarctic scenario, and to the great hemispheric asymmetry of atmospheric and ocean circulation that this situation would imply. Evidence of the existence of just such a situation during the late Tertiary period is introduced, lending weight to the argument that the scenario merits sober consideration. Finally, climatic implications of such a unipolar climatic asymmetry are examined, for instance, changes in the global water budget, a world-wide rise in the sea level, and melting of the continental ice caps.

2 NATURAL INTERNAL CLIMATOGENIC PROCESSES

2.1 THE ROLE OF POLAR SEA ICE

2.1.1 *The General Process of Ice Formation and Melting*

Large areas in both polar regions are permanently or seasonally covered by a thin blanket of ice floes separated by narrow strips of open water (polynyas or leads). The ice floes are covered by snow for most of the year and have an albedo of almost 80%. This is in contrast to the albedo of open water, which is only 8–12% in polar regions when the sun is low in the sky. During the melting season (which in the central Arctic is restricted to about ten weeks between mid-June and the end of August), the albedo of the ice floes decreases to about 60%; superficial ponds of meltwater occur, which appear light blue when seen from an airplane.

The area of polynyas relative to ice floes varies between 2 and 3% in winter and up to 12–20% in the melting season (Vowinckel and Orvig 1970, Untersteiner 1975). The thickness of the Arctic drift ice is often quoted to be 2–3 m on the average. However, the thickness of individual floes actually varies with age and ranges between 0.5 m and more than 6 m (Thorndike 1975). This has been verified by submarine expeditions and satellite microwave measurements of surface emissivity.

Typical values for the heat and radiation budget of the polar ice are very difficult to determine under such conditions. In winter the turbulent fluxes of sensible and latent heat from the polynyas – where the open ocean water (water temperature $T_w \approx -2^\circ\text{C}$) is in direct contact with the cold air below the polar inversion (air temperature $T_A \approx -30^\circ\text{C}$) – are more than 100 times as large as those at the surface of the ice floes, and sometimes have an opposite sign (Vowinckel and Orvig 1973). Recent measurements of the sensible heat flux at natural leads (with the fetch varying between 7 and 80 m) north of Barrow, Alaska yielded values of 250–450 W/m^2 ; this exceeds the solar radiation in the Sahara (Andreas *et al.* 1979). Even during polar summer with

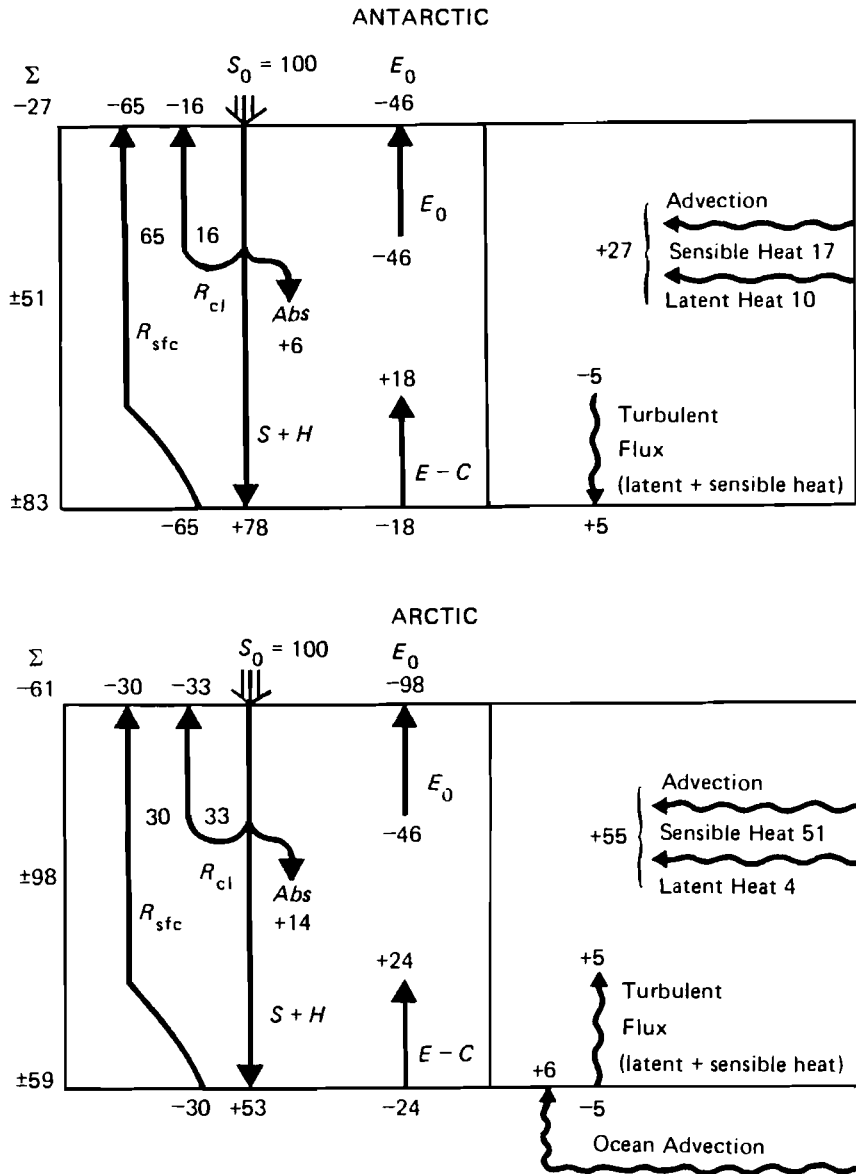


FIGURE 2 Estimated heat budgets of the atmosphere above the Antarctic and the Arctic, in 100 units of solar radiation at the top of the atmosphere (S_0). E_0 is outgoing terrestrial (infrared) radiation; Abs is solar radiation absorbed by the atmosphere; R_{cl} (R_{sfsc}) is radiation reflected by clouds and the earth's surface; $S + H$ is global (sun and sky) radiation at the earth's surface; $E - C$ is effective infrared surface radiation. The data, with some modifications, are taken from Schwerdtfeger (1970) and Vowinkel and Orvig (1970). Source: Flohn (1978a).

permanent daylight, polynyas with a diameter of several kilometers can suddenly freeze over because of cold air advection. Thus, the heat budget values given in Figure 2 can only be rough estimates.

In a very careful study, Maykut and Untersteiner (1971) simulated the physical processes of ice formation and melting, on the basis of observations made in 1957–1958 and assuming a horizontally homogenous ice cover. In this one-dimensional model of the ocean–ice–snow–air multiphase system, two processes are particularly effective in reducing ice thickness: lowered surface albedo (e.g., related to the duration of the melting season and to pollution by dust or oil wastes) and increased ocean water temperature. Model runs showed that during the melting season about 50 cm of ice melts from above, while during the rest of the year a similar amount freezes from below. A possible increase in salinity (and thus density) of the ocean water is not considered in the model. This could occur, for instance, after an artificial deviation of part of the freshwater flow from big rivers in Siberia and Canada for irrigation purposes (Aagard and Coachman 1975; for new data on future plans for Siberia and Central Asia see Hollis 1978). More sophisticated three-dimensional time-dependent models of the multiphase system are now under development in large international research programs, and more complete solutions, including all feedback mechanisms, may be expected (Washington *et al.* 1977, Hibler 1979).

2.1.2 *Arctic Drift Ice*

At present the ice-forming processes occur in a shallow (≈ 50 m), but very stable, surface layer of the Arctic ocean (Figure 3). Excess low-saline water and ice leave the Arctic basin with the strong and narrow East Greenland Current. If the freshwater inflow is significantly reduced, the salinity and density of the surface layer of the ocean must increase, reducing its stability. In a non-stratified ocean with turbulent vertical exchange, no permanent ice cover would be possible.

Arctic drift ice is driven by winds and ocean currents. A large anticyclonic gyre circles clockwise around the central core of the Arctic ice between Greenland, Alaska, and Siberia (Rothrock 1975). The total area of the Arctic drift ice varies between 7×10^6 km² in late summer and 14×10^6 km² in spring (Walsh and Johnson 1979). Thus only one-half of the maximum ice cover is seasonal, with a thickness of 50–100 cm. The average residence time of an ice crystal in a floe between freezing and melting is on the order of 5–10 years.

2.1.3 *Recession and Advancement of Arctic Drift Ice in the Past*

In contrast to the high stability of the central core of Arctic ice, which has existed for at least 7×10^5 years and probably for more than 2×10^6 years,

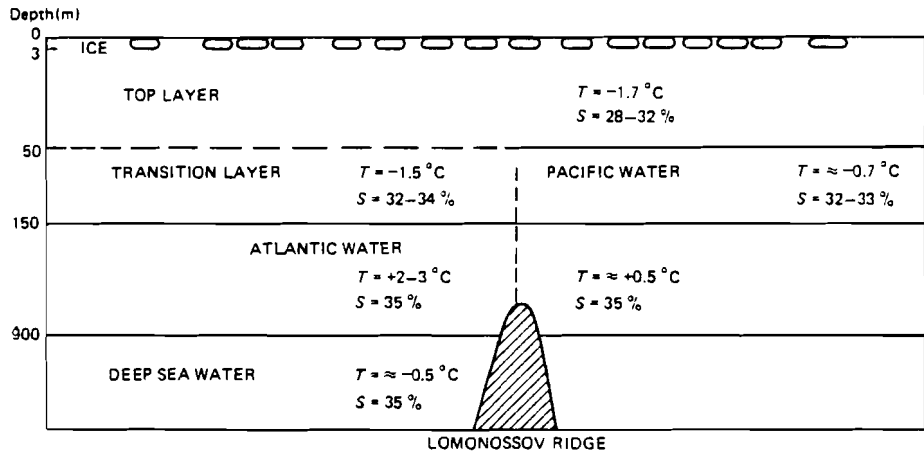


FIGURE 3 A schematic diagram of the stratification of the Arctic Ocean. T is temperature ($^{\circ}\text{C}$); and S is salinity (%).

the marginal parts of the ice in the Atlantic sector between Greenland, Svalbard, and Novaya Zemlya underwent large fluctuations within historical times. After gradually receding to Greenland's northern coast ($\approx 81^{\circ}\text{N}$), the ice began to advance along the eastern coast about the year 1320, sometimes blocking Iceland and the Denmark Strait until late summer. During the late seventeenth and early eighteenth centuries, the ice advanced several times towards the Faroes and even Norway (Lamb 1979). Occasionally Eskimos and polar bears stranded on a floe were carried as far as the coast of Scotland. The total area of Arctic ice may have varied by more than 20% during the last millenium, while the southern edge of the ice shifted by more than 2,000 km.

The large-scale advance of the ice during the Little Ice Age (1550–1850, with severe precursors around 1320 and 1430) seems to be correlated with several phenomena: a rearrangement of cyclone tracks in the far south, a much more frequent occurrence of blocking anticyclones above the then cold surface waters north and west of the British Isles, frequent outbreaks of polar air across the Alps in western and central Europe, and an increase in cyclonic activity and rainfall in the Mediterranean. "Low index" circulation patterns prevailed over most parts of the mid-latitude belt of westerlies in the northern hemisphere, and – as happens occasionally today – cold high-tropospheric troughs frequently penetrated into the interior tropics, causing anomalous rainfall. The contrasts between albedo and heat budget along the edges of the ice are of paramount importance for the formation of cold air above the ice and thus for the position of tropospheric frontal zones.

Polar ice shifts were rare during the warm period of 1931–1960. Since then, however, there has been some modest readvancement of the ice (shown in Figure 4 for Iceland), coinciding with some of the most unexpected climatic

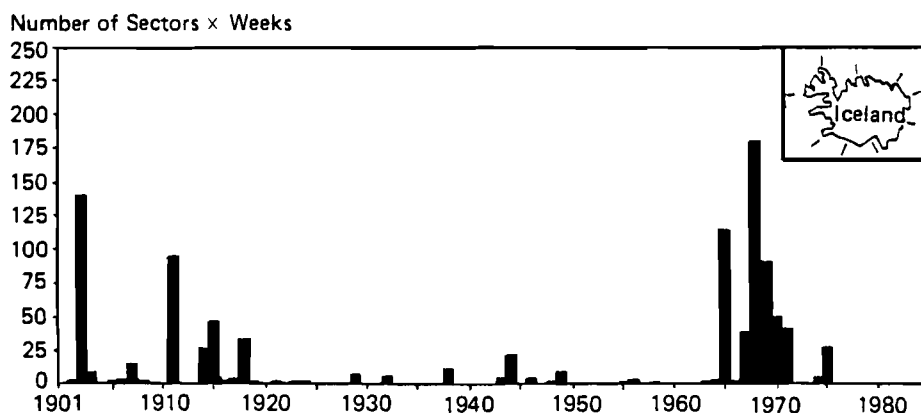


FIGURE 4 Sea ice fluctuations on the coasts of Iceland (measured in terms of the number of coastal sectors affected times duration of the ice in weeks), 1901 to the present. Source: Meteorological Service of Iceland (G. Sigtryggson).

anomalies of recent years. Among them were the severe winters of 1968/69 in the USSR and 1976/77, 1977/78, and 1978/79 in parts of North America, an unbroken series of six or seven unusually mild winters in western and northern Europe, and the coincidence of a serious western European drought with abundant rainfall in the central part of the USSR during the summer of 1976. Other anomalies were the three most severe seasons in this century of Greenland icebergs in the Newfoundland area (1971–1973) and frequent heavy gales in the North Sea area between 1972 and 1976.

Such quasi-stationary, atypical weather patterns demonstrate the simultaneous occurrence of large positive and negative anomalies of temperature and rainfall, known as the “North Atlantic seesaw” (van Loon and Rogers 1978). This phenomenon is correlated with a general cooling of the interior Arctic (see Figure 9), but masks the small temperature variations averaged along the parallels of latitude.

The physical reasons for such cooling (or warming) in the polar zone are not well understood. Flohn (1974a) hypothesizes the occurrence of one or more volcanic explosions which produce great masses of stratospheric particles; due to the stratospheric circulation system, these particles converge and subside above the interior Arctic (north of $\approx 75^\circ\text{N}$) and Antarctic, forming a dust layer at an altitude of 10–15 km (easily visible from an airplane). At this altitude the dust layer lasts longer than in mid-latitudes because of the relative absence of exchange processes between the troposphere and the stratosphere. By back-scattering and absorption, the dust layer may reduce solar radiation, surface temperature, and the duration of the melting season. Consequently, the average thickness of the ice may increase, reducing the heat flow between ocean and atmosphere. This in turn may lead to cooling and to an extension of the ice, for thin seasonal ice grows faster than thick perennial floes.

2.1.4 *Antarctic Drift Ice*

In contrast to the Arctic ice, the Subantarctic drift ice is largely seasonal ($\approx 85\%$). In winter an extremely cold, thin surface layer develops above the Antarctic ice dome, with average minimum temperatures below -70°C , repeatedly reaching -88°C . This cold layer spreads outward, cools the sea surface, and produces an extended seasonal cover of drift ice about 100–150 cm thick. (Unlike the situation in the Arctic, a low-salinity surface layer of the ocean does not develop). This drift ice is thus mainly produced by the extremely cold winds descending and blowing out of the Antarctic continent during the cold season, which is characterized by a strongly negative radiation balance. Its area increases from $3.5 \times 10^6 \text{ km}^2$ in late summer to about $22 \times 10^6 \text{ km}^2$ in spring. The most productive region is the Weddell Sea in the Atlantic sector; a large tongue of drift ice frequently extends from this sea towards ENE. At the end of the season, the total area of Antarctic ice is no less than $36\text{--}38 \times 10^6 \text{ km}^2$. Since both the areal extension of the coldest air and the position of the tropospheric baroclinic zone depend on the extension of drift ice, the southern hemispheric circulation is characterized by a time lag of 2–3 months with respect to the sun's radiation.

Two sharp extensions of the Subantarctic drift ice and the cold Antarctic surface water come in contact with the warmer water of the middle latitudes. In the Atlantic sector the drift ice and cold surface water reach lat $48\text{--}50^\circ\text{S}$, while in the vast South Pacific they extend approximately to lat 60°S . Thus, in contrast with the Arctic, the climatic influence of the Antarctic is strongest in the Atlantic sector; Bouvet Island (54°S) is almost completely glaciated, whereas Helgoland (54°N) is a summer bathing resort.

In addition to the enormous area of sea ice, the large-scale tabular icebergs of the Antarctic should be mentioned. These have an average depth of 200–400 m and extend for many square kilometers. In extreme cases they are as big as the Netherlands ($\approx 30,000 \text{ km}^2$). They break off from the large Antarctic ice shelves, their last debris reaching sometimes as far as lat 35°S in the Atlantic. From the point of view of climate, they are mainly important because of the large amount of heat they need for the melting process.

2.2 THE ROLE OF THE ANTARCTIC CONTINENTAL ICE SHEET

About 15 years ago a new, unorthodox ice age hypothesis was proposed by the New Zealand geochemist A.T. Wilson (1964). His basic assumption was that the combined action of pressure from above and geothermal heat flow from below must necessarily lead to melting at the bottom of a sufficiently thick body of ice. In this case the quite stable "cold" ice could become mobilized with the help of regelation processes, which are well known from "temperate" or "warm" glaciers in mid-latitude mountains. He assumed that a latent instability of the Antarctic ice parallels the rare surges of some Arctic or mountain

glaciers. Thus the Antarctic ice could possibly move forward catastrophically on all sides, forming a quasi-permanent ice shelf of $20\text{--}30 \times 10^6 \text{ km}^2$; the consequence would be a general cooling of the earth and the sudden initiation of a glaciation of the continents in the northern hemisphere. One of the most exciting discoveries that confirmed one of Wilson's basic assumptions was made by Gow *et al.* (1968) at Byrd station (80°S , 120°W). They observed how the bottom of an ice core (2,163 m) met with meltwater under high pressure.

Discussion of this hypothesis has led to some important modifications (e.g., Hughes 1973, Flohn 1974b), but has left the fascinating basic idea untouched. Model computations by Budd (1975a, 1975b) have demonstrated the interaction of the physical processes involved. Hughes (1975, 1977) has outlined the current form of Wilson's hypothesis in the following terms. While the bulk of the eastern Antarctic ice is stable and rests at a level well *above* sea level (except for a few small, widely dispersed meltwater lakes), the smaller ice dome of western Antarctica (between South America and long 140°W) rests on bedrock largely *below* sea level. In western Antarctica the ice may not be stable; the boundary between the floating shelf ice and the slowly moving parts of the continental ice is not fixed, and it has been suggested (see Hughes 1975, Mercer 1978) that the western Antarctic ice sheet once disappeared in the geological past. The present situation has apparently not yet reached an equilibrium stage (Hughes 1975); thus there is some risk of a catastrophic deglaciation of parts of western Antarctica in the foreseeable future (Mercer 1978). An event of this kind could create a worldwide rise in the sea level of 4–6 m (Mercer 1978). Its possible mechanism and time scale are unknown (see p. 68 for further discussion).

The Antarctic ice sheet, with a volume of about $26 \times 10^6 \text{ km}^3$, contains by far the largest freshwater reserve of the globe, at an average temperature below -30°C . Its mass balance is probably positive (Schwerdtfeger 1970), on the order of 3 cm water-equivalent per year. This figure is somewhat uncertain since some of the outflow components of this vast continent, such as snow-drift, are not yet well known. It should be mentioned that the possible positive mass balance of the Antarctic ice sheet is inconsistent with the very slow worldwide rise in the sea level of about 1.1 mm/yr. Geophysically, however, sea level fluctuations are extremely complex and far from being understood.

2.3 THE ASYMMETRY OF THE GLOBAL ATMOSPHERIC CIRCULATION

One of the basic features of global atmospheric circulation, and consequently of the wind-driven mixed oceanic layer, is its asymmetry with respect to the equator – a fact not covered satisfactorily by most textbooks. The asymmetry is accounted for by one of the fundamental parameters of atmospheric circulation, the *thermal Rossby number* Ro_T :

$$Ro_T = U_T / r\Omega$$

where $U_T = \Delta z \partial u / \partial z \propto \Delta y \partial T / \partial y$ is the vertical shear of zonal wind u (or the “thermal wind” proportional to the meridional temperature gradient $\partial T / \partial y$) of a layer Δz , r is the earth’s radius, $y(z)$ the meridional (vertical) coordinate, and Ω the angular speed of the earth’s rotation. This dimensionless number describes the thermal zonal wind, depending on the temperature difference between equator and pole, in units of the rotational speed of a point on the earth’s equator (464 m s^{-1}).

It is easy to determine the meridional equator–pole temperature difference in the troposphere, at least for the layers above the surface of the Antarctic ice dome. This is done at the Amundsen–Scott station at 90°S , altitude 2,800 m. Table 1 gives the results of a survey based on data for an uninterrupted seven-year period. If the results of the South Pole station survey (in which the surface pressure averaged 681 mbar) are used to represent the 700 mbar level, the error introduced is only about 0.5°C . Taking into account the systematic error, the data presented in Table 1 demonstrate that the Antarctic troposphere is actually about 11°C colder than the Arctic troposphere in the equivalent seasons. This is true in spite of the fact that in summer the Antarctic ice dome has the highest solar radiation of the whole globe; its surface albedo of 84–89% is also the highest.

A meridional equator–pole temperature difference results that is almost symmetric during northern winter/southern summer, but greatly asymmetric (17°C versus 44°C) during northern summer/southern winter. This causes a much stronger atmospheric circulation in the southern hemisphere, which crosses the equator and displaces the intertropical convergence zone (ITCZ) towards the north. The zonally averaged position of the “meteorological equator” – defined as the latitude of lowest pressure in the tropics and of a change in sign of the average meridional wind component – varies seasonally between 0° and almost 15°N , and reaches 6°N on an annual average (Flohn 1967). In July the thermal Rossby number is more than 250% higher above the southern hemisphere than above the northern hemisphere.

The quite different heat and radiation budgets of the two polar regions explains this asymmetry. The nearly landlocked Arctic ocean (85%) with a thin and perforated cover of drift ice contrasts with the isolated Antarctic continent with an ice sheet more than 2 km thick. Figure 2 (from Flohn 1978a) compares the preliminary data that are available on the heat and radiation budgets of Antarctica (Schwerdtfeger 1970, partly revised) and the Arctic interior (Vowinckel and Orvig 1970). Among the most essential points of difference are the higher albedo (reflectivity R_{sfc}) of the Antarctic ice, the region’s lower cloudiness and atmospheric water vapor content [that affect the reflection from clouds (R_{cl})], and the varying atmospheric infrared emission (E_0). Of minor importance are the turbulent fluxes of sensible and latent heat (evaporation) from the surface, which are directed upward above the Arctic Ocean and downward above Antarctica.

TABLE 1 Average temperatures ($^{\circ}\text{C}$) in the 300/700 mbar layer.

	January	July	Annual average
Equator (E)	.. ^a	.. ^a	-8.6
North Pole (N)	-41.5	-25.9	-35.9
South Pole ((S)	-38.3	-52.7	-47.7
Difference E-N	32.9	17.3	27.3
Difference E-S	29.7	44.1	39.1

^aThe difference in the average temperature of the mid-troposphere in January and July is less than 0.4°C .

SOURCE: Flohn (1967, 1978a).

In both regions the negative radiation budget at the top of the atmosphere must be maintained by quasi-horizontal advection from temperate latitudes; this advection is much higher in the Arctic, due to the variation of the land-sea distribution with longitude. Compared with atmospheric advection, the oceanic advection in the Arctic is rather small, since the warm Atlantic water submerges below cold, shallow surface waters.

The significance of the asymmetry of the global atmospheric circulation for climate change will be shown in Chapter 6, in which the possibility of an ice-free Arctic is discussed.

2.4 EQUATORIAL UPWELLING, EL NIÑO, AND THE HYDROLOGIC BALANCE

One of the most unusual cases of climatic variability is the irregular fluctuation of sea surface temperatures and of rainfall in a long, narrow belt along the equator across both the Pacific and the Atlantic (but not across the equatorial Indian Ocean). This belt coincides with the "equatorial dry belt" of classical climatology, for which a physical interpretation was first given by J. Bjerknes (1969).

In the Pacific and Atlantic Oceans the actual sea surface temperature drops, in a latitudinal belt between about 0° and 4°S , from the average value of tropical oceans ($26\text{--}27^{\circ}\text{C}$) to $18\text{--}22^{\circ}\text{C}$. In some cases, especially on the leeward side of islands, it drops to even less than 15°C . The occurrence of penguins on the equatorial Galapagos Islands is a striking example of bi-climatic adaptation to the lower sea temperature. Bjerknes's explanation of this phenomenon starts with the wind-driven Ekman flow in the shallow upper mixed layer of an ocean, which extends down only $50\text{--}100\text{ m}$ to the top of the thermocline; it separates, with several strong discontinuities, the cold waters of the deep ocean from the warm mixed layer. By integrating the Ekman drift with increasing depth down to the level where the wind-driven component disappears, one obtains a direction perpendicular to the wind, with an anti-cyclonic deviation of the current to the right in the northern hemisphere, and

to the left in the southern hemisphere. Since zonal winds prevail in tropical latitudes, several phenomena (see Figure 5) can be interpreted by means of the meridional component of the Ekman drift (ED_y). This can be written as follows:

$$ED_y = -(\rho f)^{-1} \bar{\tau}_x$$

Here x and y denote the zonal and meridional components, $\bar{\tau}$ the surface stress vector of wind \mathbf{v} (proportional to v^2), ρ the density, and f the Coriolis parameter ($f = 2\Omega \sin \phi$, with angular velocity Ω and latitude ϕ). Because of $\sin \phi$, the sign of f is reversed at the equator, and ED_y diverges on both sides of the equator in a generally easterly wind. In the Indian Ocean, where westerlies prevail throughout the year in a narrow band along the equator, the change in the sign of f leads to a convergence of the Ekman drift at $\phi = 0$, where $(\rho f)^{-1}$ becomes indefinite.

A more thorough elucidation should start from the rotation (vorticity) of the wind stress field. At the lower boundary of the ED layer, the vertical flow component w of the water can be expressed as:

$$w = (\rho f)^{-1} \text{rot}_z \bar{\tau}$$

where the vorticity $\text{rot}_z \bar{\tau} = \partial \bar{\tau}_y / \partial x - \partial \bar{\tau}_x / \partial y$, and x , y are the zonal and meridional coordinates, respectively.

Due to the asymmetry of the atmospheric (and oceanic) circulation, as discussed above, the southeast trade winds cross the equator and reach about lat $5-8^\circ\text{N}$, with the streamlines usually turned clockwise. This clockwise turn is equivalent to a cyclonic curvature in the southern hemisphere ($\text{rot}_z \mathbf{v}$ negative); but with the crossing of the equator and the change in the sign of f , the curvature of the flow by definition becomes anticyclonic in the northern hemisphere (Figure 5). Since the sign of vorticity is the same on both sides of the equator (see Figures 2-6 in Hantel 1972), while f in the denominator disappears at the equator ($\phi = 0$) (and is quite small in its immediate vicinity), w must be highly positive just south of the equator, indefinite at $\phi = 0$, and highly negative just north of the equator. In this case one observes a more or less permanent trend of upwelling (or downwelling) just south (or north) of the equator, together with a marked increase in water temperature when the equator is crossed from south to north.

The asymmetry of the circulation peaks in northern summer/southern winter, with a lag of 1-3 months with respect to the sun's position. As a result, the seasonal maximum of upwelling in the belt $0-4^\circ\text{S}$ occurs from June to September, i.e., at the time when the symmetry of the wind field (in relation to the equator) reaches its minimum and southerly components of the trade winds predominate. The upwelling cool water (with an average w on the order of $0.5-1$ m/d) stabilizes the atmosphere if the temperature of the sea surface T_w is less than that of the air T_A . In this case the flux of sensible heat proportional to the temperature difference $T_w - T_A$ is directed downward to the sea;

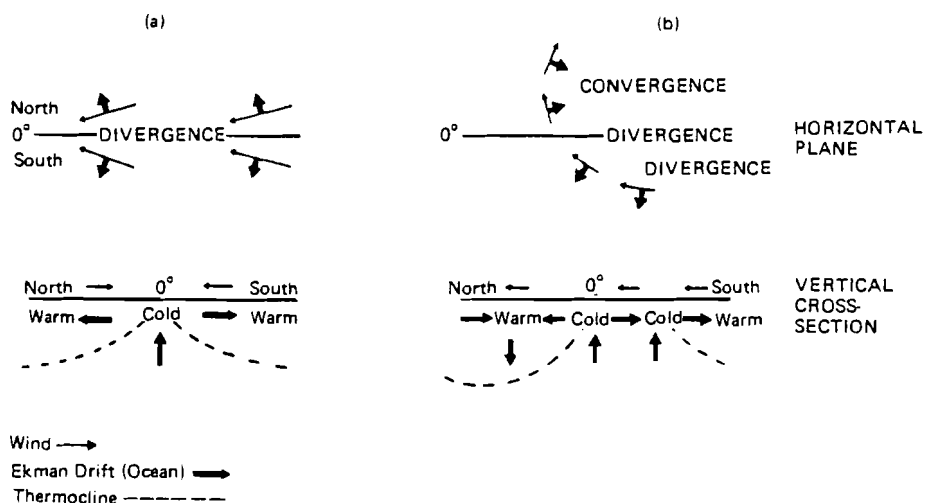


FIGURE 5 Equatorial flow patterns and upwelling for (a) the symmetric case and (b) the asymmetric case.

the relative humidity of the air increases, and evaporation (which is proportional to the vertical gradient of specific humidity at the surface of the water q_w minus the specific humidity of the air q_A) decreases sharply. Recent evaluations of maritime observations made on a meridional strip at the Galapagos (long 85–90 °W) have revealed that the average evaporation in the belt 0–3 °S decreases to 1.0 mm/d in winter (May–October) and to 0.8 mm/d in summer (November–April), compared with 2.8–3.5 mm/d in the adjacent latitudes on both sides (Trempe 1978); representative values for tropical oceans are somewhat higher (120–150 cm/yr). Similar values have been obtained from a larger data set (1953–1965) for the equatorial Atlantic (Henning and Flohn 1980).

Equatorial upwelling currently prevails in the air–sea system. However, marked changes and reversals do occur at irregular intervals, frequently during northern winter/southern summer, when the southern circulation nearly equals the intensity of the northern circulation. At such times the intertropical convergence zone (ITCZ), representing the boundary between both circulations (also called the meteorological equator), tends to be close to $\phi = 0^\circ$. Along the coasts of Ecuador and Peru, these abnormal periods coincide with the replacement of upwelling cool and nutritious water by a sterile layer of warm water. The result is a drastic reduction in the fish catch for man and seabirds. At the equator, the sign of the vertical flow component w apparently reverses, producing a downwelling trend. This anomaly usually starts around Christmas and has therefore been called *El Niño* (“the little boy”).

Recent investigations (Barnett 1977, Wyrtki 1977) have demonstrated the large variability of the winds and ocean currents, in addition to the variability

of sea surface temperature and rainfall. The average intensity of the large zonal ocean currents – which is nearly proportional to the small zonal slope of the sea level – varies by $\pm 50\%$ over the period of 12 consecutive months. Similarly, the wind stress varies on the average between $+44\%$ and -25% over similar periods and as much as $+100\%$ and -52% during particular months (Wyrtki 1977). Upwelling or downwelling is controlled by the divergence of the Ekman drift only in the central equatorial Pacific. In the Galapagos area and along the Peruvian coast, changes in the wind field over large distances ($\approx 10,000$ km) are much more effective than local variations (Barnett 1977). While upwelling coincides with high zonal winds (trade winds), downwelling occurs during periods of diminishing trade winds. An equatorial (Kelvin) wave reverses the vertical circulation in the ocean, causing the El Niño phenomenon to occur almost simultaneously between 80°W and about 160°E , i.e., over a distance of 120° longitude or approximately 13,000 km (Doberitz 1968). It is accompanied by torrential rainfall, by thermodynamic instability ($T_w > T_A$), and by lower relative humidity, which in turn causes increased evaporation. Since the correlation between sea surface temperature and rainfall is positive (and well above the 3σ level of significance; see Flohn 1972), rainfall variations are enormous and larger than anywhere else in the world. For instance, at Nauru (0.5°S , long 169°E), the rainfall during consecutive 12 month periods varies between 95 mm and over 5,000 mm (as was observed between 1916 and 1918). Irregular fluctuations suppress the usual seasonal variations.

Generally speaking, equatorial upwelling, with rainfall and evaporation at a minimum, occurs during periods of strong atmospheric circulation (today mainly controlled from the southern hemisphere); equatorial downwelling (El Niño), with high rainfall and evaporation, is coincident with periods of weak circulation. The fact that the Pacific and Atlantic are practically closed basins in equatorial latitudes leads to some complications. In past epochs with stronger or weaker zonal circulation – i.e., during some parts of the glacial (strong) and interglacial (weak) epochs – upwelling or downwelling may each have occurred more than 90% or even 100% of the time.

There is evidence that the fluctuations in water temperature T_w and thus also in evaporation were even stronger during the glacial and interglacial epochs. A permanent southerly flow like that which existed in glacial times increases upwelling, and continuously spreads cool water to both sides (Doberitz 1968 and 1969). While thermal stability ($T_w < T_A$) increases, evaporation decreases and may even be reversed to condensation (“dew”) on the cool surface of the water (with $q_w < q_A$). Conversely, in interglacial periods with distinctly weaker circulation, the tropical warm water (with temperatures of $26\text{--}27^\circ\text{C}$) may have affected the weather and climate more than 90% of the time, with high instability, evaporation, and rainfall. Since the change between upwelling and downwelling modes depends on \bar{v} , which is proportional to v^2 , relatively weak variations in atmospheric circulation can lead to enormous variations in evaporation and rainfall.

The great importance of these processes for oceanic evaporation as well as for the global water balance will be illustrated by an analysis of conditions during the peak of the last glaciation (about 24,000 to 14,000 years ago) and of the last interglacial period (about 125,000 years ago). The climate during these two epochs was almost everywhere more arid or more humid than at present. This may be tentatively interpreted in the following way. The area involved in the temperature fluctuations may have been only an equatorial ocean belt in the Pacific and Atlantic between lat 10°S and 10°N , extending over $52 \times 10^6 \text{ km}^2$. Little evidence is available for the Indian Ocean. Gardner and Hays (1976) and Prell *et al.* (1976) have evaluated T_w on the basis of a great number of ocean cores. Of particular interest is core A 180-73 located at lat 0° , long 23°W . The investigators found that 18,000 years ago, at the peak of the last glaciation, T_w in August was approximately 16°C , $7\text{--}8^{\circ}\text{C}$ colder than it is now at this location. During an earlier glacial peak 55,000 years ago, T_w dropped to about 14°C . In contrast, at the peak of the last interglacial period 125,000 years ago, T_w was approximately 26°C . (In subtropical latitudes, however, T_w has remained essentially unchanged.) February temperatures were only $1\text{--}3^{\circ}\text{C}$ cooler at the peak of the last glaciation 18,000 years ago than they are today; this indicates a strong upwelling during southern winter with an extension of the southerly circulation (due to an expansion of the Subantarctic seasonal ice).

These data, obtained for a sufficient number of ocean cores, using different biostatistical techniques, are accurate within $\pm 1\text{--}2^{\circ}\text{C}$. They indicate that the low value of evaporation E (obtained by Trempel at the Galapagos) of $0.8\text{--}1 \text{ mm/d}$ or $30\text{--}36 \text{ cm/yr}$, with $T_w = 18\text{--}19^{\circ}\text{C}$, is not exceptional; when T_w drops to 14°C , the value of E may reverse completely.

The present value of E for the area involved in temperature fluctuations, as discussed above, is about 132 cm/yr or $69 \times 10^3 \text{ km}^3/\text{yr}$ (Baumgartner and Reichel 1975). In a glacial phase, 36 cm/yr may be considered representative of this large area, yielding only $19 \times 10^3 \text{ km}^3/\text{yr}$, i.e., a regional loss of $50 \times 10^3 \text{ km}^3$, or 72%, occurs. For the global budget, one must take into account the decrease in E caused by the Arctic sea ice and extending to lat 45°N (Atlantic only). For an area of $14 \times 10^6 \text{ km}^2$, this yields a loss ranging from $E = 73 \text{ cm/yr}$ to $E = 15 \text{ cm/yr}$, or $8 \times 10^3 \text{ km}^3$. Furthermore, the drop in the global sea level by at least 100 m produces a loss in ocean area of $20 \times 10^6 \text{ km}^2$ and of $E = 12 \times 10^3 \text{ km}^3$. The expansion of the Subantarctic drift ice 600 km northward in summer and winter (Hays *et al.* 1976) and over an area of about $14 \times 10^6 \text{ km}^2$ yields a further loss in evaporation of at least $5 \times 10^3 \text{ km}^3$. One obtains altogether a loss of $50 + 12 + 8 + 5 = 75 \times 10^3 \text{ km}^3$, which is 15% of the global annual budget ($496 \times 10^3 \text{ km}^3$), or 18% of total oceanic evaporation ($425 \times 10^3 \text{ km}^3$).

In a warm interglacial phase with permanent downwelling, E may have reached 155 cm/yr or $81 \times 10^3 \text{ km}^3/\text{yr}$ (for the Pacific and the Atlantic together). Here we may take into consideration the change in the area of the

Arctic drift ice from 10^7 km² to 7×10^6 km²; this may further increase E by 2×10^3 km³. The total increase in E is then $12 + 2 = 14 \times 10^3$ km³/yr or 3% of the global evaporation. This figure may be too small, however, because continental changes have been neglected. Even more significant is the drastic change in the evaporation of equatorial oceans from about 80×10^3 km²/yr during the interglacial period to 20×10^3 km²/yr during the glacial period. This is the physical background for the nearly complete disappearance of equatorial rain forests during the glacial phases and their replacement by semihumid grasslands (see Shackleton 1977).

The equatorial ocean belt discussed above plays a key role in large-scale climatic change. J. Bjerknes (1969) has shown empirically the effects of changes in T_w in that area on worldwide atmospheric flow patterns. The circulation model developed by Rowntree (1972) also demonstrated these effects. The importance of the equatorial ocean belt has become even more evident since Bacastow (1976) and Newell (1978) showed, on the basis of records from Mauna Loa, Hawaii, and South Pole stations, that, after accounting for seasonal fluctuations, the time variations of the increase in atmospheric CO₂ are in line with the irregular change between upwelling and downwelling. Newell (1978) indicated that this correlation essentially depends on the nutrient content of the upwelling deep water; during a cool phase the photosynthesis rate in this water is high and much CO₂ is removed from the atmosphere, while during a warm phase the uptake of CO₂ by the ocean is weak. This leads to a marked positive correlation between the annual increase in atmospheric CO₂ and the sea surface temperature in the equatorial Pacific. During the 1958–1974 period, the average increase in CO₂ in the air during five downwelling years was 1.11 ppm/yr; in contrast, during five years with maximum upwelling, the average CO₂ increase was only 0.57 ppm/yr (Keeling and Bacastow 1977, data averaged from Mauna Loa and the South Pole). In the latter case, time variations in water vapor content and in the CO₂ increase rate are positively correlated. This contributes much to a better understanding of the internally coherent processes controlling the climatic variations on a 1,000-year scale during the peak of the last glacial period and the Holocene period. These variations included aridity and drastic reduction of tropical forests 18,000 years ago, together with strong cooling of equatorial (but not of subtropical) oceans; they included as well a peak in precipitation and expansion of tropical forests far into the arid zone 12,000–6,000 years ago, together with equatorial warming and weakening of the trade winds (see Shackleton 1977).

3 MAN-MADE CLIMATOGENIC PROCESSES: THE “COMBINED GREENHOUSE EFFECT” OF CARBON DIOXIDE AND ATMOSPHERIC TRACE GASES

3.1 FACTORS CONTRIBUTING TO THE GREENHOUSE EFFECT

Any analysis of the impact of an increasing “greenhouse effect” (warming of the earth’s surface and the lower layers of the atmosphere) on future climate must take into account that, in addition to CO₂ (Schneider 1975), some other, at least partially man-made, gases play an important role in creating the effect. Like CO₂, these gases absorb terrestrial radiation, particularly in the window region between 7.5 and 12 μm, just below the region of strong CO₂ absorption (12–18 μm) (Ramanathan 1975, Wang *et al.* 1976). Also involved in the greenhouse effect is water vapor, the strongest absorber of infrared radiation. The global amount of evaporation (and precipitation) has recently been estimated to be 496×10^3 km³/yr, equivalent to a water column of 973 mm/yr (Baumgartner and Reichel 1975). Man-made evaporation over land areas amounted to 1,800 km³/yr in 1965 (Lvovich 1969), and may rise to about 2,500 km³/yr by the beginning of the 1980s (Flohn 1977a). This amount is equivalent to only 0.5% of the global value, which is certainly within the limits of error. With a global warming of the atmosphere, the evaporation of the oceans will rise appreciably. This has been simulated by some of the most realistic models available (see Manabe and Wetherald 1975, Wetherald and Manabe 1975). Also, because of the importance of equatorial upwelling and downwelling for evaporation (see Chapter 2), other significant changes in the atmospheric water vapor content are to be expected. Even a slight increase in “precipitable water,” which is at present equivalent to a water column of only 25 mm, will contribute to the greenhouse effect (Manabe and Wetherald 1980).

While future increases in CO₂ concentrations have been investigated by many authors, the role of trace gases has only recently been recognized. Wang *et al.* (1976) have used a one-dimensional radiative–convective model with fixed relative humidity to study the impact of these gases. In their model the role of clouds is accounted for in two ways, by assuming a fixed cloud-top altitude (CTA) and a fixed cloud-top temperature (CTT). According to their

investigations, the combined effect of man-made trace gases is on the same order of magnitude as the effect of CO_2 . Thus any neglect of these processes would cause a serious underestimation of the total greenhouse effect. Table 2 presents data from Wang (1976) in condensed form.

As well, Table 2 contains results from a similar one-dimensional radiative-convective model describing the CO_2 -temperature relationship (Augustsson and Ramanathan 1977; also see Figure 6). In contrast to the frequently cited Manabe-Wetherald model (Manabe and Wetherald 1975), these models are one-dimensional and neglect atmospheric dynamics and transports. The radiation-cloud interaction is not included, nor is feedback between temperature and snow-ice albedo. Thus their results are only representative of low and middle latitudes; in subpolar and polar latitudes, the effect of CO_2 on the temperature must be multiplied by a factor of about 3, as recent empirical data indicate (Borzenkova *et al.* 1976). Results from the Augustsson-Ramanathan model (Figure 6) do not differ greatly from the results obtained by Manabe and Wetherald (1975). With a doubling of CO_2 , the former model yields a warming of 1.98 °C (CTA) and 3.2 °C (CTT), while the latter model yields a warming of 1.92 °C for lat 0–30° and of 2.20 °C for lat 0–50°. Figure 7 provides results from a more recent version of the Manabe-Wetherald model, showing the role of a quadrupling of the CO_2 content. The results of other recent radiation models of the CO_2 -temperature relationship are scattered around the model results described above (Schneider 1975, Bach 1978, Rowntree and Walker 1978; for a review see Ramanathan and Coakley 1978). In a recent critical examination of all existing model results, an independent Ad Hoc Study Group of the US National Research Council estimated that the most probable global warming which would result from a doubling of CO_2 is near 3 °C, with an error possibly as great as ± 1.5 °C (National Academy of Sciences 1979). Further discussion would go beyond the scope of this paper.

The first two rows in Table 2 show that both the Augustsson-Ramanathan and the Wang models agree quite highly in estimating the CO_2 greenhouse effect, assuming that temperature increases nearly linearly with CO_2 until the amount of CO_2 doubles for the first time (Figure 6). The future changes in the O_3 and H_2O content of the stratosphere, due to increasing supersonic traffic, are probably too high as calculated by the Wang model, since it is doubtful that this traffic will reach the levels assumed in the model. While infrared absorption, influenced by a decrease in O_3 and an increase in stratospheric H_2O , may produce additional warming, it is assumed here that the two effects tend to cancel out (third and fourth rows in Table 2).

One of the most important atmospheric trace gases is nitrous oxide (N_2O), produced by denitrification of fertilizers in the soil. A large increase in this gas seems unavoidable, if one considers all the complexities of the nitrogen cycle in the environment, including the atmospheric residence time of nearly 70 years (Söderlund and Svensson 1976, Hahn and Junge 1977). During the 1962–1974 period, the annual average increase in nitrogen fertilizers was as high as

TABLE 2 Infrared-absorbing trace gases and their greenhouse effect.

Constituents	Present concentration	Expected Increase in concentration(%) ^a	Greenhouse effect (° C)	
			CTA ^b	CTT ^c
CO ₂	320 ppm ^d	+100%	1.98	3.2
CO ₂	330 ppm ^d	+25%	0.53	0.79
O ₃	0.34 cm	-25%	-0.34	-0.47
H ₂ O (Stratosphere)	3 µg/g	+100%	0.65	1.03
N ₂ O	0.28 ppm ^d	+100%	0.44	0.68
CH ₄	1.6 ppm ^d	+100%	0.20	0.28
CCl ₂ F ₂ + CCl ₃ F	0.2 ppb ^e	factor of 20	0.36	0.54
CCl ₄ + CH ₃ Cl	0.6 ppb ^e	+100%	0.01	0.02
NH ₃	6 ppb ^e	+100%	0.09	0.12
C ₂ H ₄	0.2 ppb ^e	+100%	0.01	0.01
SO ₂	2 ppb ^e	+100%	0.02	0.03

^aAll the growth rates assumed in the Wang model are estimated for 2020 AD; the Augustsson-Ramanathan model is independent of time.

^bModel version in which the cloud-top altitude is held constant.

^cModel version in which the cloud-top temperature is held constant.

^dParts per million.

^eParts per billion (10⁹).

SOURCES: The CO₂ data in the first line are taken from the Augustsson-Ramanathan model (Augustsson and Ramanathan 1977); all others are taken from the Wang model (Wang *et al.* 1976).

10.7% (Pratt *et al.* 1977). Even with just a linear growth rate, one could expect an increase of 170% by the year 2000, rather than 100% as Wang assumed for 2020. Pratt estimates an increase of 200 to 450% between 1974 and 2000, while Hahn and Junge more cautiously estimate a rise of 100 to 160%. Using conservative assumptions, Hahn (1979) estimates the greenhouse effect of N₂O alone to be about 25% of that of CO₂; together with NH₃ and HNO₃, the effect of N₂O is estimated by Hahn to be about 37% of that of CO₂.

Another important atmospheric trace gas is CH₄, which is considered a conversion product of CO. Its presence is strongly correlated with the burning of fossil fuels. Finally, the contribution of chlorofluoromethanes (CFMs) to the greenhouse effect derives from their chemical inertness and thus from their long atmospheric residence time, estimated at 30–50 years. Since strong efforts are being made to prohibit the use of these substances in refrigerators, aerosol spray cans, and so on, we may expect a drastic reduction in their rate of increase in the atmosphere (from a factor of 20 to a factor of 3), and assume a linear reduction in the corresponding greenhouse effect. The greenhouse effect of all other gases is small compared to that of the gases discussed above.

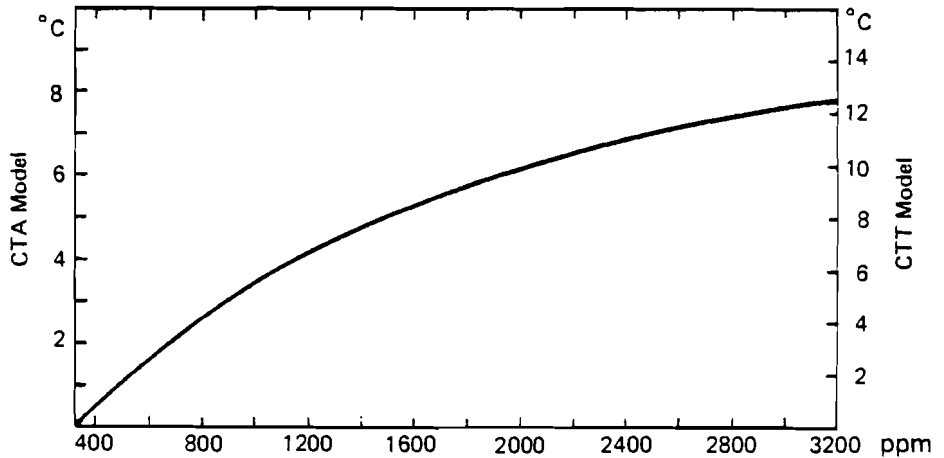


FIGURE 6 CO₂ concentrations (ppm) and increases in surface temperatures (°C) at representative middle latitudes. Results from both the CTA (fixed cloud-top altitude) and CTT (fixed cloud-top temperature) versions of the Augustsson–Ramanathan model (1977) are shown.

The selection of an appropriate model to account for the role of clouds deserves attention, since, due to our ignorance of some important parameters, we still cannot handle adequately the important cloud–radiation feedback. While Augustsson and Ramanathan prefer to hold the cloud-top altitude (CTA) constant, Wang *et al.* consider a constant cloud-top temperature (CCT) a more plausible assumption. The CTA model appears to be more consistent with the assumption of constant relative humidity. Table 2 shows that the CTA model is less sensitive to the presence of CO₂ and atmospheric trace gases than the CTT model. Though the results of the CTA model may seem somewhat more convincing at the present time, results from the CTT model should also be considered. In any case, the possible role of clouds should not be overestimated, as was argued in Chapter 1.

3.2 ESTIMATION OF THE FUTURE COMBINED GREENHOUSE EFFECT

Taking the results from Wang's model for CO₂ and using his estimated growth rates as a first order assumption, one may expect an increase in atmospheric CO₂ from 330 to 412 ppm, equivalent to a warming of 0.53 °C (CTA) or 0.79 °C (CTT). In addition, one may expect a warming of 0.81 °C (CTA) or 1.19 °C (CTT) associated with the presence of N₂O, CH₄, CFM, and other gases. This produces 150% more warming, with both the CTA and the CTT models, than would be caused by CO₂ alone. If one includes the full effects of supersonic transport (O₃ and H₂O) as calculated by Wang *et al.*, the atmosphere

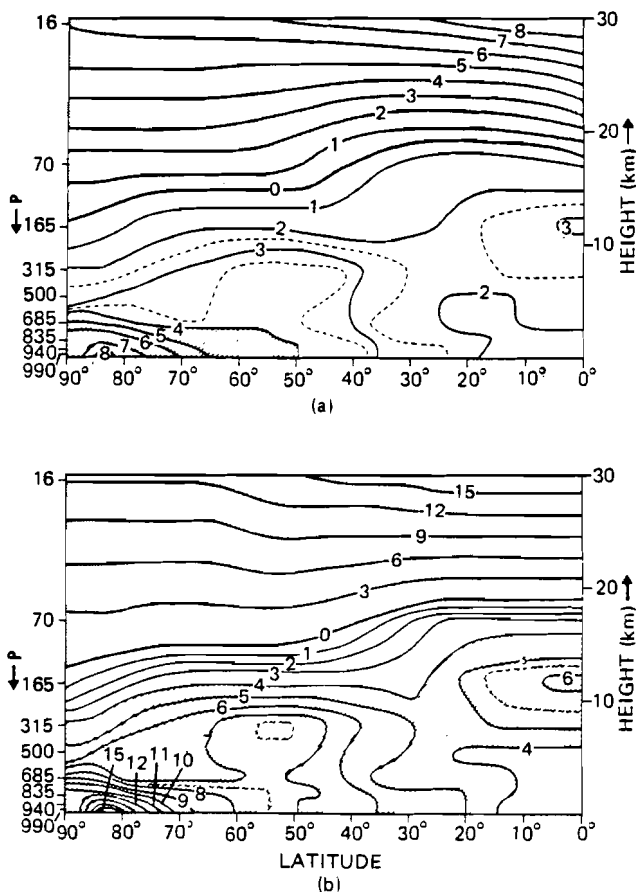


FIGURE 7 Temperature change ($^{\circ}\text{C}$) in a vertical-meridional section of the atmosphere after (a) doubling and (b) quadrupling of the CO_2 content, including atmospheric dynamics. The ocean is treated as a swamp. Note the strong warming of the lower polar atmosphere due to the snow-albedo-temperature feedback. Source: Manabe and Wetherald (1980).

would be further warmed by 0.31°C (CTA) or 0.56°C (CTT). In other words, the greenhouse effect would be 212% or 288% larger than if CO_2 alone were considered. However, this possible additional effect is disregarded in this paper, and thus the estimates given here are more likely too low than too high (see Flohn 1978c). This is especially true in view of the possible increase in water vapor discussed in Chapter 5.

Like the well-known ozone band at $9.6\ \mu\text{m}$, the atmospheric trace gases dealt with above have narrow absorption bands in the infrared window between the strong absorption bands of H_2O and CO_2 . It should be realized, however,

that two of the N_2O absorption bands are situated on the flanks of the much stronger bands of H_2O and CO_2 (at $7.78 \mu m$ and $17.0 \mu m$ respectively) (Wang *et al.* 1976, Figure 1). In view of the enormous differences in concentration among the atmospheric gases, it is necessary to further investigate the question of overlapping. According to Wang *et al.*, an additive effect can be safely assumed. The physical processes of trace gases in the window region ($7.5-12 \mu m$) are similar to those of H_2O and CO_2 on both flanks of the window; together these gases act as venetian blinds attached to the atmospheric window.

In an unpublished paper Ramanathan recently described a sophisticated radiative-convective model for estimating in detail the role of other infrared trace gases. Model results indicate that a possible increase in tropospheric O_3 may play a significant role, due to photochemical processes involving CO and CH_4 . Preliminary results from Ramanathan's model do not differ greatly from the estimates used below.

To account for the effects of the atmospheric trace gases, 50% will be added to the expected future increase in CO_2 content (i.e., to the 320 ppm base used by Wang *et al.*), and this combined greenhouse effect (CGE) will be expressed in units of virtual CO_2 concentration given in ppm. This would be equivalent to a 67% contribution of real CO_2 to the virtual CO_2 level at any given time. A less conservative approach would be to add 100% to the expected increase in CO_2 content, equivalent to only a 50% contribution of real CO_2 to the virtual CO_2 level. The right-hand columns of Table 3 give the real CO_2 value for given levels of virtual CO_2 , using the relation between the combined greenhouse effect and temperature shown above in Figure 6. Although the more conservative assumption of a 50% addition to the expected increase in CO_2 is preferred, results obtained using the assumption of a 100% addition are also presented in Table 3.*

The expected increase in atmospheric CO_2 strongly depends on the future evolution of the global CO_2 budget. A report of a working group of specialists at the Dahlem Conference (Stumm 1977) – based on various models with logistic growth curves – estimated maxima of atmospheric CO_2 concentrations at between 1,100 ppm and 1,600 ppm. At a more recent IIASA workshop (Williams 1978), participating specialists tentatively concluded that there would be a “manifold increase” in CO_2 if all economically exploitable fossil fuels were burned, and if the CO_2 growth rate could not be reduced to less than 3%. In a critical survey, Junge (1978) estimated an increase in atmospheric CO_2 by a factor of nearly 3 until the year 2050, with a further increase after this date. A rather realistic model of the global carbon cycle and the biosphere (Olson 1978) yielded a doubling of atmospheric CO_2 around 2040, and an increase by a factor of 4–6 (or even higher) by the twenty-second century. These model estimates of a possible manifold increase in atmospheric CO_2 due to fossil fuels

*In a recent lecture (Münster, March 1980), Ramanathan proposed the assumption of a 30% addition at the current time, increasing to 70% over the next 50 years.

TABLE 3 Atmospheric CO₂ content equivalent to estimated temperature differences (ΔT) during selected paleoclimatic phases.

Paleoclimatic phase	ΔT (°C) ^a	Virtual CO ₂ content ^b (ppm)		Approximate real CO ₂ content (ppm)			
		CTT ^c	CTA ^d	CTT ^c		CTA ^d	
				+100% ^e	+50% ^f	+100% ^e	+50% ^f
Current perception of warming	+0.5 ^g	365	395	342	350	360	375
Medieval warm phase	+1.0	420	490	370	386	405	432
Holocene warm phase	+1.5	475	580	398	422	450	492
Eem Inter-glacial	{ +2.0 +2.5	530	670	426	460	495	555
		590	760	455	500	540	610
Ice-free Arctic ocean	+4.0	780	1150	555	630	740	880

^aEstimated temperature increase over the current temperature.

^bUnit expressing the combined greenhouse effect stemming from real CO₂ and atmospheric trace gases.

^cVersion of the Augustsson–Ramanathan model in which cloud-top temperature is held constant.

^dVersion of the Augustsson–Ramanathan model in which cloud-top altitude is held constant.

^eAssuming a 100% contribution of trace gases to the expected increase in virtual CO₂.

^fAssuming a 50% contribution of trace gases to the expected increase in virtual CO₂.

^gBased on the current CO₂ concentration of 330 ppm.

SOURCE: The data presented in this table are based on results from the Augustsson–Ramanathan model (Augustsson and Ramanathan 1977).

would remain unchanged, if the net contribution of the biosphere to the CO₂ budget would indeed remain small. This important point has been made independently by many specialists at recent conferences (i.e., presentations made by B. Bolin, W.S. Broecker, C.D. Keeling, H. Oeschger, and others at the Conference on Energy and Climate, Münster/Westfallen, March 1980).

In respect to the future evolution of the global CO₂ budget, a very controversial question is the role of the widespread destruction of existing virgin forests – 110,000 km²/yr according to FAO statistics (see Polunin 1980). This destruction is another source of increases in atmospheric CO₂.

In light of the findings discussed above, it is clear that a scenario of future climatic evolution for the case of man-made global warming should be based on the role of the combined greenhouse effect – described in terms of atmospheric CO₂ content – with respect to temperature. In Table 3, best estimates of temperature differences (ΔT) during selected paleoclimatic stages are given, based on all available data (without regard to unknown geophysical causes); these estimates are then converted into equivalent threshold values of CO₂ with the aid of the Augustsson–Ramanathan model (see Figure 6). In this way

past climatic stages can be used as scenarios for possible future climate modifications.

Results from the CTA version of the Augustsson–Ramanathan model, as well as from the more sensitive CTT version, are presented in Table 3. The first threshold that may be selected is the level of warming that can be unambiguously derived from current data sources. This “level of perception” of a quasi-global warming is estimated at 0.4–0.5 °C. Looking at results from the CTA version and the last two columns in Table 3, one finds a corresponding real CO₂ level of 360–375 ppm.

The other threshold values shown in Table 3 are estimates of representative temperature changes over land areas during some selected paleoclimatic stages, such as the early Middle Ages (about 900–1100 AD), the Postglacial (Holocene) Optimum (about 6,500–5,500 years ago), and the Eem stage of the last Interglacial.

Considering possible consequences, one of the most important questions is, When will these combined greenhouse effect thresholds occur? The answer depends heavily on developments and decisions in the fields of economics and politics in a pluralistic society – events far outside the author’s field of expertise. Only a first-order estimate, based on a logistic growth rate model, can be tentatively given. Figure 8 gives a time scale for the expected temperature levels derived from the CTA version of the Augustsson–Ramanathan model, shown previously in Figure 6. (The curves labeled temperature in Figure 8 are in fact curves of virtual CO₂ content.) Figure 8 is also based on the combined greenhouse effect and the logistic CO₂ growth rate model developed by Zimen (1977a, 1977b). Zimen’s model is based on the assumption that the biosphere does not act as a CO₂ source and that the airborne fraction of CO₂ (presently 53–56%) remains constant. Assuming that recent CO₂ growth rates of 3.5–4% per year continue, the 0.4–0.5 °C “level of perception” of a quasi-global warming will be reached between 1990 and 2000. Under the same assumption the CTT model would yield a date between 1985 and 1990.

Assuming a logistic growth rate between 3 and 4%, the 1.5 °C threshold (equivalent to the Holocene warm period) could be reached between 2005 and 2030, and the 2.5 °C threshold (equivalent to the Eem period) between 2020 and 2050. Figure 8 also contains estimates based on the apparently unrealistic growth rates of 1–2%; on the basis of these rates any immediate climatic risk appears to be avoidable. Several processes contribute to the uncertainty of the time scale: on one hand, the airborne fraction of CO₂ should increase with time, due to the increasing CO₂ content and acidification of the oceanic mixed layer; on the other hand, the thermal inertia caused by the storage capacity of the ocean may be responsible for a time-lag of an equilibrium temperature of several years or even decades. Thus for present purposes, it seems more appropriate to label the stages of the scenario using approximately equivalent levels of virtual CO₂ instead of fixed calendar years.

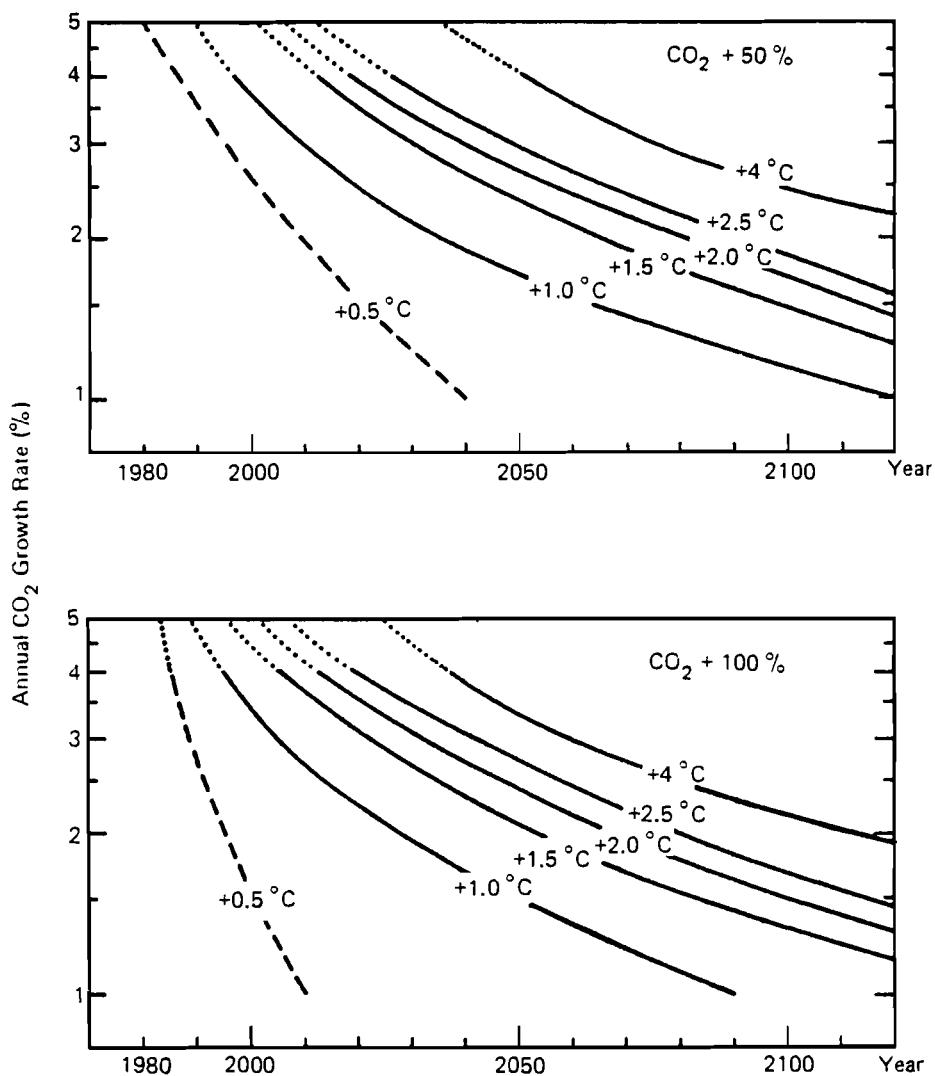


FIGURE 8 Extrapolation of the combined greenhouse effect to the year 2120 using logistic CO₂ growth rates. In the upper graph the contribution of trace gases to the combined greenhouse effect is taken into account by adding 50% to the estimated CO₂ level; in the lower graph the contribution of trace gases is taken into account by adding 100% to the estimated CO₂ level. The logistic CO₂ growth rates are taken from Zimen (1977a), and the temperature values are taken from Figure 7 of this paper.

4 RECENT CLIMATIC HISTORY AND THE PERCEPTION OF A GLOBAL WARMING

At the present time, global or hemispheric variations in surface temperature T_a can be detected only with the help of an existing network of climate stations situated almost exclusively on the continents and on a number of islands. This network has many gaps, especially in oceanic regions where the small number of stationary weather ships has been reduced drastically since 1973. The unevenly distributed stations are not sufficiently representative to account for the large irregular anomalies occurring over months, seasons, and years — a lot of noise is due only to the inadequacy of the station network. Thus interannual hemispheric temperature variations on the order of 0.2–0.3 °C can be hardly distinguished from noise.

Several papers provide an overview of the most recent temperature fluctuations. Yamamoto *et al.* (1975) have presented monthly data on T_a from 343 stations on the northern hemisphere for the period 1951–1973. They objectively analyzed the data with a cubic spline technique using moving three-month averages. Typically the most striking variations occurred in the latitude belt 60–85 °N; a significant reduction in temperature occurred after a volcanic eruption, with time delays on the order of 3 to 12 months. The effect of stratospheric dust of volcanic origin has also been analyzed with a much longer data series by Oliver (1976) and Mass and Schneider (1977). Yamamoto *et al.* (1977) have also extended their analysis to 431 stations, including some in the southern hemisphere, using time-series data for the 1957–1972 period. Still longer series of annual averages have been analyzed by Borzenkova *et al.* (1976) for several latitudinal bands between 82.5 °N and 17.5 °N, including the meridional gradient in the belt between 75 and 25 °N. The interannual fluctuations are large, especially in Subarctic and Arctic latitudes. For example, such fluctuations amounted to 0.5 °C in the belt between 57.5 and 72.5 °N, and to 0.63 °C in the polar belt between 72.5 and 87.5 °N, both in the 1940–1975 period. The hemispheric average reached a maximum around 1938, dropped approximately 0.5 °C by about 1963, and has been rising slightly since then, especially at the polar cap.

In high southern latitudes the period since 1943 has been characterized by a weak warming trend (Damon and Kunen 1976, Yamamoto *et al.* 1977). Records kept over long periods in the Subantarctic (Limbert 1974) and New Zealand (Salinger and Gunn 1975) indicate the same trend. The equatorial belt has undergone only short-lived fluctuations. According to a quite recent synthesis presented by nine investigators from the USA, Japan, and the FRG (Kukla *et al.* 1977b), interannual fluctuations explain most of the variance observed, and occur over most of the northern hemisphere and over parts of the southern hemisphere. The long-term trends are significantly weaker – i.e., on the order of 0.01–0.02 °C per year (also see Walsh 1977) – than the interannual fluctuations. This noise apparently demonstrates the role of internal feedback mechanisms within the climatic system and of short-lived external effects, such as volcanic events. These data do *not* show a reversal in the cooling trend of the last decades, especially not in the temperature of the upper air; only the surface temperature data from the Arctic and Subantarctic show an increase or remain more or less constant.

A comparison of these findings indicates the great difficulty in obtaining representative data on current temperature changes. This is especially true for the Arctic region, where the Asiatic and American sectors can have quite opposite trends (Walsh 1977); this indicates a longitudinal displacement of the center of the polar cold vortex, as is demonstrated by averages for the tropospheric layers (e.g., 500/1000 mbar).

Since all climatic variations are subject to large longitudinal changes which can frequently mask the latitudinal changes, it is preferable to use maps (van Loon and Williams 1976, 1977) and/or empirical orthogonal functions (Walsh 1977) for an adequate description of climatic change, at least for parameters such as pressure, geopotential, or temperature. A good example of climatic variability dependent on longitude is the Greenland/NW Europe seesaw (van Loon and Rogers 1978), which has been known for more than two centuries. Similar cases probably also occur in other areas because of the quasi-stationary behavior of the long waves of the atmospheric westerlies.

Unfortunately, most investigations have concentrated on temperature changes, and little is known about large-scale rainfall patterns, which have perhaps the greatest impact on economy and society. Here records from single stations often are unrepresentative and inhomogeneous. The use of areal averages is meaningful only if the available data are internally coherent. This is often not the case because of the rather rapidly diminishing spatial correlations, such as in the Mediterranean. Recent evaluations have demonstrated the role of the longitudinally-oriented Walker circulation in the tropics (Bjerknes 1969, Doberitz 1969, Flohn and Fleer 1975, Hastenrath 1976, 1977).* This circulation today is responsible for a seesaw correlation between equatorial

*The Walker circulation was so named by J. Bjerknes in 1969; it was originally called the Southern Oscillation by Sir Gilbert Walker in the 1920s. An index for the Walker circulation has been given by Wright (1975).

upwelling and downwelling in the Atlantic and in the Pacific (Doberitz 1969; see also Chapter 2 of this report). This is similar to the seesaw between the Pacific and Indonesia with the Indian Ocean, as was outlined by Walker and his successors (Berlage 1957, 1966). For a review of the numerous investigations in this context, see Wright (1977).

The recent *cooling* of the northern hemisphere, starting about 1940, has been on the order of -0.3 or -0.4 °C; this is apparently contradictory to the hypothesis of man-made *warming*. But note that the temperature trend in middle and high southern latitudes has at the same time reversed. One interpretation has been given by Damon and Kunen (1976), who consider the development in the southern hemisphere to represent the true CO₂ warming trend. This trend is masked in the northern hemisphere by cooling, due to man-made particles and volcanic eruptions. Both explanations are not very convincing; in particular the latter is brought into question by the recent occurrence of volcanic eruptions in the tropics south of the meteorological equator (Bali, 1963; Galapagos, 1968). Another possible interpretation is that the natural cooling of the northern hemisphere – probably partly due to volcanic activity, which was at a minimum between 1912 and 1948 – would have reached -0.6 °C, without the assumed warming due to CO₂ and equivalent to about $+0.2$ °C. Because of the high interannual variability, this argument cannot be verified. A look at past climatic data indicates a variation of ± 0.5 – 0.6 °C around a moving 100-year average during the last centuries; this is a reasonable limit for natural fluctuations. In the northern hemisphere, such a warming can be observed on the basis of 5-year or 10-year averages; this is above the noise level produced by interannual variability.

There are some signs (see Kukla *et al.* 1977b) that the post-1945 cooling has already passed its climax. Since about 1974 the polar region has not been as extremely cold as it was between 1964 and 1972, when the Arctic ice was progressing toward Iceland and Newfoundland (see Figure 9). The years 1978 and 1979 still do not show an upward trend; indeed, for the polar cap (65–90 °N), 1979 is the coldest year. Other evidence can be found in the monthly surface temperature maps *Grosswetterlagen Europas* issued by the FRG Weather Service (also see Walsh 1977 and Walsh and Johnson 1979). The opposite trend in high latitudes of both hemispheres and the small changes observed in low latitudes indicate that the cooling of the Arctic between 1940 and 1970 was *not* a global phenomenon. If future man-made warming is superimposed on the natural fluctuations occurring at irregular intervals over several decades, it should intensify the natural warming episodes and weaken (or even reverse) the natural cooling episodes. A warming of about 0.5 °C above the noise level, maintained for a period of about ten years, would coincide with the expected tendency. Only this might be a sufficiently convincing argument to override scientific scepticism. Using an objective procedure (based on records from 12 stations along 60 °N), Madden and Ramanathan (1980) have shown that at present no convincing sign of a CO₂-induced warming can be detected. This may result from other

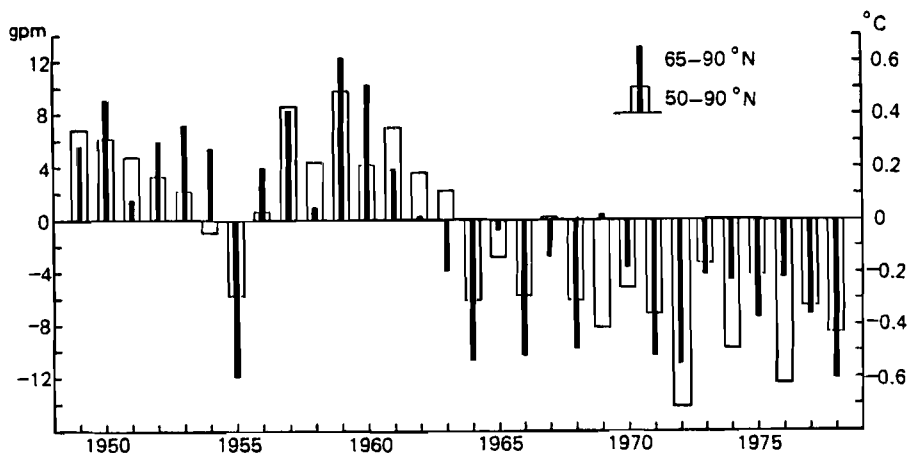


FIGURE 9 Deviations of the average annual temperature of the 500/1000 mbar layer above the polar caps from the 1949–1973 average, 65–90 °N and 50–90 °N. Gpm stands for geopotential meters. Source: Dronia (1974) with amendments provided by the author.

(natural or man-made) climatogenic effects and/or from failure to consider thermal ocean inertia. It is also not clear whether all short-lived fluctuations are of a deterministic or a stochastic nature. An interesting attempt to outline possible CO₂-induced climatic change until the year 2000 has been made by Wigley *et al.* (1980), comparing the 5 warmest and 5 coldest years during the last 50 years.

The evidence presented above thus suggests that a *global warming of 0.5 °C* can be assumed to be a reasonable threshold for a general perception of warming – even if it may still be impossible to distinguish quantitatively between the contributions of natural versus anthropogenic processes. Beginning about 1990, a repetition of some climatic patterns of the 1931–1960 reference period (to avoid the misleading term “normal”) can be expected; this reference period was one of the warmest periods during the last 500 years, and was also characterized by a relatively low interannual variability in some regions (such as India), but not in western and central Europe, where severe winters and exceptional wet or dry summers were observed in the 1940s (see, for example, Ratcliffe *et al.* 1978).

A more general notion of recent short-lived climatic fluctuations can be obtained from the monthly maps of the 500/1000 mbar layer for large areas of the northern hemisphere, published in *Grosswetterlagen Europas* since 1949, as mentioned above; the thickness of this layer is proportional to the temperature, and represents the average temperature of the lower half of the atmospheric mass ($\approx 0\text{--}5$ km).

Figure 9 (updated after Dronia 1974) gives the deviation of area averages from a 25-year average (1949–1973) for the polar cap 65–90 °N and for lat 50–90 °N for each calendar year. This procedure suppresses all longitude-dependent variations. In the 500/1000 mbar layer, the systematic deviations of the individual radiosondes are generally below 0.5 °C and can be neglected, at least in the case of area averages. The year-to-year variations are still relatively large. A good example is the year 1955, when a great anomaly centered in the Pacific. The marked cooling during 1962–1964 cannot be interpreted as having been caused by the Agung eruption in Bali in early March 1963, although this event probably contributed to the cooling. Since 1963 the average temperature of the lower troposphere in polar latitudes has remained a few tenths of a degree cooler than it was before. A worldwide comparison for the years 1958–1976, based on 63 evenly spaced radiosonde stations (Angell and Korshover 1978), has verified a warming trend in high southern latitudes, indicating a cooling in northern and southern temperature latitudes, as well as increasing temporal variability in the tropics. In all latitude belts, 1976 was one of the coldest years on record.

In addition to such temperature data, it is necessary to obtain in the near future continuous records of some integrating parameters, such as the extension of sea ice at the end of the melting season in the northern and southern hemispheres (in August or late February, respectively). This is especially important for the North Atlantic sector where the greatest fluctuations are to be expected. The Commission on Snow and Ice of the International Union of Geophysics and Geodesy (IUGG) collects data for many mountains on glacier variations. For our purposes the extended permanent ice fields and snowbeds in high latitudes are of paramount interest, rather than valley glaciers in alpine mountains that, in quite a number of cases, only respond to local conditions. The variations in the size of glaciers at the end of the melting period should be monitored, including the relative area of snowbeds in the partly unglaciated Queen Elizabeth Islands (Canadian Archipelago) and in similar islands in the Siberian sector of the Arctic.

Special mention should be made of the following ice fields (Hattersley-Smith 1974): Iceland–Vatnajökull, Hofsjökull, Langjökull (partly controlled by volcanic and geothermal activity), Drangajökull (NW); Baffin Island–Penny Ice Cap (66–67 °N), Barnes Ice Cap (70 °N); Devon Island–field at 75 °N; Axel Heiberg Island–field at 79–81 °N, (studied since 1959); Norway–Folgefonn (60 °N), Hardangerjökull, Jostedal Breen, Svartisen (67 °N); Svalbard–Edge Island, Nordaustlandet; and Severnaja Zemlja–field at 78–81 °N. In the southern hemisphere, the large Patagonian ice field situated at lat 48–50 °S should also be mentioned (Schwerdtfeger 1956, 1958).

A continuous evaluation of the snow-covered land area based on satellite data (Kukla *et al.* 1977b) is also necessary. According to recent experience (1971–1972), the early appearance of a continuous snow cover in the autumn is of great importance for the evolution of cold-season surface temperatures on boreal continents.

5 EXAMINATION OF PAST CLIMATES AS A BASIS FOR A GLOBAL WARMING SCENARIO

5.1 MEDIEVAL WARMING

According to the wealth of evidence collected by Lamb [1977a (see especially Chapters 13 and 17), 1979] the early Middle Ages represent the warmest period of the last millennium. The temporal peak of this warm period differs slightly between areas (Dansgaard *et al.* 1975, Alexandre 1977, Wigley 1977). The most remarkable period was between about 900 and 1050. It was characterized by unusually warm and hospitable conditions in Arctic latitudes. (Barry *et al.* 1977), with a disappearance of sea ice in the East Greenland Current, cereal cultivation in Iceland and Norway up to 65 °N (and even experimentally in Greenland), and Eskimo settlements as far north as Ellesmere Land and the New Siberian Islands.

During this period, forests in Canada advanced up to 100 km north of the present timberline, simultaneously with an upward shift of the tree line in many European mountains. This indicates a temperature increase of around +1 °C, compared with average temperatures between approximately 1916 and 1950 (Table 4). Frequent droughts occurred all over Europe south of 60 °N. The Caspian Sea stood at -32 m, i.e., lower than today's level, after losing much water for irrigation. (This sea subsequently rose 12 m by the 14th century.) In the Mediterranean region, the Dead Sea was nearly as low as it is now (Klein 1977), but the northern part of the Sahara was definitely wetter. Crossing the desert by horse caravan has been reported for that time (Nicholson 1980), and the end of earlier cattle rearing around the Kufra oasis (now near the center of aridity) has also been traced to this period. China and Japan had warm summers (Chu 1973, Yoshino 1978), but severe winters in China, with freezing of the lakes near the banks of the Yangtse Kiang River, have been reported.

In North America, there is evidence of large cultivated areas and a remarkable urban center in Illinois and Iowa (Bryson and Murray 1977). Tree ring data from California mountains also indicate higher temperatures but low

TABLE 4 Estimated climate parameters for Central England during selected periods.

Climatic Periods	Temperature (°C)			Rainfall		Annual Evaporation ^b	Annual Runoff ^b
	Annual average	July–Aug.	Dec.–Feb.	Annual	July–Aug.		
“Atlantic” ^c (6,000 yrs ago)	10.7	17.8	5.2	110–115 ^a	– ^e	108–114 ^a	112–116 ^a
Little Optimum ^d (1150–1300 AD)	10.2	16.3	4.2	103 ^a	85 ^a	104 ^a	102 ^a
Little Ice Age (1550–1700 AD)	8.8	15.3	3.2	93 ^a	103 ^a	94 ^a	92 ^a
Recent warm period (1916–1950 AD)	9.4	15.8	4.2	932 mm		497 mm	435 mm

^aPercent of 1916–1950 average.

^bCalculated according to Turc’s formula.

^cHolocene warm period.

^dData probably also valid for 900–1050 AD.

^eNo evidence available.

SOURCE: Lamb (1977).

rainfall, similar to southwest Colorado. Evidence from the tropics is very scanty. Rains concentrated in the southern part of Ethiopia (Nicholson 1976), while Nile floods were low and Lake Turkana was high. No data are available for India. Long-lasting warming on the Antarctic coast, together with a period of marked drought and forest fires in New Zealand, has been reported.

One interpretation of these data (Lamb 1977a) suggests a northward shift of the cyclone track by 3–5° latitude to 60–65°N and high pressure conditions over Europe, similar to the warmest and driest summers of the 1931–1960 period; in winter, a similar pattern occurred during this period in the north, which has frequently been related to a “blocking” pattern with severe winters and extended droughts, especially in eastern Europe. Such a pattern would be consistent with the marked retreat of ice from the Greenland seas during the early Middle Ages. Since the speed of the East Greenland Current is higher than the melting time of ice floes, a retreat of the Atlantic drift ice to latitudes north of 80°N is indicated. Cooling in northern Greenland after 1160 (Dansgaard 1975) coincides with a marked advance of glaciers in the Alps and other mountain ranges, and with a reappearance of Arctic sea ice around 1320. Extreme climatic anomalies and severe famines also occurred throughout Europe and a long drought period (200 years) affected Iowa and Illinois, leading to mass emigration from these areas (Bryson and Murray 1977).

This wave of anomalies announced, after several interruptions, the transition towards the Little Ice Age (1550–1850).

5.2 THE HOLOCENE WARM PERIOD AND THE HUMID SAHARA

The history of the retreat of the melting ice domes of North America and northern Europe after the peak of the last ice age 18,000 years ago is fairly well known (see Lamb 1977a, Chapter 16). While the smaller Scandinavian ice sheet finally disappeared more than 8,000 years ago (Figure 10), the North American ice sheet still covered about 50% of its former area at that time (Figure 11), disintegrating after a catastrophic incursion of the sea into Hudson Bay, probably about 7,800–7,600 years ago (Hughes 1977). Separate ice sheets remained; the Labrador ice did not disappear until about 4,500 years ago, while some ice fields of about 35,000 km² in interior Baffin Island have apparently survived until today. This created a marked longitudinal asymmetry of the atmospheric circulation between 8,000 and 6,500 years ago (Lamb 1977a), which faded out 4,500 years ago. During this episode, Eurasia and Africa experienced the warmest epoch of the last 75,000 years, but eastern North America remained relatively cool, especially in summer, with frequent outbreaks of polar air. This caused a predominance of southwesterly winds over the Atlantic, probably producing an intensification of the Gulf Stream and its northward-flowing branches. In winter, the frequent occurrence of anticyclonic ridges at long 0–20 °W would be consistent with frequent outbreaks of polar air also over central and eastern Europe, extending with copious precipitation to the Mediterranean Sea and northern Africa.

The present description of the climate during the Holocene warm period refers mainly to the peak of the epoch, around 6,000 years ago. Data are given here in radiocarbon years; their conversion into calendar years, with a possible difference of up to 12%, appears to be a matter of controversy. Insufficient time resolution of the data available does not yet allow treatment of the existing fluctuations on a 100-year or even a 500-year scale.

During the peak of the Holocene period, forests in western Canada and in western Siberia extended 200–300 km farther north than they do today. The summer temperature has been estimated to have been 2–3 °C higher than at present. Subarctic forests also covered the northernmost islands of Norway and the whole of the Taimyr peninsula. This warm period, however, came to an end around 4,800 years ago, when, because of a polar outbreak lasting no longer than about 200 years, the Canadian timberline moved more than 300 km south (Nichols 1975). Almost simultaneously with this relatively brief event, important climatic shifts towards a “neoglacial” climate – similar to the Little Ice Age between 1550 and 1850 AD – occurred in many areas, together with a gradual desiccation of the present Arid Belt.

At the peak of the warm period the waters of the Kuroshio, between Taiwan and Japan, were up to 6 °C warmer than now (Taira 1975). With some

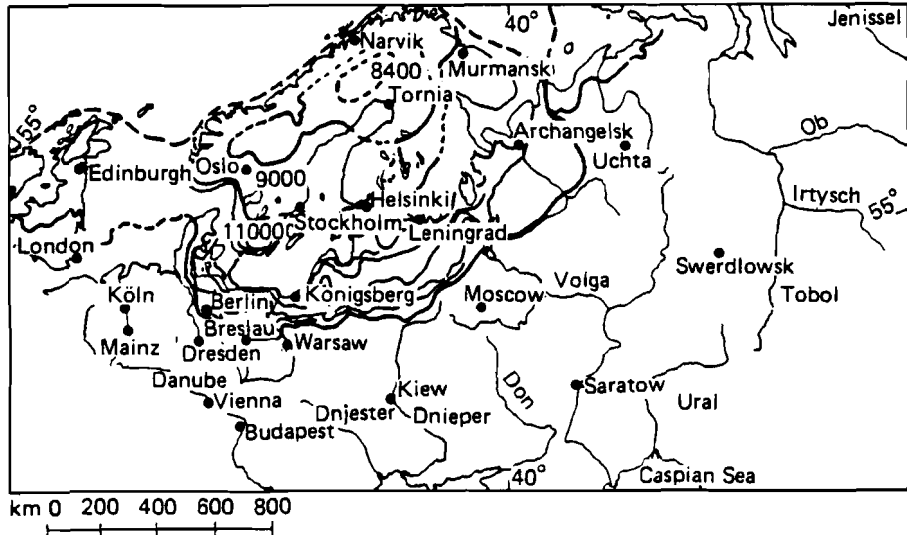


FIGURE 10 European ice margins during the last glaciation, 18,000–8,000 years ago. The map is based on Woldstedt (1969).

delay, the interior Arctic experienced its warmest level during the Holocene period about 4,500 years ago; open waters flowed in the fjords and along the northern coasts of Spitzbergen, Greenland, and Ellesmere Island, allowing Siberian driftwood to reach these coasts up to lat 83°N (Vasari *et al.* 1972, Barry 1977). However, there is no indication that the core of the present Arctic drift ice between Greenland, Alaska, and eastern Siberia disappeared during the Holocene warm period. Regarding the sea level, only conflicting evidence is available for a worldwide rise of a few meters at the time; this question will be considered in the following chapter of this report.

In the Subantarctic ocean, the very rapid shrinking of the mainly seasonal Antarctic drift ice led to a warming peak as early as 9,000 years ago (Hays 1978). Similarly, the Holocene warm period had already started more than 7,000 years ago (Starkel 1977) in eastern Siberia, an area in which no major ice sheets had formed during the previous glaciation. At Lake Biwa in central Japan, the warm period was initiated over 8,000 years ago (Fuji 1976). The transition between the glacial and interglacial (Holocene) modes of the atmospheric–oceanic circulation was very complex, superimposed by a series of abrupt changes between cold and warm phases (i.e., Bölling, Alleröd phases: see Lamb 1977a) between about 13,500 and 10,800 years ago. At the end of this period, the tropical oceans became slightly warmer than they are now; this was probably accompanied by a substantial weakening of the tropical (Hadley) circulation. Increasing evaporation raised the water vapor content of the tropical air, leading to a rapid expansion of the tropical rainbelt and

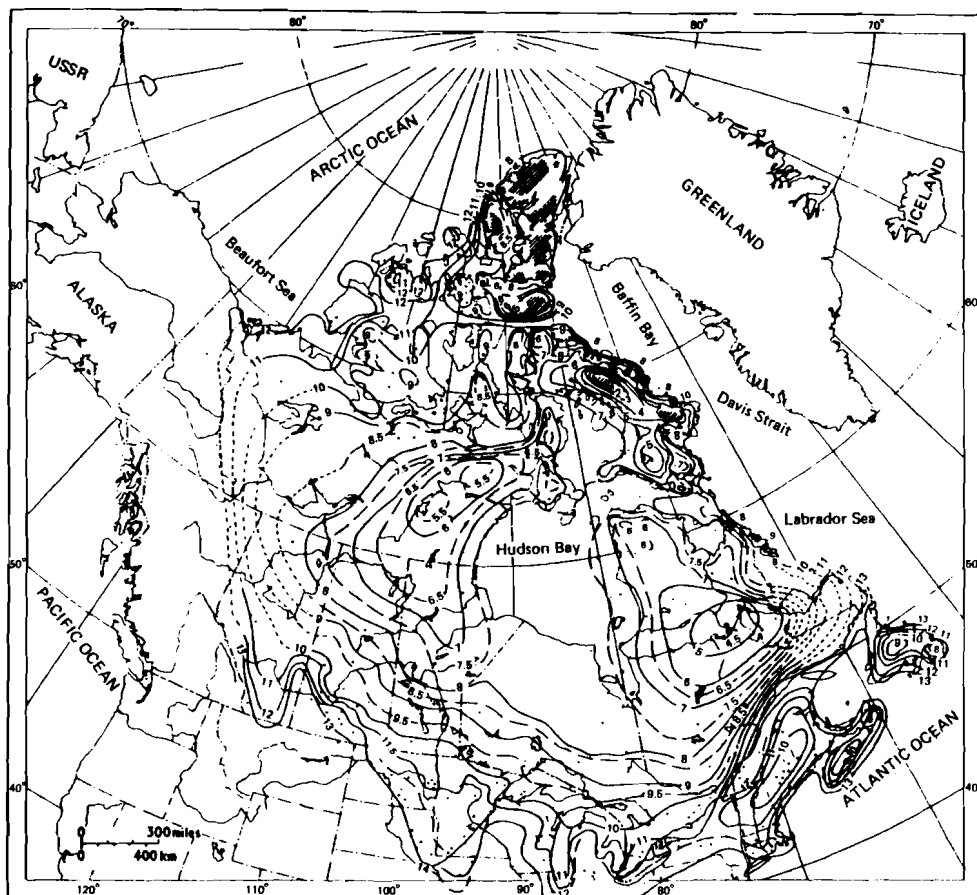


FIGURE 11 Isochrones of the withdrawal of the North American (Laurentide) ice sheet. The numbers in the body of the map are dates expressed in 10^3 years before the present time. Dots show where radiocarbon dates have been established. Moraines, coastlines, and all other available evidence have been used. Source: Bryson *et al.* (1969), reprinted in Lamb 1977a.

rain forests (which had been drastically reduced during the previous ice age) towards higher latitudes (Rognon and Williams 1977, Shackleton 1977).

For England and Wales, Lamb has given estimates of the basic climatic parameters, including those representing other climatic stages of interest (see Table 4). On the mid-latitude oceanic coasts the probable temperature increase was $1.5-2^{\circ}\text{C}$.

In other continental areas the increase was lower, at least in northeastern North America. In the area between 85° and 95°W , a triangle of prairie vegetation extended into Wisconsin and Illinois, reaching a maximum about 7,000 years ago (Bernabo and Webb 1977). Together with some areas in southwest Siberia

and in eastern Turkey, this is one of the few areas that was drier during the Holocene period than it is now. The occurrence of thermophilous species in European and Asiatic forests (Frenzel 1967, 1968a, 1968b) indicated somewhat higher temperatures and rainfall. Permafrost in eastern Siberia retreated several hundred kilometers north of its present position; a similar retreat in Canada and Alaska can be assumed because of the northward extension of the vegetation lines. In the mountains the upper tree line shifted upward by 100–150 m, which indicates a warming of nearly 1 °C compared to current temperatures.

In subtropical latitudes, the present arid areas enjoyed wetter conditions during the Holocene warm period. Since everywhere the temperature was higher or similar to today's temperature, this humid climatic phase (Sarnthein 1978) must have been related to higher precipitation and caused by higher evaporation of the tropical oceans (see the discussion in Chapter 2 of this report on equatorial upwelling, El Niño, and the hydrologic balance). This was probably correlated with a weakening of the subtropical anticyclones and the trade winds. In this connection, there is evidence of a correlation between a prolonged warm and humid period and a weakening of the coastal oceanic flow (with upwelling) in California earlier than 5,400 years ago (Pisias 1979).

Perhaps the most surprising feature of the Holocene warm period is the recently established occurrence of a marked humid period in the Sahara, as well as in the deserts of the Middle East (Nicholson 1976, Williams and Faure 1980). Since parts of this humid phase occurred simultaneously on both flanks of the desert, the model of a parallel shift of climatic zones towards north or south, as the seasonal variations suggest, cannot be considered applicable in all cases. Evidence based on current data supports the idea of a tendency towards synchronous shrinking or expansion of the Arid Belt on *both* flanks. (On a much shorter time scale, Nicholson (1980) found this tendency in the 16th and 19th centuries, together with a prolonged rainy summer season.) During the first phase of this moist period – between about 11,000 and 8,000 years ago (see Figure 12) – tropical rains expanded northward. Mediterranean rains, under the influence of the dwindling northern ice sheets, still dominated along the northern margins, with frequent outbreaks of cold air occurring even during summer (Flohn and Nicholson 1980). Marked troughs in the high tropospheric layer, extending diagonally across the Sahara, could have induced tropical disturbances; these in turn could have crossed the arid zone as “Sahara depressions,” initiating more frequent rains even in the central belt between lat 21° and 26° N, as shown in Figure 13 (Flohn 1971). Lake Mega-Chad stood about 40 m higher, with an area of nearly 320,000 km² (comparable to the present Caspian Sea). During the peaks of the Holocene period this lake had an outlet to the Benué–Niger catchment. The onset of the Holocene rainfall caused the sedimentation rate in the sea off the Niger delta to increase by a factor of 20 (Pastouret *et al.* 1978). Similarly, Lake Turkana (formerly Lake Rudolf) emptied into the White Nile catchment (Butzer *et al.* 1972). Even in

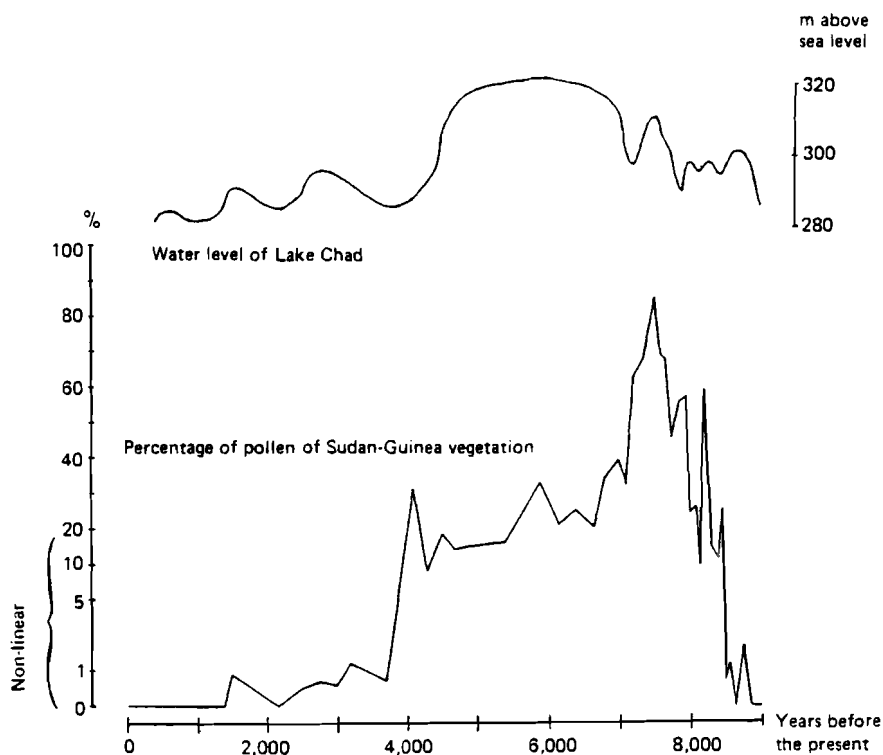


FIGURE 12 Upper curve: water level of Lake Chad (Mega-Chad) during the Holocene period. Lower curve: percentage of pollen in Sudan–Guinea vegetation over time during the Holocene period, representing the contribution of tropical rainfall to the total amount of rainfall. This vegetation may represent an area with an annual rainfall of 80–120 cm. The time scale 8,000 and more years before the present may be too compressed, possibly due to errors in C_{14} -dating. The upper curve is after Servant (1973) and the lower curve is based on Maley (1977a and 1977b).

the now hyperarid center of the Sahara between the Kufra Oasis and the Tibesti Mountains – which today has less than 5 mm of rain per year – permanent rivers were flowing (Pachur 1975), indicating at least 200 mm, and more probably 300–400 mm, of rainfall per year. The grasslands in this area were utilized by many groups of cattle-raising nomads (Gabriel 1977).

Similar evidence has been found throughout the Arid Belt of the Old World between Mauretania (long 17°W) and Rajasthan (long 77°E), including the Afar–Danakil depression and the Arabian interior. At the margin of the Tharr desert in India (which now has an average annual rainfall of about 250 mm) rainfall increased to values of 500–800 mm during a long moist period between about 10,500 and 3,600 years ago (Singh *et al.* 1974, Bryson and Murray

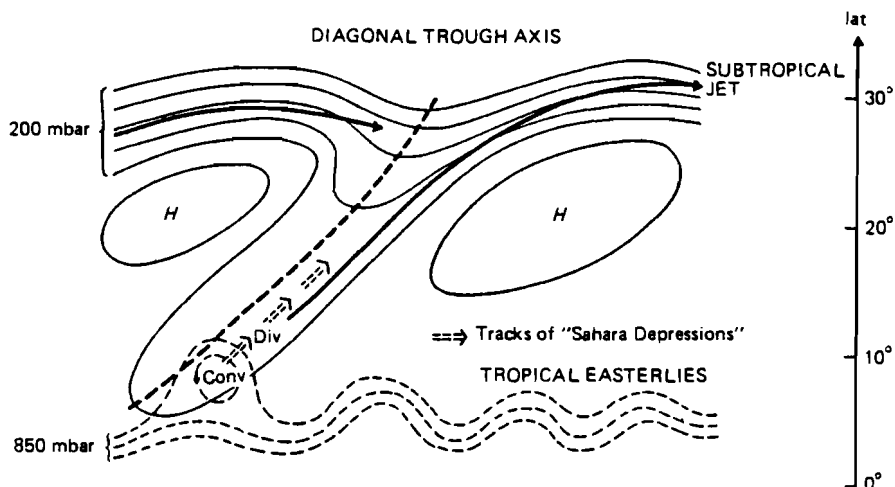


FIGURE 13 Interaction between “diagonal” upper troughs in the subtropical westerlies (200 mbar or ≈ 12 km) and tropical easterlies with traveling vortices (850 mbar or ≈ 1.5 km). Coincident low convergent (CONV) and upper divergent (DIV) motions produce “Sahara depressions”; these move in a northeast direction ahead of the upper trough, which is visible from satellites as an elongated cloud band. Source: Flohn 1971.

1977). This temporal variation in rainfall is shown in Figure 14. The individual fluctuations may be uncertain, as well as the dates for the beginning and the end of the moist period; still, the occurrence of a long moist period at this time agrees well with evidence from more than 30 other spots lying more than 8,000 km apart [*cf.* the summary review by Rognon and Williams (1977)]. Here again, both monsoonal summer rains and extratropical winter rains increased, overlapping in many parts of the Arid Belt.

Throughout the area of the present Arid Belt, gradual desiccation set in about 5,500 years ago, interrupted by relatively wetter periods. It seems noteworthy that according to most recent data, the early high civilizations (the Old Empire of Egypt from the first to the fourth dynasties, the Near East urban centers between Jericho and Ur, the Indus culture) started at the end of this relatively wet period, and had to fight increasing desiccation. North of about lat 35° N the displacement of the winter rains towards the south lead to a dry period in Anatolia and Iran (Butzer 1975); good evidence has been found of a simultaneous lowering of Lake Van in eastern Anatolia by 300–400 m and salinization of its waters (Kempe 1977).

Evidence about the Holocene climatic history of the arid southwest of the USA is poor, except for the existence of a freshwater lake in central New Mexico in this moist period.

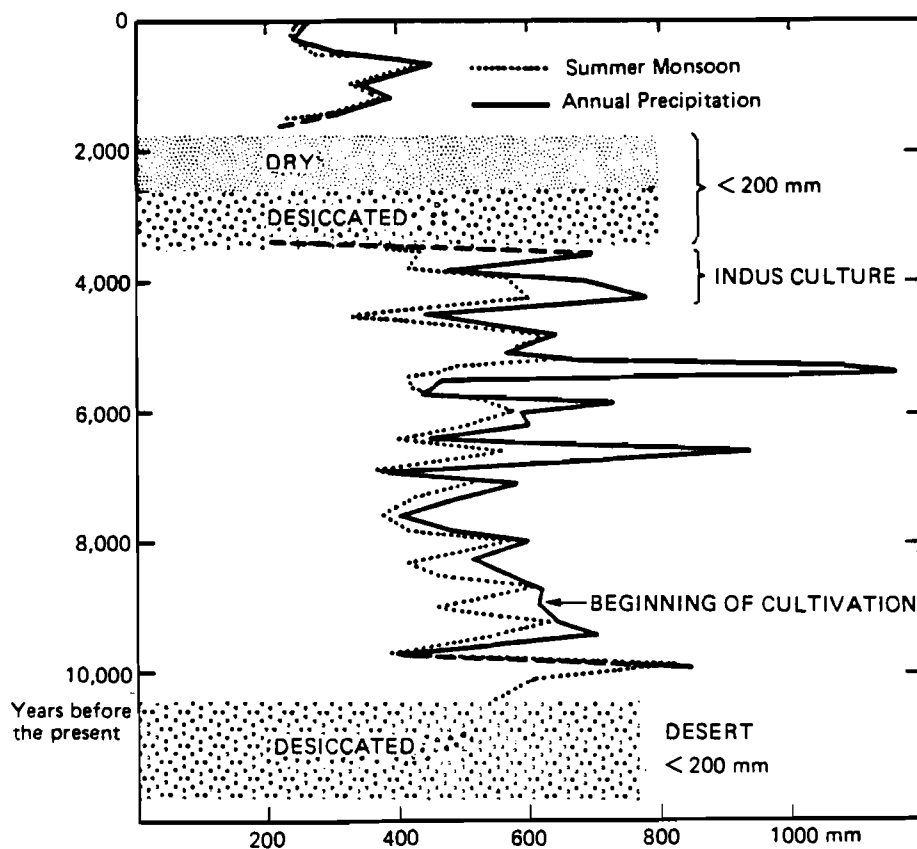


FIGURE 14 Rainfall estimates for Rajasthan, India, 10,000–2,000 years ago, based on evidence from pollen. (In the periods indicated by shaded areas, no pollen and thus no rainfall data are available.) The data are taken from Bryson and Murray (1977) and Singh *et al.* (1974).

Climatic conditions in Australia during the Holocene warm period were quite similar; increased precipitation occurred at the northern *and* southern margins of the desert together with a slight warming in the mountains of New Guinea, even at altitudes above 2,500 m (Bowler *et al.* 1976a). In contrast, the evidence available for southern Africa (van Zinderen Bakker 1976) indicates that the interior plateau had warmer, but drier, semidesert conditions.

At this point it is necessary to raise the question, To what extent can this climatic history repeat itself under varying boundary conditions? There were two such essential boundary conditions during the early Holocene period, i.e., until about 5,500 years ago: the presence of limited and shallow, but not

negligible, permanent ice sheets in eastern Canada, and the absence of desertification processes triggered by man.

These permanent ice sheets seem to have disappeared eventually, fairly parallel to the desiccation which started about 5,500 years ago. The importance of these ice sheets as a boundary condition can be understood if one takes into account the effect which a permanent cold source in eastern Canada could have had on the circulation pattern in the European section; similar to today's conditions in spring, the effect would have been frequent blocking anticyclones in the region of the British Isles and Scandinavia, with increasing cyclonic activity in the Mediterranean. This would have been effective especially in late spring, summer, and fall, and would have been accompanied by frequent deep troughs over eastern and central Europe, extending diagonally into northern Africa (see Figure 13). Similar conditions could only be expected in the near future if a permanent snow cover were to develop in the area of Baffin Island and Labrador; this is unlikely to occur in the next decades, but is not absolutely impossible, as will be discussed in the concluding chapter of this report.

Increasing desertification triggered by man (Hare 1977) has probably contributed to the slow and gradual desiccation process. Rainfall data collected in many arid regions since 1890 (Rajasthan) or 1904 (southern Tunisia) do *not* reveal a downward trend. Models designed by Charney (1975), Berkofsky (1976, 1977), Ellsaesser *et al.* (1976), and Joseph (1977) describe man-made destruction of vegetation as the cause of increasing surface albedo and intensification of the subsidence processes which should reduce effective rainfall. A reversal of such desertification processes (soil erosion, deflation, destruction of vegetation, groundwater depletion, and salinization) seems possible only if repeated large-scale rainfall triggers the growth of an adequate vegetation cover that can be protected against overgrazing and the ever-increasing strain caused by rapid population growth. Only then could the weak positive feedback effect, "desertification—increasing albedo—increasing subsidence—less rainfall—extended desertification," be interrupted and (possibly!) reversed. This would necessitate a major concerted effort on the part of many nations. From the discussion of the Holocene ice sheets in eastern Canada, one may conclude that no substantial change in rainfall along the northern margins of the Old World Arid Belt is to be expected. On the southern flank this might be possible if, as is expected, the subtropical anticyclones become slightly less intensive and are displaced towards higher latitudes. This would weaken the trade winds of the northern hemisphere and decrease coastal and equatorial upwelling, leading to increased evaporation and a higher water vapor content.

From the discussion of desertification triggered by man, it appears that, given our present population growth, reconstruction of the natural vegetation cover is a socioeconomic problem; several decades may pass before a reliable long-term increase in rainfall could be achieved through such reconstruction. Here much additional research of a truly interdisciplinary nature is certainly needed.

5.3 THE LAST INTERGLACIAL PERIOD (EEM SENSU STRICTO)

Recent investigations of ocean cores in low and middle latitudes, as well as of continental loess deposits in Austria and Czechoslovakia, have indicated that over the past 2–2.5 million years a sequence of at least 17 large-scale glaciations has occurred on northern continents. These were interrupted by an equal number of interglacial periods with a climate similar to the present one. Detailed data are available only for more recent events, especially for the last glaciation between about 73,000 and 14,000 years ago. This glaciation had two major glacial peaks at the beginning and end, and at least five shorter periods with a slightly warmer climate (interstadials). For the controversial subject of chronology, see, for example, Kukla (1977a).

The last interglacial period, defined here as stages 5a–5e after Emiliani and Shackleton (1974), lasted, with two important interruptions, from about 130,000 to 75,000 years ago. While the climate in Europe and Asia during this period has been carefully described by Frenzel (1968a), information on North America is hardly adequate for a regional description, and evidence for other continents is almost completely lacking. Detailed investigations of the climate at the earliest peak of the last interglacial (Eem sensu stricto, or stage 5e as defined above) around 125,000 years ago are being carried out by the CLIMAP group (Cline and Hays 1976). The group is evaluating the large number of accessible ocean cores to obtain a realistic estimate of sea surface temperatures and salinities. Since the Eem sensu stricto was apparently the warmest of all interglacial periods, a climatic interpretation of this subperiod is given below.

In northern and eastern Europe the climate during this subperiod was much more oceanic than it is at present. This was mainly due to the high sea level, about 5–7 m above today's level. Scandinavia was isolated from the continent by an oceanic channel between the Baltic and the White Sea. The sea also penetrated deeply into the continent in western Siberia, along the Ob and Yenisey flood plains up to lat 62°N. Table 5 gives a selection of climatic data from polar and mid-latitudes in Eurasia and North America. Temperatures were generally 2–3 °C higher than today, (even higher in some areas) and slightly more humid (for details, see Frenzel 1967, 1968a, and 1968b). The forests in the current cool/temperate zone were then thermophilous; deciduous trees like oak, linden, elm, hazel, and hornbeam prevailed. The occurrence of hippopotamus, forest elephants, and lions in southern England is a remarkable feature of this warm climate (Lamb 1977a, p. 188). Thermophilous forests in eastern Siberia indicated a marked retreat of permafrost up to lat 57°N (now around lat 50°N); boreal forests extended up to the coastlines of the time. While the coasts were inundated by the high eustatic sea level, the high temperature estimates suggest a seasonal retreat of Arctic drift ice far away from the coasts. Marginal parts of the Arctic drift ice were probably displaced poleward, but the central core of the ice in the ocean between Greenland, Alaska, and eastern Siberia has remained unchanged, at least since the beginning of the

TABLE 5 Estimated climatic differences between the Eem period and the present.

Area	Temperature (°C)			Annual rainfall (mm)
	January	July	Annual average	
Denmark	+2	+1–2	+1.5	0
GDR and northern FRG	+1–2	+3	+2.5	0
Central Poland	+3–4	+3	+3	+50
Northeast Poland	+3–5	+3–5	+5	+50
Byelorussia	+5–6	+5	+6	0
Central Russia	+9–10	+2	+5	+100
Northwest Ukraine	+2–3	±0	+1	+50
Western Siberia	+4	+3	+3	+100 ^b
Central Siberia	– ^a	– ^a	+6	– ^a
Toronto	+3–4	+2	+2–4	+250
Southeast Alaska	– ^a	+4–5	– ^a	– ^a
Banks Islands (72°N)	– ^a	+4–5	– ^a	– ^a

^aNo evidence available.

^bRough estimate.

SOURCE: Frenzel (1967).

Brunhes paleomagnetic epoch 700,000 years ago (Herman 1977). Worldwide comparisons of ocean cores indicate that during this stage the sea level stood at least 6 m higher than at present, as evidenced at Barbados, Hawaii, New Guinea, Mallorca, and on the lower Thames.

The duration of the Eem (stage 5e) was only on the order of 10,000 years. It was terminated by a markedly abrupt and relatively short period of cooling, during which the global ice volume both increased and decreased, possibly causing a change of 60–70 m in the sea level (rather than 100 m or more as occurred during the last ice age). In the Eem period, Atlantic polar water with some seasonal ice retreated north of lat 76°N for about 8,000 years, while subtropical waters, which apparently did not extend north of 44°N in the Holocene period, reached 52°N (Kellogg 1976).

Two other warm phases (5c and 5a) followed, but with fewer thermophilous forests and a lower sea level. Figure 15 gives a simplified diagram of the vegetation history of a peat bog core in northeast France (Woillard 1975, 1978), illustrating the apparent brevity of the two interrupting cold episodes on the continent. The second cooling (locally called Melisey II), which occurred during stage 5b (Emiliani and Shackleton 1974), apparently coincided with several marked events in northern Greenland at lat 76°N (Dansgaard *et al.* 1972), in a deep cave in southern France (Duplessy *et al.* 1970), in peat bogs in California and northern Greece (Adam 1978, Wijmstra 1978), and in many ocean cores of the Caribbean (Kennett and Huddleston 1972). The worldwide occurrence

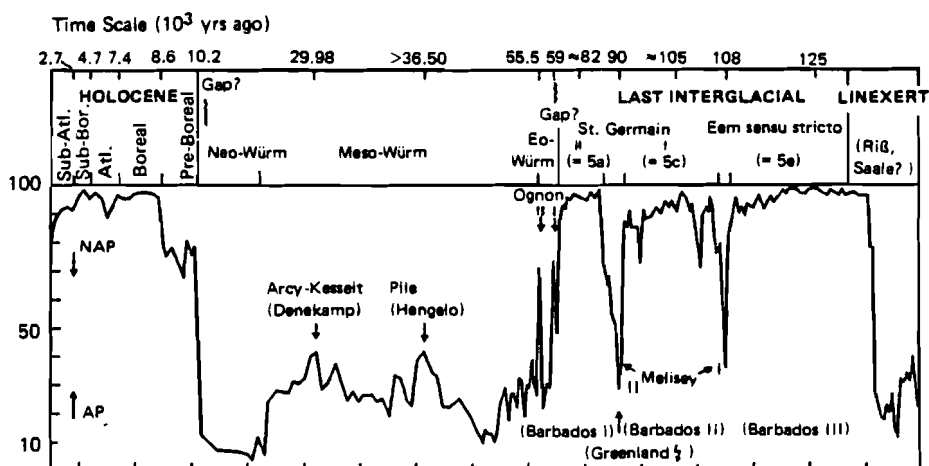


FIGURE 15 A simplified vegetation history from a fossil bog in southern Vosges (north-east France). The time scale in 10^3 years before the present is given on the x-axis, and the percentage of forest pollen (AP) vs. nonarboreal pollen (NAP) is given on the y-axis. Sub-Atl. is Sub-Atlanticum; Sub-Bor. is Sub-Boreal; Atl. is Atlanticum. Emiliani–Shackleton stages (5a, 5c, and 5e) are shown in the ‘Last Interglacial’ portion of the graph. The beginning of the Eem sensu stricto is misplaced slightly to the left; it should coincide with the sudden rise of AP. The figure is a simplified version of a figure appearing in Woillard (1975).

of stages 5a–5e (Emiliani–Shackleton) is verified by many complete oceanic and continental cores in all latitudes.

In all interglacial periods for which good evidence exists, except for the present one, such rather abrupt coolings with a Subarctic or Arctic climate have been observed to last only for several centuries or 1,000–2,000 years (“abortive glaciations”) (see Woillard 1979). The physical mechanism of such abrupt, but certainly natural events, recurring approximately once every 10,000 years, is not yet known; the possible role of clustering of volcanic eruptions or of Antarctic surges is still an open question (see Chapter 2 of this report and Flohn 1979).

Little is known about low latitudes; the occurrence of a long humid phase, with a deep lake in the Afar Triangle west of Djibouti (see Gasse and Delibrias 1976), and also along the western African coast (Diester–Hass 1976), suggests conditions similar to those prevailing during the early Holocene period.

6 IS A COEXISTENCE OF AN ICE-FREE ARCTIC AND A GLACIATED ANTARCTIC POSSIBLE?

6.1 CAUSES AND TIME SCALE OF A POSSIBLE OPENING OF THE ARCTIC OCEAN

The most fascinating, and also most controversial, problem of the future evolution of man's climate is the possibility of a complete disappearance of the drift ice of the Arctic ocean (which was discussed in Chapter 2). The sensitivity of the multiphase air–snow–ice–ocean system (see Figure 1) is demonstrated by the relatively large amount of seasonal melting (from above) and freezing (from below), on the average about 50 cm/yr. Unfortunately, no figures are available for a sample of years; recent experience based on ice and weather ship data suggests high interannual variability. In particular, the system is highly sensitive to the heat flow of the ocean below, to the albedo of the ice–snow surface during the melting season, and certainly to the length of the melting season (which ends with the first snow cover). After demonstrating the sensitivity of the system, Budyko discussed the possibility of artificial removal of the Arctic sea ice, and then designed simple semiempirical models based on the heat balance of the earth–atmosphere system (Budyko 1962, 1969, 1972). He noted that small increases in the solar constant or an increase in the atmospheric CO₂ content might lead rather rapidly to an ice-free Arctic ocean, substantially increasing the surface temperature by about 6–8 °C in summer, but by more than 20 °C in winter.

Since Budyko's work, arguments for and against such a drastic evolution – which probably went beyond the imagination of many responsible scientists – have been discussed, in private circles much more than in publications. Since no sufficiently realistic model of the climatic system is available, including the physical and dynamical interaction and the feedback processes between atmosphere, drift ice, and ocean, this problem cannot be satisfactorily resolved at the present time. Fletcher *et al.* (1973) made one of the first attempts to simulate atmospheric circulation under the conditions of an ice-free Arctic ocean, on the basis of the Mintz–Arakawa model. As Figure 16 shows, the essential result of the

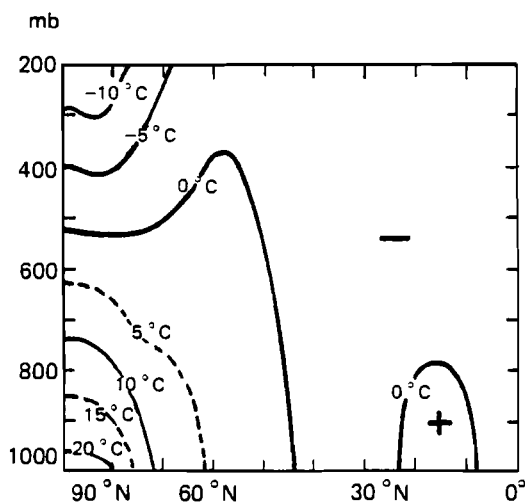


FIGURE 16 Temperature change obtained from the simulation of atmospheric circulation under conditions of an ice-free minus an ice-covered Arctic, using the Mintz–Arakawa model. The figure is based on Fletcher *et al.* (1973).

simulation is a warming of the lower troposphere north of about lat 45°N , together with a cooling of the upper troposphere and a marked destabilization of the polar atmosphere. Changes in tropical latitudes are probably uncertain.

Simple one-dimensional models have also frequently been investigated since Budyko's initiative (e.g., Sellers 1969, 1973). One of the most important simplifications was to define the latitude of boundary ϕ_p of the polar zone as equivalent to an average latitudinal temperature of the warm half-year of -1°C (Budyko 1974); then the planetary albedo, as seen from space, was taken to be 0.62 for the northern polar cap and 0.77 for the southern polar cap. This procedure introduces parameterization of the highly effective snow–albedo–temperature feedback. According to Budyko's 1974 monograph, the relationship between ϕ_p and solar radiation has the form of a hysteresis loop; ϕ_p is larger when the incoming radiation, as the determining parameter, increases from a value lower than the original value, and smaller when the incoming radiation decreases from a value higher than the original value. This is shown in Figure 17 (after Figure 8 in Budyko 1974). In another diagram (Budyko 1974, Figure 9) he demonstrates the relation between the average planetary air temperature and solar radiation; there the difference between points E (ice-free regime) and 3 (present situation) is equivalent to a change of about 4°C from the current temperature. This is higher than the temperature increase in all warm phases ($1\text{--}2.5^{\circ}\text{C}$) during the last 2×10^6 years, but the difference is not very big. If one accepts Budyko's model as a reasonable first guess, the possibility of such an ice-free regime cannot be excluded. Furthermore, temperature

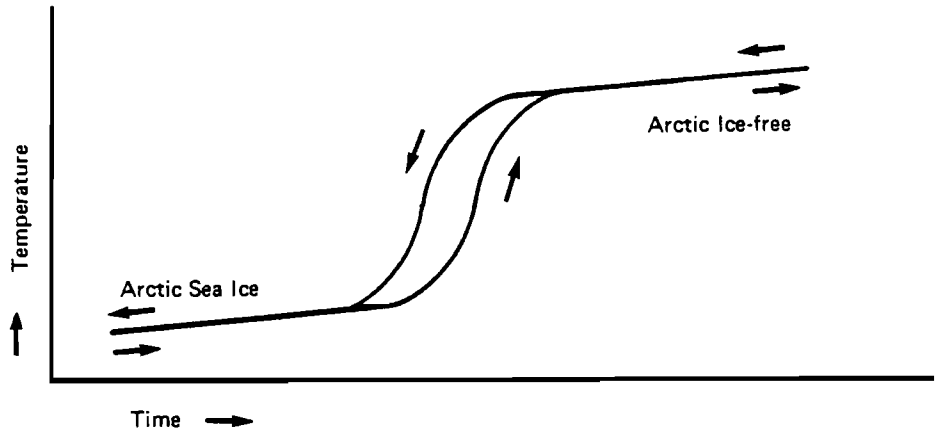


FIGURE 17 Expected temperature change due to hysteresis in the case of formation or disappearance of Arctic sea ice. The arrows pointing to the left indicate ice formation, while arrows pointing to the right indicate disappearance of the ice. The graph is a simplified version of a graph appearing in Budyko (1974).

estimates based on vegetation patterns during relevant past epochs, as the late Tertiary, also suggest a temperature about 4 °C higher than the present temperature in the northern hemisphere (see the next section of this chapter). In this case, however, the hysteresis loop is followed from above and not from below, as must be expected in a possible future evolution.

Looking at seasonal variations in the heat budget of the Arctic sea ice, Maykut and Untersteiner (1971) have stressed the roles of surface albedo and oceanic heat flow; their estimate of the oceanic heat flow ($1.5 \text{ kcal/cm}^2/\text{yr} \approx 2 \text{ W/m}^2$) is much too small according to more recent data, and should be increased by a factor of 6 to 7 (Aagard and Greisman 1975). Surface albedo during the melting season plays an effective role only in the case of surface pollution through dust or oil wastes. As for the oceanic heat flow, the flux of sensible heat is, on an annual average, slightly less than 10% of net solar radiation as well as of the infrared terrestrial radiation (Figure 2; see also Vowinkel and Orvig 1970); this is also true for the flux of latent heat (evaporation) in the same upward direction. Since the annual net radiation at the surface is quite small at present, the heat flux from the ocean is approximately equal to the sum of the flux of sensible heat and the flux of latent heat into the atmosphere.

During the melting season the melting process of the sea ice takes only 50–60 days (plus an additional 20 days for snowmelt), leading to a phase transition of about 15–20% of the average mass of an ice floe. In the remaining months a similar amount freezes from below. It is obvious that interannual changes in the heat budget – which should be on the order of $\pm 20\%$ or even

higher — may significantly alter these estimates. They have been verified in substance by only a few 12-month surveys. If one assumes only a 10% increase in summer melting and a 10% decrease in cold season freezing, for a period of a few years, the destruction of a 2–3 m ice floe would take a short time. If the melting season started 1–2 weeks earlier, perhaps as a consequence of advective warming, this would most certainly lead to a substantial imbalance in the sensitive mass budget. However, there is also a negative feedback; in winter the accretion rate is negatively correlated with thickness, i.e., thin ice accretes much faster than thick ice, because of the higher value of the upward heat flux (Thorndike *et al.* 1975). In contrast, a positive correlation exists during melting.

Under given assumptions, a seasonal disappearance of the Arctic sea-ice cover has recently been found in two model computations. Manabe and Stouffer (1979) used a spectral atmospheric model coupled with a static mixed-layer ocean, which allows for seasonal heat storage, evaporation, and the formation and decay of sea ice. If the CO₂ content of the atmosphere is assumed to be 1,200 ppm, model results show a disappearance of sea ice during summer and fall after about 10 model-years, when fairly stable climatic conditions have been reached (see Figure 18). Parkinson and Kellogg (1979) arrived at a similar result with a newly developed sea-ice model, under the assumption of a general increase in the air temperature of 5 °C. None of these models has been run over a longer period, taking into consideration storage of radiational heat in the open sea with its low albedo during summer.

According to the large areal fluctuations of the ice over the last millenium (discussed in the section on Medieval warming in Chapter 5), there is little doubt that at least the marginal sections of the Arctic drift ice can disappear rather rapidly. This argument is not valid for the central core; its existence has been verified by several independent lines of evidence at least for the period since the Brunhes–Matuyama boundary 0.7 million years ago, and it has probably existed for the last 2.3 million years. However, if the global warming exceeds the range of temperature fluctuations (up to +2.5 °C) during the last 6–8 glacial–interglacial cycles, this argument is no longer true; with an average warming of 4 °C or more, as occurred in the late Tertiary, disappearance of the central core of the drift ice is almost certain. This would be equivalent to an increase in the virtual CO₂ level by a factor of almost 3. The equivalent increase in the real CO₂ level would be by a factor of about 2.5 (see Table 3).

The atmospheric heat budget above an ice-free Arctic ocean is completely different from that which presently exists. Disregarding earlier attempts to analyze this heat budget, some calculations by Vowinckel and Orvig (1970, p. 220) will be presented here as the most complete approach available. The heat budget equation for a column above the Arctic cap (75–90° lat) between the earth's surface (sfc) and the top of the atmosphere (TA) may be written as follows:

$$R_{\text{sfc}} \downarrow - R_{\text{TA}} \uparrow + F_a + F_s \triangleq 0$$

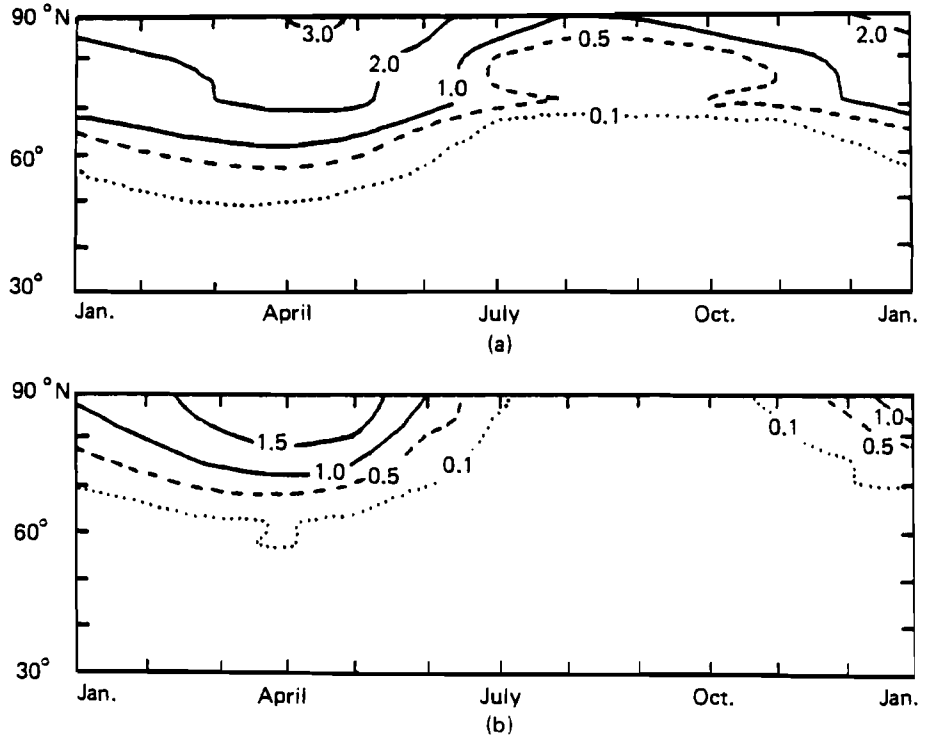


FIGURE 18 Seasonal variations in Arctic ice thickness (m) in (a) the standard case and (b) after quadrupling of the CO_2 content. A thickness of 10 cm may represent the southern boundary of sea ice. The figure is based on computations from Manabe–Stouffer's spectral atmosphere/mixed ocean model (1979).

where R = net radiation flux, F = northward heat transport across lat 75°N by ocean (s) and atmosphere (a). In equilibrium, the divergence of the downward radiation flux, $\text{div } R = R_{\text{sfc}} - R_{\text{TA}}$, must equal the convergence of the horizontal flux of sensible and latent heat. Table 6 gives estimates for the individual terms, assuming, in the case of an ice-free Arctic ocean, either a cloudless atmosphere or a closed stratus cover. Both assumptions are unrealistic, but the role of clouds of different altitude, thickness, and extension for the radiation fluxes is not yet well understood. Somewhat more realistic is the assumption of a cloudless sky during summer (from May to August), when the continents favor a thermal circulation with subsidence over the sea; for the rest of the year a closed stratus should prevail (see the last line of Table 6). The data are given in watts/m^2 ($1 \text{ kcal/cm}^2/\text{yr} = 1 \text{ kilolangle/yr} = 1.327 \text{ W/m}^2$).

The most interesting result is that of a positive annual net radiation budget, $\text{div } R$ (Table 6, last line); in this case heat would be available for export from the Arctic. The advective oceanic heat flux F_s is, according to the most recent evaluation (Aagard and Greisman 1975), 10.6 W/m^2 – much larger than

TABLE 6 Energy budget estimates (W/m^2) for an ice-free Arctic ocean.

	R_{sfc}	R_{TA}	$\text{div } R$	$F_a + F_s$
Present conditions	+3.3	+100.8	-97.5	+97.5
Ice-free, no clouds	29.4	59.1	-29.7	+29.7
Ice-free, closed stratus	42.7	92.9	-50.2	+50.2
Ice-free, seasonally varying ^a	62.1	58.3	+3.8	-3.8

^aAssuming a cloudless sky during summer, and a closed stratus cover during the rest of the year.
SOURCE: Vowinckel and Orvig (1970).

the value calculated in most earlier investigations. (For instance, Vowinckel and Orvig arrived at the value $\approx 7 \text{ W}/\text{m}^2$). One of the most important factors is the export of ice by the East Greenland Current; this contributes about 50% to the warming of the Arctic ocean, since the ice is melted externally. In an earlier analysis with much greater uncertainties, Donn and Shaw (1966) obtained an imbalance of +26.3 kilolangle/yr ($\approx 35 \text{ W}/\text{m}^2$). The heat surplus is in line with the obvious consideration that, during the cold season, heat and water vapor should be exported from an ice-free ocean towards the continents; the continents certainly should be colder than an open ocean in subpolar latitudes. An open Arctic ocean should receive an annual net radiation of 30–60 W/m^2 at the surface (Table 6). If one assumes $R_{\text{sfc}} = 45 \text{ W}/\text{m}^2$, allowing 40% for evaporation in summer (when the small flux of sensible heat is probably downward), then 27 W/m^2 or 20 kcal/cm^2 are available for heat storage in the sea. For a 50 m mixed surface layer, this yields an average heat storage of 4 cal/g, which is equivalent to a warming of 4 °C in one single summer. In winter, infrared emission increases with temperature; therefore if the surface temperature increases from -35 °C to 0 °C, the blackbody radiation increases by only about 60%. But due to the much higher water vapor content, atmospheric counter-radiation will also rise substantially, so that the net infrared radiation of the ocean surface may not change much. These estimates permit the conclusion that a new equilibrium water temperature will be reached after a few years, which should be indeed substantially higher than the melting temperature of saltwater; Budyko's estimate of +8 °C cannot be so far from reality. This would also be consistent with the air temperatures estimated for late Tertiary vegetation at the highest latitudes.

It should not be forgotten that the fate of the Arctic sea ice also depends on the low salinity of the shallow upper layer of the sea (see Figure 3). A balance exists between the outflow of the surface water via the East Greenland Current and the seasonal inflow of fresh water from the enormous Siberian and Canadian rivers. Due to the urgent need for increased irrigation in the central Asian part of the USSR, several large diversion schemes have been developed for western Siberia, including an advanced canal system (Hollis 1978). In this scheme, provision is made for a diversion of up to 300 km^3 freshwater per year, which is about 23% of the present runoff into the Kara Sea (1,283 km^3/yr).

It has been pointed out that any large-scale loss of freshwater inflow tends to raise the salinity of the Arctic Ocean, to decrease its stability, and to contribute eventually to a reduction in the present sea-ice balance; no quantitative investigation is available as yet.

6.2 COEXISTENCE OF AN OPEN ARCTIC OCEAN AND A GLACIATED ANTARCTIC CONTINENT DURING THE LATE TERTIARY

One of the main arguments against a possibly ice-free Arctic ocean in the foreseeable future has been the existence of the highly glaciated Antarctic continent. Indeed it is not easy to imagine a completely asymmetric planet with one pole ice-free, and the other one covered by an ice sheet more than 2 km thick. Still, a similar asymmetry probably existed for more than 20–30 million years during the Permo–Carboniferous glacial period about 250 million years ago. At that time, however, several of the earth's continents formed one giant supercontinent (Gondwana); it was situated at higher latitudes of the southern hemisphere and included the pole. In the northern hemisphere most of our present coal deposits were formed during this period in forest swamps similar to the Everglades in southern Florida. The boundary conditions on the earth's surface are different today, but not so much different: one pole is situated on a fairly large, completely isolated ice-covered continent, while the other pole is situated in a deep, almost landlocked ocean with a thin skin of floating ice. To some extent, this causes an asymmetric circulation of atmosphere and ocean, as was discussed in Chapter 2 (see also Flohn 1978a).

Regarding the background of a possible evolution of an ice-free Arctic ocean, it is of paramount interest that exactly the same situation did in fact exist immediately before the onset of the Pleistocene, with its sequence of glacial and interglacial periods in the northern hemisphere and a more or less constant glaciation of the Antarctic. As the results of the Deep Sea Drilling Program have shown, the Antarctic ice had developed to its present size about ten million years (i.e., a period five times the duration of the Pleistocene) before the formation of Arctic drift ice. In two recent reviews Kennett (1977a) and Frakes (1978) evaluated the available evidence, and arrived at only slightly different results. At the end of the period in which a glaciated Antarctic and ice-free Arctic coexisted, in the Pliocene (about 2–5 million years ago), the early hominids, our ancestors, lived in a savanna environment in equatorial East Africa learning how to use pebbles as weapons and as tools. (Unfortunately they did not yet know how to record climate.) To what extent climatic changes may have affected the ape–man transition is not yet known.

For the last 50–70 million years, Antarctica has been situated near the South Pole. It was once connected with Australia and other parts of the former Gondwana continent. Both poles were ice-free throughout the Mesozoic and the early Tertiary (about 200–50 million years ago) (Schwarzbach 1974). During these eras the atmospheric circulation was probably dominated by the

tropical Hadley cells reaching to lat 50–60°, with strong seasonal variations (Flohn 1964b). The meridional extension of Australia and Antarctica caused warm oceanic currents and prevented any glaciation until the beginning of the Eocene (55 million years ago). Soon thereafter, Australia separated from Antarctica and drifted northward at an average speed of 5 cm/yr, while Antarctica remained nearly fixed (Kennett *et al.* 1977c). After a long period of increasing winter snow, with possible local glaciations in West Antarctica and steadily decreasing water temperatures (small surface–bottom differences), the first significant drop in temperature occurred 38 million years ago, near the boundary between the Eocene and Oligocene eras. This drop especially affected the bottom layers (i.e., a 5 °C decrease within less than 10⁵ years, which was remarkably abrupt for the time; see Figure 19).

At this time substantial Antarctic sea ice formed, coinciding with the development of widespread glaciation in parts of the Antarctic continent (Kennett 1977a). As under present conditions, the cold and dense bottom water spread outward into all oceans, causing a considerable worldwide crisis for deep-sea fauna. After further climatic fluctuations of more geological importance, including a significant global cooling during the Oligocene (38–22 million years ago), a notable Antarctic ice cap formed during the middle Miocene epoch (15–12 million years ago) and became a permanent feature; it probably was still “warm,” i.e., with temperatures close to the melting point. This formation occurred roughly at the same time as volcanic activity sharply increased, as many ocean drillings have shown (see Figure 20; also Kennett *et al.* 1977c). After the formation of the ice cap, the first mountain glaciers in southern Alaska appeared, as well as the first cold-water fauna in northernmost Japan (Kanno and Masuda 1978); a marked drop in the surface temperature also occurred in the high latitudes of the Pacific (Savin *et al.* 1975).

The highest glacial maximum, characterized by a “cold” and slowly moving Antarctic ice dome, was reached at the end of the late Miocene or Messinian (6.5–5 million years ago), when the ice volume was larger than it is today. At this time the height of the ice dome must have been several hundred meters higher, and the Ross shelf ice extended several hundred km farther north. This glacial maximum was accompanied by a remarkable global cooling, by an extension of cold Antarctic surface waters 300 km northward, and by a high carbonate sedimentation rate at the equatorial Pacific, indicating strong upwelling of nutritious cool water (Saito *et al.* 1975). Seven to ten cyclic temperature changes were observed, with minima as cold as in the cold phase of the last glaciation. This is not necessarily indicative of a global cooling, but does show the intensity of the equatorial upwelling. One of the most important consequences was a “glacial-eustatic” drop in sea level 40–50 m below today’s level, due to the storage of water in the Antarctic ice dome. During each drop the Gibraltar Strait, or its predecessor, became dry and isolated the Mediterranean; the latter completely evaporated 8–10 times to a depth of 3,700 m and filled

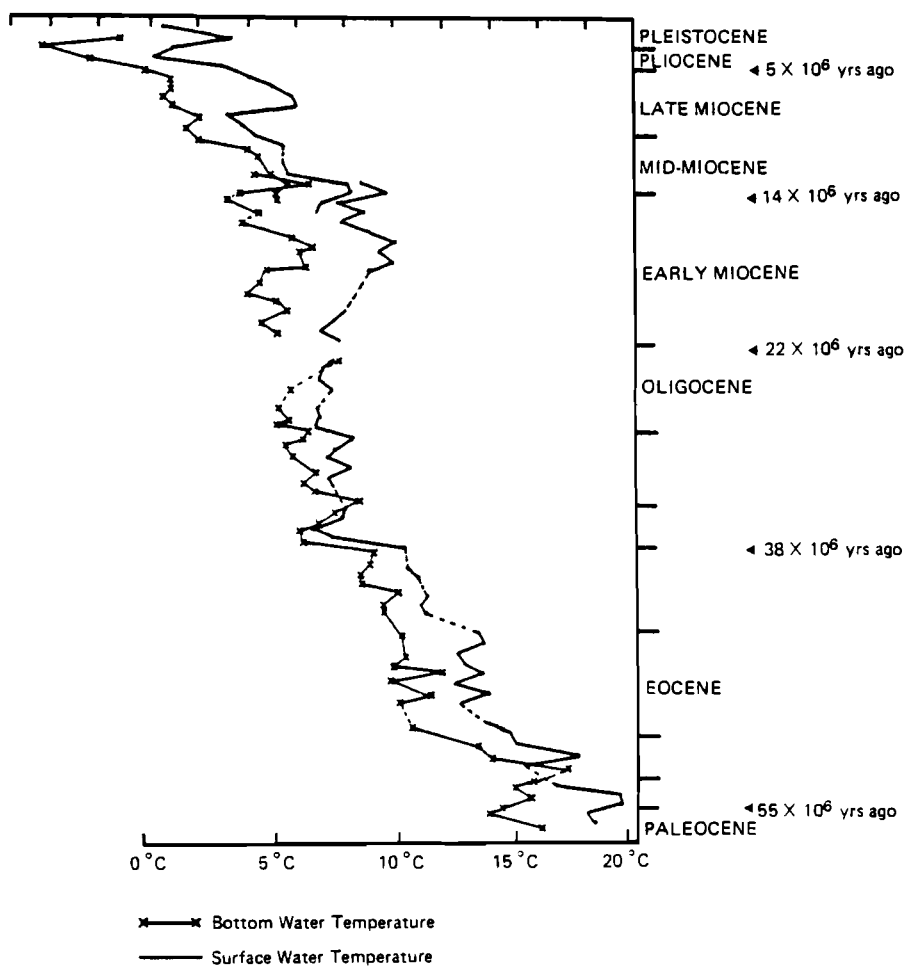


FIGURE 19 Evolution of surface and bottom (isotopic) temperatures in the Subantarctic (about 50 °S, 160 °E) since the late Paleocene about 58 × 10⁶ years ago. The figure is based on two figures which appeared in Kennett (1977a).

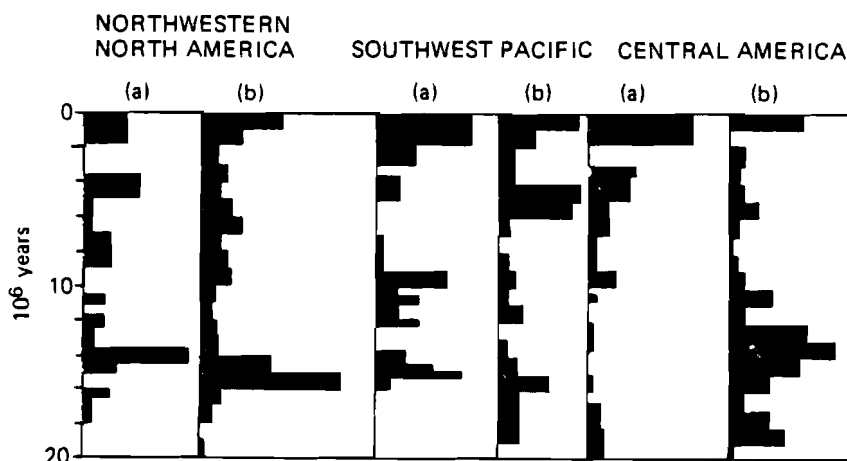


FIGURE 20 Volcanic activity in some circum-Pacific provinces during the late Tertiary and Quaternary, measured by volcanic ash from (a) deep sea sediments and (b) terrestrial volcanic sequences. Source: Kennett *et al.* (1977c).

again, leaving a laminated salt layer 300–500 m thick (Hsü *et al.* 1973, 1977). This lamination and the paleoclimatic history of equatorial Pacific sediments indicate a cyclic behavior on a time scale of about 10^5 years, lasting for about 0.5 million years; the cyclic behavior was probably caused by orbital elements similar to those in effect during the Pleistocene.

During and after that time, the Arctic enjoyed a cool to temperate climate with boreal forests extending up to the northernmost tip of land. In the late Miocene and Pliocene the entire shelf north of Asia and Alaska fell dry, and the continents extended 200–600 km farther north, e.g., in Siberia up to 81°N , and in Canada up to 83°N (Hopkins 1967). The distribution of vegetation in Siberia shortly before the first appearance of ice on the European continent (during the late Pliocene, about 2.5 million years ago) has been mapped with the aid of a rich data base, published mainly by Soviet authors (Frenzel 1968a, 1968b). No evidence of tundra or widespread permafrost could be found. Summer temperatures have been estimated to have been about 3°C higher in western Europe, but $4\text{--}5^\circ\text{C}$ higher in eastern Europe. There and in Siberia annual and winter temperatures must have been $5\text{--}10^\circ\text{C}$ higher than at present (Frenzel 1968a, 1968b). Since the relative and absolute heights of many mountains were significantly lower than they are now (as is demonstrated by the flat or rolling topography now covering the highest levels of some mountains – the Rax “plateau” in Austria is a good example) oceanic rainfall could penetrate farther inland. Precipitation has been estimated to have been 300–400 mm higher (Frenzel 1968a, 1968b). In a few areas, such as in California and northwest Iceland, local glaciers were formed simultaneously with the boreal forests, but produced no significant large-scale climatic effect. Simultaneous glaciation of parts of Greenland can be assumed, but there is no

evidence for it, due to the strong, and probably permanent, glacial erosion since that time. Along the coasts of Alaska well-developed boreal mixed forests extended more than 800 km north of some of the present tree lines. The fossil insect fauna at lat 66°N resembled the insect fauna now living in the Vancouver–Seattle area at lat 48–50°N (Hopkins 1971).

During the Pliocene (5–2 million years ago) the Ross Ice Shelf in Antarctica extended beyond its present boundary, and glaciation started in southern South America [about 3.6 million years ago (Mercer 1976)]. From ice-rafted pebbles one may infer that, simultaneously with a northward shift of the boundary of the cold Antarctica surface water, Antarctic tabular icebergs occurred and also spread northward, reaching even farther north than during the Pleistocene glaciations.

Of special interest is the climate of the middle and lower latitudes. After many careful investigations, Lotze (1964) compiled maps of the position of the evaporite belt during past climatic periods, i.e., the position of the arid zone of playas and sebkhas, where soluble salts were sedimented in dry pans. The northern limits of the northern arid belt during the Quaternary, late Tertiary, and early Tertiary, taken from Lotze's maps, is presented in Figure 21; a southward shift from an average latitude of about 47°N in the early and middle Tertiary to 42°N in the late Tertiary, and to 38°N in the Quaternary is indicated in the figure. In the context of this paper, only the displacements during the latter epochs are important. The multiple desiccation of the Mediterranean that occurred during the Messinian – a short portion of the Miocene/Pliocene epoch 6.5–5 million years ago – aggravated the arid conditions in southern Europe. Evidence of a similar southward shift of the vegetation belts of North America has been compiled by Dorf (1960) (Figure 22).

During the Messinian, even the southern part of central Europe was partly arid, with steppes or desert vegetation near Vienna (Schwarzbach 1974, Hsü 1974). Southwest Germany was also drier than it is now (Schwarzbach, in Nairn 1964). While tropical marine microfossils had occurred abundantly in the Atlantic up to lat 58°N before these events, this boundary retreated during the desiccation of the Mediterranean on the eastern side of the Atlantic to about lat 33°N. Tropical species could not enter the Mediterranean after its reopening during the early Pliocene (5 million years ago), though such species were able to reach farther than lat 50°N in the Gulf Stream region. This indicates a great longitudinal contrast, probably caused by the wind-driven surface currents of the oceans.

Many regional temperature and precipitation estimates have been made (e.g., Mägdefrau 1968, Schwarzbach 1974). Since in the late Tertiary many of our present mountains existed only in rudimentary form, these numerical data cannot be considered representative of conditions in the near future. This is obvious, for example, in the case of the now arid continental basin of Nevada or the Mojave desert, which enjoyed a rather moist maritime climate near sea level during the late Miocene. Summer temperatures were then 4°C lower, and winter temperatures were 8–10°C higher than at present (Schwarzbach



FIGURE 21 Displacement of the northern boundary of the northern hemisphere arid zone during the early Tertiary ($30\text{--}50 \times 10^6$ years ago), late Tertiary ($5\text{--}15 \times 10^6$ years ago), and Quaternary ($0\text{--}2 \times 10^6$ years ago) periods, measured by the position of the evaporite belt. The figure is based on several figures which appeared in Lotze (1964).

1974). During the same time periods, southwest Germany enjoyed a subtropical or, later, warm to temperate climate (Mägdefrau 1968). In the tropics, the extension of savanna climates with seasonal rains was much wider than it is today, but the equatorial rain forest with perennial rain was smaller. In the Oligocene and Miocene (Maley 1980), the vegetation patterns of the African continent revealed the same marked asymmetry as in the Miocene and Pliocene. While the southern Sahara was covered with a tropical humid or at least semihumid vegetation (which has persisted in southern Nigeria), southern Africa and the Zaire basin were dry and sometimes fully deserts. Evidence of the same aridity has also been observed in northern Australia, especially for the period after the Messinian peak of the Antarctic glaciation (Kemp 1978).

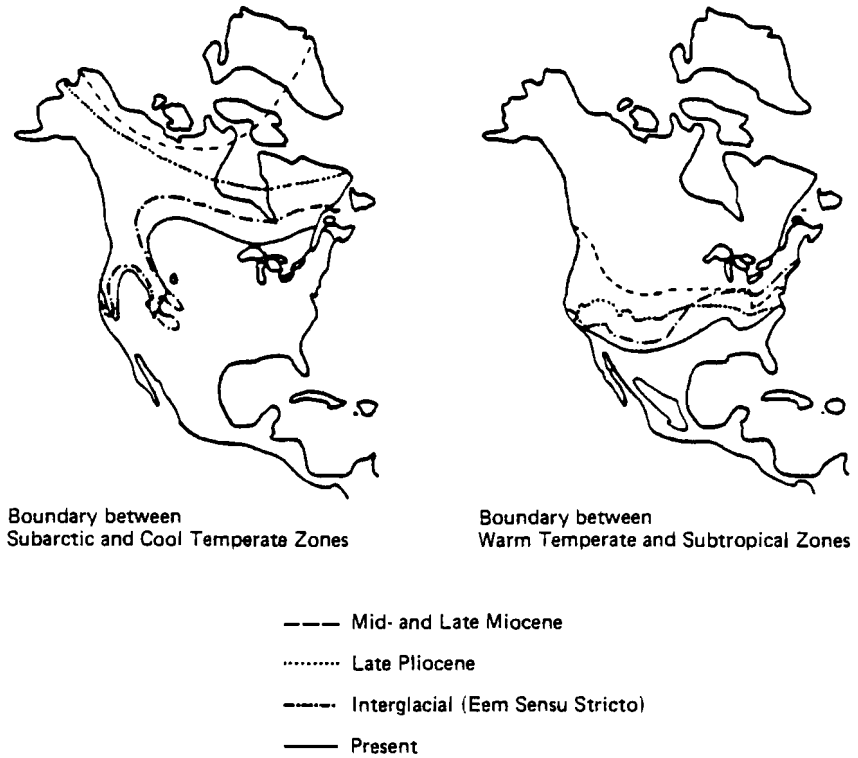


FIGURE 22 Displacement of vegetation boundaries in North America from the mid- and late Miocene periods to the present. The figure is based on Dorf (1960).

Although certainly still incomplete, this evidence indicates that the hemispheric asymmetry of the general atmospheric and oceanic circulation was substantially greater between the middle Miocene and the Pliocene than it is now (Flohn 1978a). The shape and position of the continents was then by and large similar to present conditions. Large-scale glaciation of the northern continents did not start until 2.5×10^6 years ago; the formation of Arctic drift ice began only after that date, about 2.3×10^6 years ago, when the meltwater produced a shallow, stable low-saline upper layer in the Arctic ocean (Herman 1977). Further evidence of an ice-free Arctic ocean earlier than 3×10^6 years ago is found in the vegetation boundaries described by Frenzel (1968) for Siberia and by Hopkins (1967, 1971) for Arctic North America and the Chukchi peninsula. Thus, the simultaneous existence of a continental ice dome in the Antarctic and a substantially ice-free Arctic ocean is well established for the period between, at least, about 12 and 2.5×10^6 years ago, a period characterized by a high degree of stability in spite of second-order climatic fluctuations. This strange situation must have caused marked hemispheric circulation asymmetries of both the atmosphere and the ocean.

6.3 SOME IMPLICATIONS OF A UNIPOLAR CLIMATIC ASYMMETRY

The discovery of the coexistence of a fully glaciated Antarctic continent and an open Arctic ocean, for no less than 10×10^6 years immediately before the Pleistocene, is indeed important. It could be made because of the evidence accumulated by the "Glomar Challenger" during the Deep Sea Drilling Project. The notion appears so contradictory to traditional climatological views that no more than reluctant adoption can be expected. One of the most urgent tasks to pursue next is a careful and critical survey of the vast geological literature on a global scale. This must be done, however, in cooperation between geologists and meteorologists, and with full knowledge of the basic laws of planetary circulation and their consequences.

Attention must be paid, first of all, to the fundamental circulation theorem set forth by V. Bjerknes in 1897 (see Palmén and Newton 1969); according to this theorem, temperature decreases with height and latitude in the three-dimensional baroclinic structure of the earth's atmosphere, while atmospheric density decreases with height but increases with latitude. Not being parallel, isothermal and isopycnic surfaces cut each other at small angles, forming flat tubes (solenoids). The circulation theorem states that in such a baroclinic field the intensity of a thermal circulation (which is driven by differences in heating according to latitude and height) depends only on the number of solenoids, i.e., on the temperature change (gradient) along an isopycnic surface. Since the slope of such a surface is only 1:300 to 1:2,000, the isopycnic temperature gradients nearly equal the horizontal gradients. On a rotating planet, this thermal circulation is distorted by the Coriolis force; in the earth's atmosphere, the zonal (E-W) components of motion, introduced by the earth's fast rotation, are much stronger than the meridional and vertical components.

It cannot be the task of this report to outline the physical concepts of atmospheric circulation (see, for example, Palmén and Newton 1969) or of oceanic circulation; the latter is driven mainly by the wind near the surface, and at greater depths by solenoids between surfaces of constant temperature and density (depending on salinity). Note, however, that the intensity of atmospheric circulation, given the earth's rotation and the composition (density) of the atmosphere, depends first of all on the meridional temperature difference between the equator and the poles. The data presented in Table 1 of this paper shows that, even today, the equator-pole temperature difference is about 40% higher in the southern than in the northern hemisphere.

For conservative extrapolation of the relation between temperature and height for the case of an ice-free Arctic in winter, one may assume (as in Figure 23) an average surface temperature of $+4^\circ\text{C}$ (instead of the current -34°C), and a moist adiabatic lapse rate from the cloud base at about 950 mbar up to at least 500 mbar. [This instability probably leads to a cooling of the upper troposphere, e.g., at 300 mbar (~ 9 km) from the current -58°C to about -62°C ; see also Figure 16.] This means an average tropospheric warming of

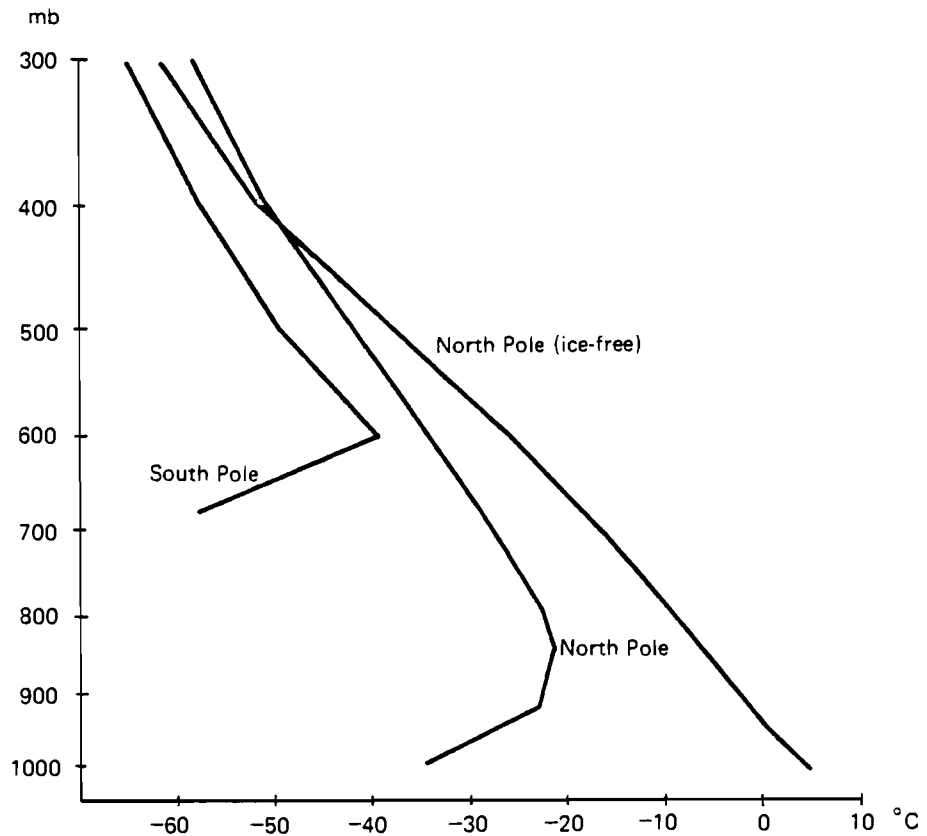


FIGURE 23 Current winter temperatures above the North Pole and South Pole, and estimated winter temperatures which might prevail above an ice-free North Pole.

11.5 °C. A corresponding tropospheric warming of only 2–3 °C can be expected for summer, when the surface inversion is shallow and unimportant. For the 300/700 mbar layer, assumed representative for the purposes of a hemispheric comparison (see Chapter 2, especially Table 1), the temperature increase in winter is only +4 °C, and the summer increase +2 °C. A conservative estimate of a +3 °C annual average increase results. In this case, the average temperature difference of this layer between the equator and the North Pole would decrease to 24 °C; still, the temperature difference would remain at 37 °C above the southern hemisphere, where it would be slightly more than 50% higher than in the northern hemisphere. Here the assumption is made that the greenhouse effect does not significantly alter the meridional temperature gradient; this is certainly not quite realistic and subject to further revision.

Under the conditions of such a unipolar temperature asymmetry, one fundamental quantity of the atmospheric circulation could be extrapolated. Remember that in a rotating atmosphere there are two fundamentally different modes of meridional exchange of conservative properties, such as angular momentum or enthalpy (Palmén and Newton 1969). The first mode can be conceptualized as a helical motion within a latitudinal band, symmetric about the rotational axis, and driven by a thermal circulation in a meridional/vertical plane between the equator and the subtropics; this is the tropical circulation or Hadley cell. The exchange processes of the second mode in higher latitudes are mainly due to traveling and quasi-stationary eddies, advecting warm or cold air poleward or equatorward on both sides of a vortex or long wave, within a belt of westerlies; this belt, identical with the meandering edge of a huge polar vortex, is part of the extratropical or Ferrel circulation. The average boundary between the two modes (which in reality permanently interact) is characterized by the belt of subtropical anticyclones near the surface and by the maximum of baroclinic westerly winds (i.e., the subtropical jet stream) in the upper troposphere, both in positions which nearly coincide.

It has been shown (Smagorinsky 1963) that the stability or instability of eddies in a baroclinic current depends on a simple criterion related to the circulation theorem, i.e., the ratio between the meridional temperature gradient and the vertical lapse rate. Since the latter depends mainly on the water vapor content of the atmosphere (as will be discussed below), the behavior of the eddies is by and large controlled by the meridional temperature gradient. The eddies tend to be unstable in the Ferrel circulation, but stable in the Hadley cell where the meridional temperature differences are weak. The latitude-dependent threshold of the so-called Z-criterion then indicates, at the same time, the seasonally varying position ϕ_{STA} of the subtropical belt. ϕ_{STA} is given by the following relation, where r = earth's radius, h = scale height of the atmosphere, θ = potential temperature, $y(z)$ = meridional (vertical) coordinate, and STA = subtropical anticyclone:

$$\cot \phi_{STA} = \frac{r \partial \theta / \partial y}{h \partial \theta / \partial z}$$

Korff and Flohn (1969) have verified this theoretical concept* using monthly averages over many years of both the latitude ϕ_{STA} of subtropical anticyclones and the meridional temperature gradient at the 300/700 mbar layer, in both hemispheres. With correlation coefficients above 0.85, this relation describes remarkably well the seasonal variation and the actual hemispheric asymmetry of ϕ_{STA} (Figure 24).

*The Z-criterion has recently been criticized by Greenhut (1977), who has demonstrated that it leads to incorrect results if applied to tropical latitudes during northern summer, when the average meridional temperature gradient reverses. Here it is only applied to the atmospheric circulation in subtropical and temperate latitudes; the empirical verification given above leaves no doubt about its applicability in this general case.

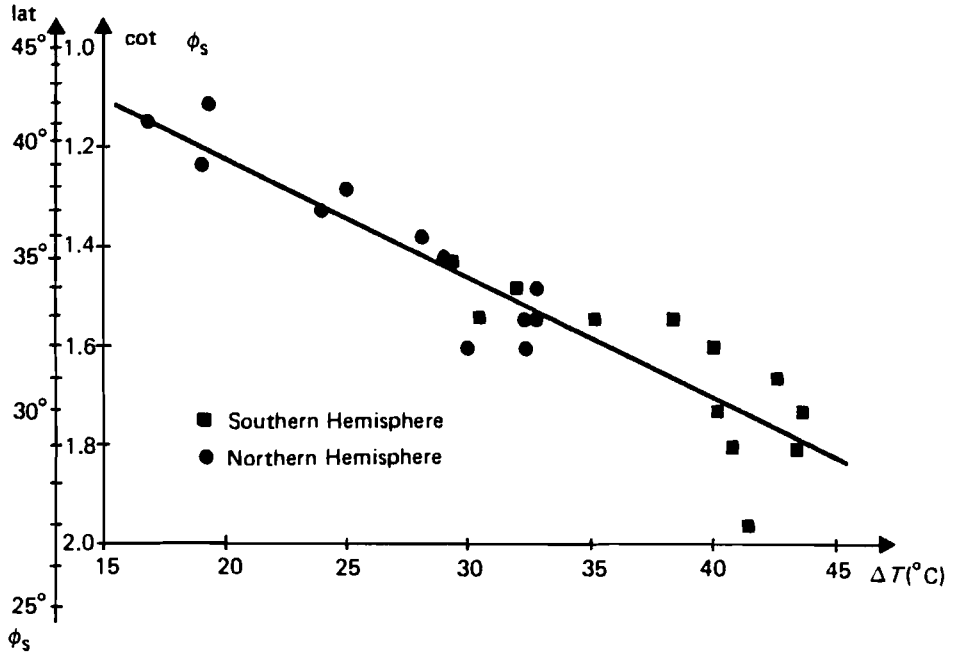


FIGURE 24 Latitude of the subtropical anticyclonic belt (ϕ_s) in each month of the year vs. the current equator-pole temperature difference. The monthly data for the 300/700 mbar layer are from Flohn (1967); data on subtropical anticyclonic belts are from Pflugbeil (1967).

The role of the lapse rate $\partial\theta/\partial z$ should be taken into account; as early as 1964 a diagram (Figure 25) was published (Flohn 1964b), which demonstrated that an increase in the lapse rate would reduce ϕ_{STA} . A quite similar diagram was published later by Bryson (see Williams 1978, p. 151).

There are two factors that impede simple quantification by means of the Manabe-Wetherald diagram (see Figure 7). First, because of theoretical considerations, it is an open question whether $\partial T/\partial y$ in Figure 25 can be taken as a linear average between the equator and the pole or as the highest value in the subtropical baroclinic zone (the latter assumption is preferred by Flohn, 1964b).

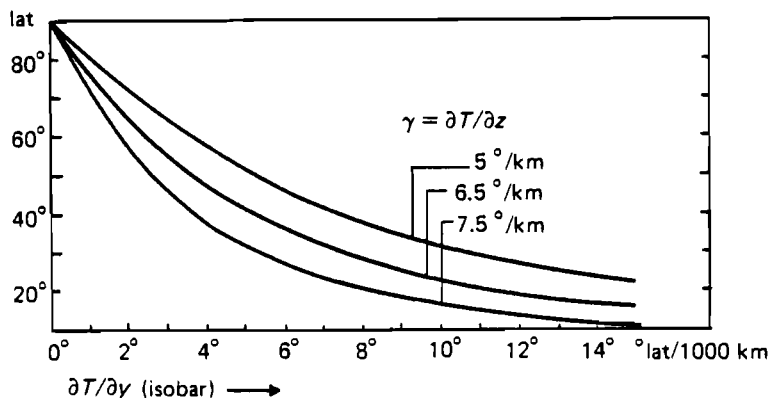


FIGURE 25 Latitudinal position of the subtropical anticyclonic belt as a function of vertical stability γ and the meridional temperature gradient $\partial T/\partial y$. y and z are the meridional and vertical coordinates, respectively. Source: Flohn (1964b).

Second, introduction of clouds into the Manabe–Wetherald (1975) model in a simplified manner yields discontinuities in the tropospheric lapse rate below 300 mbar (Figure 7), which make it difficult to use the quantitative estimate in the above formula. The combined role of meridional and vertical temperature gradients with respect to the Z -criterion merits further investigation.

A simple extrapolation based on the temperature distribution above an ice-free Arctic (see Figure 23), with the temperatures above the equator and the South Pole unchanged, would yield only a small northward displacement of the subtropical anticyclonic belt. However, neglecting the 700/1,000 mbar layer, in which most of the warming ($+21^\circ\text{C}$) occurs, leads to unrealistic results. The Z -criterion is based on the concept of baroclinic instability; the slope of the 300 mbar surface, which is representative of tropospheric baroclinicity (or the temperature gradient), depends on the temperature pattern of the troposphere as a whole. There is no way of realistically estimating the properties of the 700/1,000 mbar layer at the Antarctic (where it is completely under the surface), but one may use more realistic values, valid for the 300/1,000 mbar layer, to estimate the temperature increase above the Arctic: $+11^\circ\text{C}$ in winter, $+3^\circ\text{C}$ in summer, and $+7^\circ\text{C}$ year-round. This would produce an annual shift of the northern subtropical high-pressure belt from the present lat 37° to lat $43\text{--}45^\circ$, with the location of the southern subtropical belt remaining unchanged (31°S) (see Figure 24). In summer, the shift would probably extend not much farther than 100 or 200 km, but in winter the subtropical belt may be displaced to the north by some 800 km or even more. This would drastically reduce the extension of the subtropical belt of winter rains, now supplying California, the

Mediterranean, the Middle East up to Turkestan (USSR), and the Punjab region of India. The belt situated at 45–50 °N would probably be frequently affected by summer droughts.

Such an asymmetric displacement of the northern STA together with a constant southern STA would also shift the average position of the “meteorological equator” to lat 9–10 °N, from its current position at 6 °N. Because of the much higher intensity of the southern Hadley cell and the southern trade winds, this position may also be displaced further north, i.e., near lat 12 °N. In this case penetration of the equatorial rain belt across the mathematical equator into the southern hemisphere would occur probably only occasionally in northern winter; the seasonal displacement of the rain belt would be restricted to the belt between the equator and lat 20 °N. As a consequence, tropical summer rains south of the equator would decrease markedly, eventually leading to natural desertification in many countries situated within the belt between 0 and 20 °S. This would probably be aggravated by more frequent and more intense equatorial upwelling, causing a drastic reduction of oceanic evaporation in this belt, especially in northern summer/southern winter, when the meteorological equator reaches its northernmost position. In this case, strong equatorial upwelling can be expected to occur permanently (with El Niño situations no longer arising), at least in the Pacific and Atlantic oceans. For the equatorial Indian Ocean, no evidence of past (or present) upwelling is available.

In the big oceans, the position of the equatorial upwelling zone is controlled by the disappearance of the Coriolis force at the mathematical equator. Since no meridional climatic shift is possible in this case, the equatorial upwelling zone can serve as a marker for latitudinal shifts of tectonic plates (Winterer 1973). The different view expressed by Kozur (1976) results from a misunderstanding of the geophysical background of oceanic upwelling along the equator, which never coincides with the atmospheric intertropical convergence zone (see Chapter 2).

In the present Sudan–Sahel belt, between about lat 8 °N and 18 °N (or perhaps 20 °N), an increase in precipitation could be possible. However, this contention is based on only one argument, namely the northward shift of planetary climatic belts. But in Africa the actual seasonal advance of the rainfall belt in summer is remarkably small; this is most probably due to the tropical easterly jet, which, in an area of decreasing speed, forces the air beneath to subside (Flohn 1964a, 1966). This effect should also persist during an ice-free Arctic ocean phase. Another essential prerequisite for an increase in precipitation, if one follows the convincing model studies by Charney (1975) and many others, would be the conservation of vegetation that might reappear because of expanding summer rains, i.e., the protection of vegetation against overgrazing and other desertification processes triggered by man.

In the monsoon area of southern Asia, the planetary circulation patterns are largely controlled by and disturbed by the existence of the mountain area

north of the Himalayas. Here any rational attempt to predict the effects of disappearing Arctic sea ice seems to be impossible. Since the late Tertiary, the altitude of the giant mountain range in this area has increased considerably; vertical motions are still occurring, and climatological evidence from a period when the Himalayas did not exist can certainly not be assumed to resemble what could be expected under present boundary conditions. Striking evidence for uplifting is the Tibetan Plateau, whose weak rolling topography has risen from near sea level in the late Tertiary to a present altitude of 4–5 km. Being an elevated heat source, the plateau controls the tropical easterly jet (Flohn 1964a, 1968) and the entire monsoon circulation between western Africa and the Philippines. In this wide area, the influence of an ice-free Arctic could be rather weak or even negligible in summer. In winter, a northward displacement of the subtropical jet at lat 5–6° (like in other longitudes, see p. 65) could mean wintertime disturbances across the whole of southern Asia, perhaps with increasing rainfall in areas as remote as Chinese Turkestan, but with decreasing winter rain south of the Himalayas.

After a possible disappearance of the central core of the Arctic drift ice, one of the first consequences in the cold season would be the formation of a baroclinic zone along the northern coast of the continents, between the cold air continuously formed above the snow-covered land and the relatively warm air above the open Arctic ocean. It must remain an open question as to what extent coastal ice, and perhaps also a thin seasonal mid-ocean ice cover, could form. In any case, the rate of snowfall along the northern coasts of the continents and Arctic islands would be enhanced by such a development. In summer, the low-level stratus clouds now above the melting ice could probably disappear, and the thermal circulation arising between the heated continents and the relatively cool water could produce a distinct predominance of anti-cyclonic situations above the Arctic Ocean (which will then be characterized by subsidence and little cloudiness).

Changes in the global water budget (see Chapter 2) are difficult to estimate. While a weaker tropical circulation can be assumed for the moderate warm phases considered in the global warming scenario discussed in Chapter 5, evidence from past climates, based on signs of increasing aridity in the late Tertiary are unambiguous; the fact that the peak of Antarctic glaciation, together with the eustatic drop of the sea level, also reduced the area of ocean evaporation lends weight to this conclusion. If one assumes strong upwelling for only six months of the southern winter, the loss due to this effect is $30 \times 10^3 \text{ km}^3/\text{yr}$. On the other hand, an ice-free Arctic ocean would evaporate much faster than at present; (currently the evaporation is only on the order of 5–10 cm/yr). If one assumes a rather large increase in evaporation, i.e., by +100 cm/yr, this would yield no more than $10 \times 10^3 \text{ km}^3/\text{yr}$ for an area of 10^7 km^2 . Based on the incomplete evidence from past climates, the extension of the southern belt to lat 0–20 °S and the displacement of the northern STA to lat 35–45 °N (or even farther) would support a general increase in aridity, with a global loss of water on the order of at least 4–5%.

The prospects for a worldwide rise in the sea level as a possible consequence of global warming must be considered quantitatively. Melting of drifting sea ice does not change the sea level at all; floating ice is in static equilibrium with water, like an ice cube in a glass of whisky. Within the human time scale (~ 100 years), any worldwide rise in the sea level could only be caused by large-scale surges of continental ice caps, e.g., on the order of 10^5 km^3 or more, leading (with a density of almost 0.9) to a 25 cm sea-level rise per 10^5 km^3 of ice melted.

Only one area is prone to such a surge, the "western" part of Antarctica (between South America and long 150°W), situated on a rock foundation largely below sea level. Surges of this order have been suggested for the 19th century (Lamb 1967), as well as for the postglacial period (Wilson 1978), and the probability of such an event may increase with global warming. There seems to be a gradual transition from one surge to another (of unknown time scale!), as well as extended calving of existing ice shelves. Possibly more interesting are surges on the order of $2 \times 10^6 \text{ km}^3$, equivalent to a sea-level rise of 5 m; the last event of this kind may have occurred about 110,000 years ago (Hollin 1977) or, with more widespread evidence, about 125,000 years ago (Mercer 1978). The risk of such a global rise in the sea level – possibly produced by a mechanism of calving bays, as proposed by Hughes (1977) – has been examined by Mercer (1978). At present, the risk seems to be quite small, but certainly not negligible (see Chapter 2 of this report). Some theoretical studies have been made, but more detailed field investigations are needed, as well as monitoring of Antarctic ice shelves and coastal sea ice.*

The possibility of a significant melting of continental ice caps (e.g., in Greenland and in the Antarctic) is also rather small. The surface of the Antarctic ice cap, with temperatures between -20°C and -70°C and an albedo of 80–90%, can be considered stable. Even a very marked warming through greatly increased transport of warm air would not suffice to cause significant melting (or evaporation). After a possible disappearance of the Arctic sea ice, Greenland (lat $60\text{--}83^\circ\text{N}$) would be affected by some melting during the warm season (at least at its southern part), but it would also receive much greater winter snow-fall due to increased cyclone activity. It is difficult to estimate the ratio of both processes without model computations. But in the worst and rather unlikely case, an estimated annual net loss of as much as 50 cm water-equivalent would cause an additional sea-level rise of 2.5 mm/yr, as compared with the present value of 1.2 mm/yr.

As a result of these considerations, the probability of a catastrophic or even only appreciable rise in the sea level during the next 100 years seems small (estimated to be 1% or less) – much smaller than the probability of a large-scale shift of climatic belts due to a global warming – but is certainly not negligible.

*The possible time scale of such a disintegration could be on the order of 100–200 years, equivalent to an average sea-level rise on the order of 2–5 cm/yr. This is suggested by a similar event caused by the catastrophic incursion of the sea into the present Hudson Bay about 7,800 years ago (Andrews *et al.* 1972), simultaneously with an observed eustatic sea-level rise of 7–10 m over 200 years on the coasts of northwest England (Tooley 1974) and southwest Sweden (Mörner 1976).

7 CONCLUSIONS

Small changes in the global average temperature (see Table 3) are utterly misleading for the general reader. A temperature drop of 1 °C near the northern boundary of agricultural land (affecting, for instance, wheat in northern Canada, or hay in Iceland) may reduce the growing season by several weeks, with detrimental effects on harvests. Even more essential are the accompanying changes in the frequency of extremes in weather in lower and middle latitudes, i.e., long and cold springs, cool and wet summers, and so on. According to the present state of the art, a sudden cooling, similar to that which occurred during the Little Ice Age and its forerunners, cannot be excluded, since natural internal climatogenetic processes are at present still unpredictable (see Chapter 2). The most catastrophic years were 1316, 1430, 1570, and several years in the 1690s and 1780s (the latter apparently affecting Europe,* North America, as well as Japan). The European revolutions of 1789 and 1848 occurred after a succession of years with bad weather, bad harvests, and high cereal prices; some of the most severe climatic and economic conditions were reported in the years following some very heavy volcanic eruptions, e.g., after 1766, 1783, 1815, and finally, 1883.

The problem of natural climatic fluctuations due to the varying frequency and intensity of volcanic explosions merits some discussion. As far as can be seen, this effect alone could counteract, with a certain degree of probability, the evolution outlined in the admittedly one-sided scenario discussed in this paper (see the basic assumptions given on p. 5). Lamb (1970, 1977b) has demonstrated the time variability of volcanic eruptions using an estimated Dust Veil Index (see Figure 26). There is little doubt that the peaks of volcanic activity by and large coincide with series of particularly cool years (and especially cool summers); their role in climatic history, perhaps on all time scales (see

*These data have been derived from historical records including a comparison of some 25 long series of cereal prices (1200–1790) in northwest and central Europe. A detailed study is in preparation; see also the documented evidence given by Ladurie (1971) and Lamb (1977a).

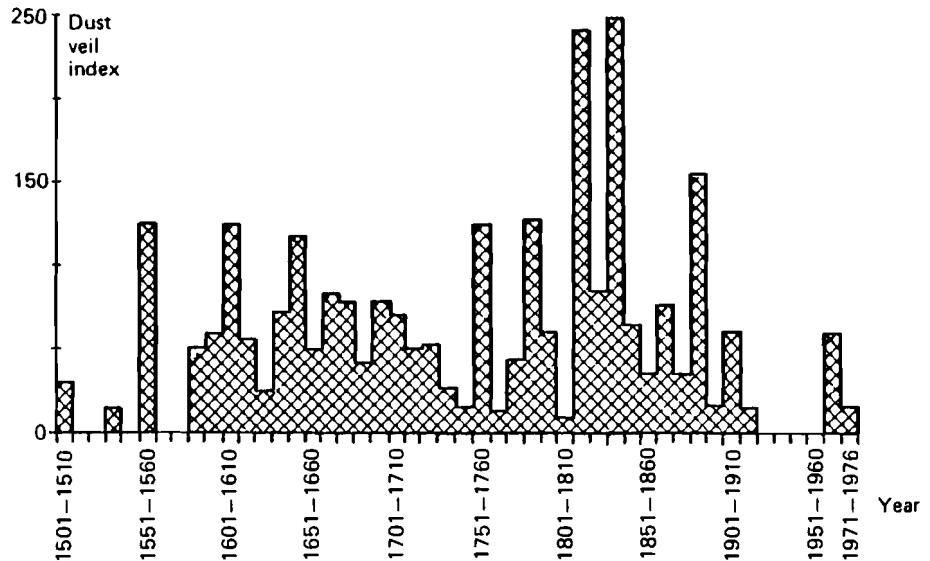


FIGURE 26 Ten-year averages of volcanic activity in the northern hemisphere since 1500, measured in terms of the Dust Veil Index. Source: Lamb (1977b).

Figure 20), can hardly be overrated. Volcanic eruptions are very difficult to forecast, as has been confirmed by recent occurrences; such forecasts are virtually impossible beyond the time scale of weeks or months. On a global scale, the geophysical concept of plate tectonics has contributed much to a better understanding of volcanic eruptions; mid-oceanic rift systems burst, hot material ascends and erupts in individual volcanoes, and plates move horizontally towards the continents, where they are subducted by heavy earthquakes. In recent years a series of unusually severe earthquakes has occurred, all of them along well-known active tectonic zones, but volcanic activity has remained moderate. Should we soon expect an increase in the frequency of really heavy volcanic explosions? There is no answer to this question, but volcanologists would be hardly surprised if this were to happen. An example of discontinuous manifestations of the slow plate motion – which is probably responsible for the observed clustering of volcanic (and possibly seismic) events – recently occurred at the mid-Atlantic rift system which crosses Iceland. In April 1977 two innocent-looking, but steaming, parallel cracks, each with a diameter of about 1 m, formed in the Myvatn area, and a geothermal power station which stood just before completion lost its resources.

Since volcanic activity has until now been unpredictable, a statistical technique can be used to estimate the probability of a cooling episode similar to the Little Ice Age occurring during the next 100 years. On the basis of Figure A 31 in the excellent report *Understanding Climatic Change*, issued by the US National Academy of Sciences (1974), one can estimate that the

probability that an event which may occur randomly once every 1,000 years will occur during the following 100 years is about 10–20%. This estimate only indicates an order of magnitude, but to disregard such a probability would be irresponsible.

In this context, our scenario leads to the following conclusions: if the atmospheric CO₂ content continues to rise, and if other man-made trace gases add another 50% (or more) to the greenhouse effect of infrared absorption, developments similar to those outlined in the global warming scenario based upon past climates in Chapter 5, must eventually be expected. The Eem period may serve as a first guide to what might happen if the real CO₂ content rises to about 500–550 ppm; if the effect of other trace gases were negligible, the relevant threshold of the virtual CO₂ content would be about 600–700 ppm (see Table 3). As the Manabe–Wetherald model (Figure 7) indicates, a doubling of the CO₂ content could be accompanied by quite serious regional consequences, some of them benign, but others deleterious. These consequences would be more profound than all climatic changes mankind has experienced during the last 10,000 years. To avoid serious risks, provision should be made to avoid exceeding about 450 ppm, as a threshold value of the real CO₂ content.

The real danger, however, is related to the possible consequences outlined in Chapter 6. Can we stop at a CO₂ content between 450 and 750 ppm? Since the necessary time of transition from one energy system to another is on the order of several decades (Häfele and Sassin 1977a, 1977b), it will soon be too late for any effective countermeasures. The report of a working group of specialists (Williams 1978, p. 315) states that “mankind needs and can afford a time window of between 5 and 10 years for vigorous research and planning . . . to justify a major change in energy politics . . .” At first glance, the idea of a planet with one pole heavily glaciated and the other ice-free seems so fantastic and inconceivable that emotional resistance against it, especially among non-scientists, will be difficult to overcome. But there is no doubt that exactly this pattern had existed and was stable for a period of ten million years; this is established as a fact.

It goes beyond the capability of a climatologist, familiar with the historical and geophysical background of his science, to predict the time sequence of future increases in CO₂ and a rise in the temperature. This depends on economic and political decisions which occur outside his sphere of knowledge and experience. As a first guide to different CO₂ growth rates, the reader is referred to Figure 8 in this paper. Taking into account all uncertainties, especially with respect to the role of the biosphere and the oceans, specialists argue that an increase in atmospheric CO₂ by a factor of 3 to 5 could be expected over the next 100 years or so (see p. 26).

From a climatological point of view the *decisive threshold* of the real CO₂ level should be somewhere between 550 and 750 ppm; that of the virtual CO₂ level is somewhat higher, e.g., between 800 and 1,000 or 1,100 ppm. Above

this threshold, the probability of an evolution toward an ice-free Arctic increases rapidly – a development of this kind could occur quite abruptly, i.e., in a matter of few decades (or less), and would then be irreversible. Since this situation had been maintained, under purely natural conditions, over a period of no less than ten million years, it would again be stable, at least for a period well beyond a millenium, before the deep ocean has absorbed the additional input of CO₂. What has happened can happen again; after a series of catastrophic weather extremes, it would lead to a nearly inconceivable displacement of climatic zones by 400–800 km (or more), definitely affecting mankind as a whole.

The author firmly believes that this risk is unacceptable and must be avoided even at very high cost. It is at least as large as, but probably much larger than, all the risks involved in the transitional use of nuclear energy under special precautions. The risk of a global warming can be avoided if decisions regarding future energy policies and all their consequences are carefully planned and can be executed, under an international agreement, without undue delay.

REFERENCES

Monographs

- Andersen, N.R., and A. Malakhov, eds. (1977) *The Fate of Fossil Fuel CO₂ in the Oceans. Marine Science, Vol. 6.* New York: Plenum Press.
- Bach, W., J. Pankrath, and W. Kellogg, eds. (1979) *Man's Impact on Climate. Developments in Atmospheric Science, Vol. 10.* Amsterdam: Elsevier.
- Baumgartner, A., and E. Reichel (1975) *The World Water Balance.* Munich: Oldenbourg.
- Bryson, R.A., and Th.J. Murray (1977) *Climates of Hunger.* Madison: University of Wisconsin Press.
- Budyko, M.I. (1974) *Izmeneniia klimata.* Leningrad: Gidrometeoizdat (in Russian). Translated into English by the American Geophysical Society in 1977.
- Cline, R.M., and J.D. Hays, eds. (1976) *Investigation of Late Quaternary Paleoceanography and Paleoclimatology.* Geological Society of America Memoir 145.
- Frenzel, B. (1967) *Die Klimaschwankungen des Eiszeitalters.* Braunschweig: Vieweg.
- Frenzel, B. (1968a) *Grundzüge der pleistozänen Vegetationsgeschichte Nord-Eurasiens.* Wiesbaden: Franz Steiner.
- Gabriel, B. (1977) *Zum ökologischen Wandel im Neolithikum der Östlichen Zentralsahara.* Berliner Geographische Abhandlungen 27.
- GARP, in B. Bolin, ed. (1975) *The physical basis of climate and climate modeling.* GARP Publication Series 16. Geneva: World Meteorological Organization.
- Gribbin, J., ed. (1978) *Climatic Change.* Cambridge: Cambridge University Press.
- Hare, F.K. (1977) *Climate and desertification.* Pages 63–167, *Desertification: its Causes and Consequences*, edited by the Secretariat of the United Nations Conference on Desertification. Oxford: Pergamon.
- Ives, J.D., and R.G. Barry, eds. (1974) *Arctic and Alpine Environments.* London: Methuen.
- Labeyrie, J., ed. (1974) *Variation du Climat au Cours du Pleistocene.* Paris: Centre Nationale de Recherches Scientifiques.
- Ladurie, E.L. (1971) *Times of Feast, Times of Famine. A History of Climate Since the Year 1000.* New York: Doubleday.
- Lamb, H.H. (1972) *Climate: Present, Past and Future, Vol. 1.* London: Methuen.
- Lamb, H.H. (1977a) *Climate: Present, Past and Future, Vol. 2.* London: Methuen.

- Lvovich, M. (1969) Water Resources for the Future. Moscow: Posveshchenie (in Russian).
- Mägdefrau, K. (1968) Paläobiologie der Pflanzen. 4th ed. Stuttgart: Gustav Fischer.
- Nairn, A.E.M., ed. (1961) Descriptive Paleoclimatology. London: Interscience.
- Nairn, A.E.M., ed. (1964) Problems in Paleoclimatology. NATO Paleoclimatology Conference at the University of Newcastle/Tyne, Jan. 7–12, 1963. London: Interscience.
- National Academy of Sciences (1974) Understanding Climatic Change. A Program for Action. Washington, D.C.
- National Academy of Sciences (1979) Carbon Dioxide and Climate. A Scientific Assessment. Washington, D.C.
- Nicholson, S.E. (1976) A Climatic Chronology for Africa: Synthesis of Geological, Historical and Meteorological Information and Data. Ph.D. thesis, Department of Meteorology, University of Wisconsin. Madison, Wisconsin.
- Olsen, J.S., H.A. Pfuderer, and Y.K. Chan (1978) Changes in the Global Carbon Cycle and the Biosphere. ORNL-1050. Oak Ridge, Tennessee: Oak Ridge National Laboratory.
- Palmén, E., and C.W. Newton (1969) Atmospheric Circulation Systems. International Geophysics Series 13.
- Pittock, A.B., L.A. Frakes, D. Janssen, J.A. Peterson, and J.W. Zillman, eds. (1978) Climatic Change and Variability. A Southern Perspective. Cambridge: Cambridge University Press.
- Schwarzbach, M. (1974) Klima der Vorzeit. Eine Einführung in die Paläoklimatologie. 3rd ed. Stuttgart: Enke.
- Servant, M. (1973) Séquences Continentales et Variations Climatiques: Elévation du Basin du Tchad Canozoïque Supérieure. Doctoral Dissertation, University of Paris.
- Stumm, W., ed. (1977) Global Chemical Cycles and Their Alteration by Man. Berlin: Abakon.
- Takahashi, K., and M.M. Yoshino, eds. (1978) Climatic Change and Food Production. Tokyo: University of Tokyo Press.
- van Zinderen Bakker, E.M., ed. (1978) Antarctic Glacial History and World Palaeoenvironments. Rotterdam: Balkema.
- Vasari, Y., H. Hyvarinen, and S. Hicks, eds. (1972) Climatic Change in Arctic Areas during the Last Ten Thousand Years. Acta Universitatis Ouluensis A3, Geologica (1).
- Williams, J., ed. (1978) Carbon Dioxide, Climate and Society. IASA Proceedings Series Environment, Vol. 1. Oxford: Pergamon Press.
- Williams, M.A.J., and H. Faure, eds. (1980) The Sahara and the Nile. Rotterdam: Balkema.
- World Meteorological Organization (1979) Proceedings of the World Climate Conference. Publication No. 537. Geneva: World Meteorological Organization.

Selected References on Geophysics, Modeling, and Related Topics

- Aagard, K., and L.K. Coachman (1975) Eos-Transactions of the American Geophysics Union 56: 484–487.
- Aagard, K., and P. Greisman (1975) Journal of Geophysical Research 80: 3821–3827.
- Andreas, E.L., C.A. Paulson, R.M. Williams, R.W. Lindsay, and J.A. Businger (1979) Boundary-Layer Meteorology 17: 57–91.
- Angell, J.K., and J. Korshover (1978) Monthly Weather Review 106: 755–770.
- Augustsson, T., and V. Ramanathan (1977) Journal of Atmospheric Sciences 34: 448–451.
- Bacastow, R. (1976) Nature 261: 116–118.
- Bacastow, R. (1977) Pages 33–44, The Fate of Fossil Fuel CO₂ in the Oceans, edited by N.R. Andersen and A. Malakhov. Marine Science, Vol. 6. New York: Plenum Press.
- Bach, W. (1976a) Review of Geophysics and Space Physics 14: 429–474.

- Bach, W. (1976b) *Bonner Meteorologische Abhandlungen* 24.
- Bach, W. (1978) Pages 141–168, *Carbon Dioxide, Climate, and Society*, edited by J. Williams, Oxford: Pergamon.
- Barnett, T.P. (1977) *Journal of Physical Oceanography* 7: 221–236, 633–647.
- Berkofsky, L. (1976) *Applied Meteorology* 15: 1139–1144.
- Berkofsky, L. (1977) *Beiträge zur Physik der Atmosphäre* 50: 312–320.
- Berlage, H.P. (1957) *Medelingen en Verhandelingen Koninklijk Nederlandsch Meteorologisch Instituut De Bilt* 69.
- Berlage, H.P. (1966) *Medelingen en Verhandelingen Koninklijk Nederlandsch Meteorologisch Institut De Bilt* 88.
- Bjerknes, J. (1969) *Monthly Weather Review* 97: 163–172.
- Bjornsson, A., K. Saemundson, P. Einarsson, E. Tryggvassen, and K. Gronvold (1977) *Nature* 266: 318–322.
- Borzenkova, I.I., K.Ya. Vinnikov, L.P. Spirina, D.I. Stekhnovskii (1976) *Meteorologiya i Gidrologiya* 7: 27–35.
- Bryson, R.A., W.M. Wendland, J.D. Ives, and J.T. Andrews (1969) *Arctic and Alpine Research* 1: 1–14.
- Budyko, M.J. (1962) *Izvestiya Akademii Nauk SSR, Seriya Geograficheskaya* 6: 3–10 (in Russian).
- Budyko, M.J. (1969) *Tellus* 21: 611–619.
- Budyko, M.J. (1972) *Eos-Transactions of the American Geophysics Union* 53: 868–874.
- Budd, W.F. (1975a) *Science* 186: 925–927.
- Budd, W.F. (1975b) *Journal of Glaciology* 14: 3–21.
- Cess, R.D. (1976) *Journal of Atmospheric Sciences* 33: 1831–1843.
- Cess, R.D. (1977) *Journal of Atmospheric Sciences* 34: 1824–1827.
- Charney, J.G. (1975) *Quarterly Journal of the Royal Meteorological Society* 101: 193–202.
- Damon, P.E., and St. M. Kunen (1976) *Science* 193: 447–453.
- Doberitz, R. (1968) *Berichte des Deutschen Wetterdienstes* 112.
- Doberitz, R. (1969) *Bonner Meteorologische Abhandlungen* 11.
- Donn, W.L., and D.H. Shaw (1966) *Journal of Geophysical Research* 71: 1087–1093.
- Dronia, H. (1974) *Meteorologische Rundschau* 27: 166–174.
- Ellsaesser, H.W., M.C. MacCracken, G.L. Potter, and F.M. Luther (1976) *Quarterly Journal of the Royal Meteorological Society* 102: 655–666.
- Fletcher, J.O., Y. Mintz, A. Arakawa, and T. Fox (1973) *World Meteorological Organization Technical Note* 129: 181–218.
- Flohn, H. (1964a) *Bonner Meteorologische Abhandlungen* 4.
- Flohn, H. (1966) *Zeitschrift für Meteorologie* 17: 316–320.
- Flohn, H. (1967) *Annalen der Meteorologie, Neue Folge* 3: 76–80.
- Flohn, H. (1968) Colorado State University, Department of Atmospheric Science Paper 130.
- Flohn, H. (1971) *Bonner Meteorologische Abhandlungen* 15.
- Flohn, H. (1972) Pages 93–102, *Studies in Physical Oceanography, Vol. I*, edited by A.L. Gordon. New York: Gordon.
- Flohn, H. (1974a) *Annalen der Meteorologie, Neue Folge* 9: 25–31.
- Flohn, H. (1975) *Bonner Meteorologische Abhandlungen* 21.
- Flohn, H. (1977a) *Applied Sciences and Development* 10: 44–58.
- Flohn, H., and H. Fleer (1975) *Atmosphere* 13: 96–109.
- Gow, A.J., H.T. Ueda, and D.E. Garfield (1968) *Science* 161: 1011–1013.
- Greenhut, G.K. (1977) *Journal of Applied Meteorology* 16: 727–734.
- Hahn, J., and C. Junge (1977) *Zeitschrift für Naturforschung* 32a: 190–214.

- Hahn, J. (1979) Pages 193–213, *Man's Impact on Climate*, edited by W. Bach, J. Pankrath and W. Kellogg. New York: Elsevier.
- Hantel, M. (1972) Pages 121–136, *Studies in Physical Oceanography*, Vol. I, edited by A.L. Gordon. New York: Gordon.
- Hastenrath, St. (1976) *Rivista Italiana di Geofisica e Science Affini* 3: 255–256.
- Hastenrath, St. (1977) *Annalen der Meteorologie*, Neue Folge 12: 84–86.
- Hattersley-Smith, G. (1974) Pages 195–223, *Arctic and Alpine Environments*, edited by J.D. Ives and R.G. Barry. London: Methuen.
- Häfele, W., and W. Sassin (1977a) The global energy system. Pages 12–25, *Annual Review of Energy*, Vol. 2, edited by J. Hollander. Palo Alto, California: Annual Reviews Inc.
- Häfele, W., and W. Sassin (1977b) On energy demand. *International Atomic Energy Agency Bulletin* 19(6): 21–37.
- Henning, D., and H. Flohn (1980) *Beiträge zur Physik der Atmosphäre* 53: 430–441.
- Hibler, W.D. (1979) *Journal of Physical Oceanography* 9: 815–846.
- Hollis, G.E. (1978) *Geographical Journal* 144: 62–80.
- Joseph, J.H. (1977) Pages 487–492, *Proceedings of a Conference on Radiation in the Atmosphere*, edited by H.J. Bolle. Princeton: Science Press.
- Junge, C. (1978) *PROMET, Meteorologische Fortbildung* 2/3: 21–32.
- Keeling, C.D., and R. Bacastow (1977) *Energy and Climate*. US National Research Council. Washington, D.C.: National Academy of Science.
- Korff, H.C., and H. Flohn (1969) *Annalen der Meteorologie*, Neue Folge 4: 163–164.
- Klein, C. (1977) Personal communication. Jerusalem.
- Kukla, G.J., J.K. Angell, J. Korshover, H. Dronia, M. Hoshiai, J. Namias, M. Rodewald, R. Yamamoto, and T. Iwashima (1977b) *Nature* 270: 573–580.
- Lamb, H.H. (1967) *World Meteorological Organization Technical Note* 87: 428–453.
- Lamb, H.H. (1970) *Philosophical Transactions of the Royal Society of London*, Series A 266: 425–533.
- Lamb, H.H. (1977b) *Climate Monitor* 6: 57–67.
- Limbirt, D.W.S. (1974) *Polar Record* 17: 303–306.
- Madden, R.A., and V. Ramanathan (1980). Paper submitted to *Science* for publication.
- Manabe, S., and J.L. Holloway, Jr. (1975) *Journal of Geophysical Research* 80: 1617–1649.
- Manabe, S., and R.T. Wetherald (1975) *Journal of Atmospheric Sciences* 32: 3–15.
- Manabe, S., and R.J. Stouffer (1979) *Nature* 282: 491–493.
- Manabe, S., and R.T. Wetherald (1980) *Journal of Atmospheric Sciences* 37: 99–118.
- Maykut, G.A., and N. Untersteiner (1971) *Journal of Geophysical Research* 76: 1550–1575.
- Mass, C., and S.H. Schneider (1977) *Journal of Atmospheric Sciences* 34: 1995–2004.
- Newell, R.E., A.R. Navato, and J. Hsiung (1978) *Pure and Applied Geophysics* 116: 351–371.
- Oliver, R.C. (1976) *Journal of Applied Meteorology* 15: 933–970.
- Parkinson, C.L., and W.W. Kellogg (1979) *Climatic Change* 2: 149–163.
- Parkinson, C.L., and W.M. Washington (1979) *Journal of Geophysical Research* 84: 311–337.
- Pflugbeil, C. (1967) *Berichte des Deutschen Wetterdienstes* 104.
- Pollack, J.B., O.B. Toon, C. Sagan, A. Summers, B. Baldwin, and W. vanCamp (1976) *Journal of Geophysical Research* 8: 1071–1083.
- Polunin, N., ed. (1980) *Growth without Disaster*. Proceedings of the Second International Conference on Environmental Future, Reykjavik, June, 1977. London: Macmillan Press.
- Pratt, R.F., *et al.* (1977) *Climatic Change* 1: 109–135.
- Ramanathan, V. (1975) *Science* 190: 50–52.
- Ramanathan, V., and J.A. Coakley (1978) *Review of Geophysics and Space Physics* 16: 465–489.

- Ratcliffe, R.A.S., J. Weller, and P. Collison (1978) *Quarterly Journal of the Royal Meteorological Society* 104: 243–255.
- Roads, J.O. (1978) *Journal of Atmospheric Sciences* 35: 753–772.
- Rothrock, D.A. (1975) *Journal of Geophysical Research* 80: 387–397.
- Rowntree, P.R. (1972) *Quarterly Journal of the Royal Meteorological Society* 98: 290–321.
- Rowntree, P.R., and J. Walker (1978). Pages 181–192, *Carbon Dioxide, Climate, and Society*, edited by J. Williams. Oxford: Pergamon.
- Sagan, C., O.B. Toon, and J.B. Pollack (1979) *Science* 206: 1363–1368.
- Salinger, M.J., and J.M. Gunn (1975) *Nature* 256: 396–398.
- Schneider, S.H. (1975) *Journal of Atmospheric Sciences* 32: 2060–2066.
- Schwerdtfeger, W. (1956) *Anales Societas Cientifico Argentina* 161: 53–82.
- Schwerdtfeger, W. (1958) *Zeitschrift für Gletscherkunde und Glazialgeologie* 4: 73–86.
- Schwerdtfeger, W. (1970) Pages 253–355, *World Survey of Climatology*, Vol. 14, edited by H.E. Landsberg. Amsterdam: Elsevier.
- Sellers, W.D. (1969) *Journal of Applied Meteorology* 8: 392–400.
- Sellers, W.D. (1973) *Journal of Applied Meteorology* 12: 241–254.
- Smagorinsky, J. (1963) *Monthly Weather Review* 91: 99–165.
- Söderlund, R., and B.H. Svensson (1976) Pages 23–73, *SCOPE Report No. 7*. London: Wiley.
- Thorndike, A.S., D.A. Rothrock, G.A. Maykut, and R. Colony (1975) *Journal of Geophysical Research* 80: 4501–4513.
- Trempel, U. (1978) *Diplomarbeit*. Universität Bonn.
- Untersteiner, N. (1975) Pages 206–224, *GARP Publication Series 16*. Geneva: World Meteorological Organization.
- van Loon, H., and J. Williams (1976) *Monthly Weather Review* 104: 364–380, 1003–1011, 1591–1596.
- van Loon, H., and J. Williams (1977) *Monthly Weather Review* 105: 636–647.
- van Loon, H., and J.C. Rogers (1978) *Monthly Weather Review* 106: 296–310.
- Vowinckel, E., and S. Orvig (1970) Pages 129–252, *World Survey of Climatology*, Vol. 14, edited by H.E. Landsberg. Amsterdam: Elsevier.
- Vowinckel, E., and S. Orvig (1973) *World Meteorological Organization Technical Note* 129: 143–166.
- Walsh, J.E. (1977) *Monthly Weather Review* 105: 1527–1535.
- Walsh, J.E., and C.M. Johnson (1979) *Journal of Physical Oceanography* 9: 580–591.
- Wang, W.C., Y.L. Yung, A.A. Lacis, T. Mo, and J.E. Hansen (1976) *Science* 194: 685–690.
- Washington, W.M., R.M. Chervin, and G. Rao (1977) *Pure and Applied Geophysics* 115(5–6): 1335–1336.
- Wetherald, R.T., and S. Manabe (1975) *Journal of Atmospheric Sciences* 32: 2044–2059.
- Wright, P.B. (1975) *CRU 4*. University of East Anglia, Climate Research Unit.
- Wright, P.B. (1977) *Report 77-13*. Hawaii Institute of Geophysics.
- Wyrтки, K. (1977) *Journal of Physical Oceanography* 7: 779–787.
- Yamamoto, R., T. Iwashima, and M. Hoshiai (1975) *Journal of the Meteorological Society of Japan* 53: 482–486.
- Yamamoto, R., M. Hoshiai, and T. Iwashima (1977) *Archiv für Meteorologie, Geophysik, und Bioklimatologie, Serie B* 25: 105–115.
- Zimen, K.E. (1977a) *Global Chemical Cycles and Their Alteration by Man*, edited by W. Stumm. Berlin: Abakon.
- Zimen, K.E. (1977b) *Zeitschrift für Naturforschung* 32a: 1544–1554.

Selected References on Paleoclimatology

- Adam, D.P. (1978) X. International Union for Quaternary Research (INQUA) Congress, Birmingham, UK. Abstracts. Page 3.
- Alexandre, P. (1977) *Annales Economies, Sociétés, Civilisations* 32: 183–197.
- Andrews, J.T., A. Mears, G.H. Miller, and D.R. Pheasant (1972) *Nature—Physical Science* 239: 147–149.
- Barry, R.G., W.H. Arundale, J.T. Andrews, R.S. Bradley, and H. Nichols (1977) *Arctic and Alpine Research* 9: 193–210.
- Bernabo, J.C., and T. Webb III (1977) *Quaternary Research* 8: 64–96.
- Bowler, J.M., G.S. Hope, J.N. Jennings, G. Singh, and D. Walker (1976a) *Quaternary Research* 6: 359–394.
- Bowler, J.M. (1976b) *Earth Science Reviews* 12: 279–310.
- Bryson, R. (1978) Pages 316–327, *Climate Changes and Variability: A Southern Perspective*, edited by A.B. Pittock *et al.* Cambridge, Massachusetts: Cambridge University Press.
- Butzer, K.W., G.L. Isaac, J.L. Richardson, and C. Washbourn-Kamau (1972) *Science* 175: 1069–1076.
- Butzer, K.W. (1975) Pages 389–410, *Problems in Prehistory: North Africa and the Levant*, edited by F. Wendorf and A.E. Marks. Dallas, Texas: Southern Methodist University Press.
- Chu, C.Ch. (1973) *Scientia Sinica* 16: 226–256.
- Cifelli, R. (1976) *Nature* 264: 431–342.
- Dansgaard, W., *et al.* (1972) *Quaternary Research* 2: 396–398.
- Dansgaard, W., N. Reeh, N. Gundestre, H.B. Clausen, and C.U. Hammer (1975) *Nature* 255: 24–28.
- Dansgaard, W. (1978) *Journal of Glaciology* 20: 3–30.
- Diester-Haas, L. (1976) *Quaternary Research* 6: 299–314.
- Dorf, E. (1960) *American Scientist* 48: 341–364.
- Duplessy, J.C., J. Labeyrie, C. Lalou, and H.V. Nguyen (1970) *Nature* 226: 631–633.
- Emiliani, C., and N.J. Shackleton (1974) *Science* 183: 511–514.
- Flohn, H. (1964b) *Geologische Rundschau* 54: 504–515.
- Flohn, H. (1974b) *Quaternary Research* 4: 385–404.
- Flohn, H. (1978a) Pages 3–13, *Antarctic Glacial History and World Paleoenvironments*, edited by van Zinderen Bakker. Rotterdam: Balkema.
- Flohn, H. (1978b) Pages 124–134, *Climatic Changes and Variability: A Southern Perspective*, edited by A.B. Pittock *et al.* Cambridge, Massachusetts: Cambridge University Press.
- Flohn, H. (1978c) Pages 227–238, *Carbon Dioxide, Climate, and Society*, edited by J. Williams. Oxford: Pergamon.
- Flohn, H. (1979) *Quaternary Research* 12: 135–149.
- Flohn, H., and Sh. Nicholson (1980) *Paleoecology of Africa* 12: 3–21.
- Frakes, L.A. (1978) Pages 53–69, *Climatic Changes and Variability: A Southern Perspective*, edited by A.B. Pittock, *et al.* Cambridge, Massachusetts: Cambridge University Press.
- Frenzel, B. (1968b) *Science* 161: 637–649.
- Fuji, N. (1976) Pages 316–356, *Paleolimnology of Lake Biwa and the Japanese Pleistocene* 4, edited by S. Horie. Otsu, Japan.
- Gardner, J.V., and J.D. Hays (1976) Pages 221–246, *Geological Society of America Memoir* 145, edited by R.M. Cline and J.D. Hays.
- Gasse, F., and G. Delibrias (1976) Pages 529–575, *Paleolimnology of Lake Biwa and the Japanese Pleistocene* 4, edited by S. Horie. Otsu, Japan.

- Hays, J.D., J. Lozano, N. Shackleton, and G. Irving (1976) Pages 337–369. Geological Society of America Memoir 145, edited by R.M. Cline and J.D. Hays.
- Hays, J.D. (1978) Pages 57–71, Antarctic Glacial History and World Palaeoenvironments, edited by van Zinderen Bakker. Rotterdam: Balkema.
- Herman, Y. (1977) Personal communication.
- Hollin, J.T. (1977) *Boreas* 6:33–52.
- Hopkins, D.M., ed. (1967) *The Bering Land Bridge*. Stanford, California: Stanford University Press.
- Hopkins, D.M. (1971) *Palaeogeography, Palaeoclimatology, Palaeoecology* 9: 211–231.
- Hsü, K.J., W.B.F. Ryan, and M.B. Cita (1973) *Nature* 242: 240–244.
- Hsü, K.J. (1974) *Die Naturwissenschaften* 61: 137–142.
- Hsü, K.J., L. Montadert, D. Bernoulli, M.B. Cita, A. Erickson, R.E. Garrison, R.B. Kidd, F. Mélières, C. Müller, and R. Wright (1977) *Nature* 267: 399–403.
- Hughes, T. (1973) *Journal of Geophysical Research* 78: 7884–7910.
- Hughes, T. (1975) *Review of Geophysics and Space Physics* 13: 502–526.
- Hughes, T. (1977) *Review of Geophysics and Space Physics* 15: 1–46.
- Kanno, S., and F. Masuda (1978) Pages 63–70. *Climatic Change and Food Production*, edited by K. Takahashi and M. Yoshino. Tokyo: University of Tokyo Press.
- Kellogg, T.B. (1976) Pages 77–110, Geological Society of America Memoir 145, edited by R.M. Cline and J.D. Hays.
- Kemp, E.M. (1978) *Palaeogeography, Palaeoclimatology, Palaeoecology* 24: 169–208.
- Kempe, S. (1977) *Mitteilungen des Geologisch-Paläontologischen Instituts der Universität Hamburg* 47:125–228.
- Kennett, J.P. (1977a) *Journal of Geophysical Research* 82: 3843–3860.
- Kennett, J.P., and R.C. Thunell (1975) *Science* 187: 497–503.
- Kennett, J.P., and R.C. Thunell (1977b) *Science* 196:1231–1234.
- Kennett, J.P., A.R. McBirney, and R.C. Thunell (1977c) *Journal of Volcanology and Geothermal Research* 2: 145–163.
- Kennett, J.P., and P. Huddleston (1972) *Quaternary Research* 2: 384–395.
- Kozur, H. (1976) *Nova Acta Leopoldina, Neue Folge* 224: 413–472.
- Kukla, G.J. (1977a) *Earth Science Review* 13: 307–374.
- Lamb, H.H. (1979) *Quaternary Research* 11: 1–20.
- Lotze, F. (1964) Pages 491–507. *Problems in Paleoclimatology*, edited by A.E.M. Nairn. London: Interscience.
- Maley, J. (1977a) *Nature* 269: 573–577.
- Maley, J. (1977b) Pages 187–197. *Recherches Françaises sur le Quaternaire*. International Union for Quaternary Research, Brussels.
- Maley, J. (1980) Pages 63–86, *The Sahara and the Nile*, edited by M.A.J. Williams and H. Faure. Rotterdam: Balkema.
- Mercer, J.H. (1976) *Quaternary Research* 6: 125–166.
- Mercer, J.H. (1978) *Nature* 271: 321–325.
- Mörner, N.A. (1976) *Palaeogeography, Palaeoclimatology, Palaeoecology* 19: 63–85.
- Nichols, H. (1975) University of Colorado, Institute of Arctic Alpine Research, Paper 15.
- Nicholson, S.E. (1980) Pages 173–200. *The Sahara and the Nile*, edited by M.A.J. Williams and H. Faure. Rotterdam: Balkema.
- Pachur, H.J. (1975) *Die Erde—Zeitschrift der Gesellschaft für Erdkunde Berlin* 106: 21–46.
- Pastouret, L., H. Chamley, G. Delibrias, J.C. Duplessy, and J. Thiede (1978) *Oceanologica Acta* 1: 217–232.
- Pisias, N.G. (1979) *Quaternary Research* 11: 373–386.

- Prell, W.L., J.V. Gardner, A.W.H. Bé, and J.D. Hays (1976) Pages 247–266, *Geological Society of America Memoir 145*, edited by R.M. Cline and J.D. Hays.
- Rognon, P., and M.A.J. Williams (1977) *Palaeogeography, Palaeoclimatology, Palaeoecology* 21: 285–327.
- Saito, T., L.H. Burckle, and J.D. Hays (1975) Pages 226–244, *Late Neogene Epoch Boundaries*, edited by T. Saito and L.H. Burckle. New York: American Museum of Natural History.
- Savin, S.M., R.G. Douglas, and F.G. Stehli (1975) *Geological Society of America Bulletin* 86: 1499–1510.
- Sarnthein, M. (1978) *Nature* 272: 43–46.
- Singh, G., R.D. Joshi, S.K. Chopra, and A.B. Singh (1974) *Philosophical Transactions Royal Society of London, Series B* 267: 467–501.
- Shackleton, N.J. (1977) Pages 401–427, *The Fate of Fossil Fuel CO₂ in the Oceans*, edited by N.R. Andersen and A. Malakhov. *Marine Science*, Vol. 6. New York: Plenum Press.
- Starkel, L. (1977) X. International Organization for Quaternary Research (INQUA) Congress. Birmingham, UK. Abstracts, Page 433.
- Taira, K. (1975) *Palaeogeography, Palaeoclimatology, Palaeoecology* 17: 333–338.
- Tooley, M.J. *Geographical Journal* 140 (Feb.): 18.
- van Zinderen Bakker, E.M. (1976) *Palaeoecology of Africa* 9: 159–202.
- Wigley, T.M.L. (1977) Interim final report to NOAA. University of East Anglia, Climate Research Unit.
- Wigley, T.M.L., D. Jones, and P.M. Kelley (1980) *Nature* 283: 17–21.
- Wijmstra, T.A. (1978) Pages 25–45, *Climatic Change*, edited by J. Gribbin. Cambridge: Cambridge University Press.
- Wilson, A.T. (1964) *Nature* 201: 147–149.
- Wilson, A.T. (1978) Pages 33–39, *Antarctic Glacial History and World Palaeoenvironments*, edited by E.M. van Zinderen Bakker. Rotterdam: Balkema.
- Winterer, E.L. (1973) *American Association of Petroleum Geologists-Bulletin* 57: 265–282.
- Woillard, G.M. (1975) *Acta Geographica Lovaniensia* 14: 1–168.
- Woillard, G.M. (1978) *Quaternary Research* 9: 1–21.
- Woillard, G.M. (1979) *Nature* 281: 558–562.
- Yoshino, M.M. (1978) Pages 63–70, *Climatic Change and Food Production*, edited by K. Takahashi and M.M. Yoshino. Tokyo: University of Tokyo Press.

THE AUTHOR

Hermann Flohn received his doctorate in 1934 from the Goethe University, Frankfurt am Main, and then joined the Reichswetterdienst. In 1946 he joined the staff of the Deutscher Wetterdienst and was appointed Director of its Research Division in 1952. In his capacity as Full Professor at the University of Bonn, he founded the University's Institute of Meteorology in 1961. In 1977 he became Professor Emeritus.

Professor Flohn is a member of the Deutsche Akademie der Naturforscher und Ärzte in Halle, the Akademien der Wissenschaften in Düsseldorf and Munich, and the Koninklijke Academie voor Wetenschappen, Letteren en Schone Kunsten van België in Brussels.

RELATED IIASA PUBLICATIONS

RR-75-45	The Carbon Cycle of the Earth – A Material Balance Approach, by R. Avenhaus and G. Hartmann. Microfiche only.	\$4.00	AS45
RR-76-1	Second Status Report of the IIASA Project on Energy Systems, by W. Häfele, <i>et al.</i> Microfiche only.	\$12.50	AS150
RR-77-8	Fusion and Fast Breeder Reactors, by W. Häfele, J.P. Holdren, G. Kessler, and G.L. Kulcinski.	\$24.00	AS280
CP-77-9	Climate and Solar Energy Conversion: Proceedings of a IIASA Workshop, December 8–10, 1976. J. Williams, G. Krömer, and J. Weingart, editors.	\$11.00	AS135
RM-76-17	On Geoengineering and the CO ₂ Problem, by C. Marchetti.	\$4.00	AS45
RM-76-22	Regional Air Pollution Impact: A Dispersion Methodology Developed and Applied to Energy Systems, by R.L. Dennis. Microfiche only.	\$4.00	AS45
RM-76-23	Evaluation of Health Effects from Sulfur Dioxide Emissions for a Reference Coal-Fired Power Plant, by W.A. Buehring, R.L. Dennis, and A. Hoelzl.	\$7.00	AS85
RM-76-35	A Non-Linear Eight Level Tandem Model to Calculate the Future CO ₂ and C-14 Burden to the Atmosphere, by F. Niehaus.	\$7.00	AS85
RM-76-79	The Impact of Waste Heat Release on Simulated Global Climate, by A.H. Murphy, A. Gilchrist, W. Häfele, G. Krömer, and J. Williams.	\$4.00	AS45

RM-77-15	Further Studies on the Impact of Waste Heat Release on Simulated Global Climate: Part I. J. Williams, G. Krömer, and A. Gilchrist.	\$4.00	AS45
RM-77-32	Energy, Entropy, and Information, by J. Thoma.	\$4.00	AS45
RM-77-34	Further Studies on the Impact of Waste Heat Release on Simulated Global Climate: Part II. J. Williams, G. Krömer, and A. Gilchrist.	\$5.00	AS60
RM-78-63	Dynamic Standard Setting for Carbon Dioxide, by E. Hoepfinger.	\$4.00	AS45
PP-77-7	Can We Predict Climate Fluctuation? by J. Williams.	\$4.00	AS45

IIASA Proceedings Series

Vol. 1	Carbon Dioxide, Climate and Society, J. Williams, ed., 1978. ISBN 0 08 023252 3H	\$30.00	
Vol. 10	Climatic Constraints and Human Activities, J. Ausubel and A. Biswas, eds., 1980. ISBN 0 08 026721 1H	\$30.00	